MASTER THESIS

Modelling the Arctic snowpack properties in Svalbard using SNOWPACK

UNIS Supervisor
Prof. Alexander PROKOP

EPFL Supervisor
Prof. Michael LEHNING

Author
Martin PRAZ

July 27, 2018

Abstract

Longyearbyen is the main settlement in Svalbard, located in the high Arctic and is known for its increasing scientific research and tourism. Most people travelling to this unique location are only concerned about the danger that polar bears can represent, but it is known that avalanche danger is more significant. This study assesses the applicability and performances of the software SNOWPACK to model the snowpack properties in Svalbard throughout the year. Simulations are performed for three different locations equipped with devices able to provide data inputs for the numerical model. The primary challenge of this study is then to evaluate if the model can simulate the snowpack accurately using these measurements. This is done by comparing the model output with snow pits realised during spring on the three test sites, namely Lia, Nybyen and Sverdruphamaren. Because wind and radiation data were not collected directly on the test sites, they had to be derived from two additional nearby stations. The impact of these data on the model output is tested through sensitivity analyses. Results indicate that radiation data does not significantly affect the snowpack in Svalbard. On the other hand, the study reveals that wind has a significant impact on the simulation outputs; hence it is crucial to measure this variable accurately. In this contribution, wind data are adjusted to the simulation sites location, knowing that the corrections are limited by different topographies and channelling effect of wind. For Lia and Sverdruphamaren stations, comparisons between the field measurements and the model outputs are satisfactory. The results are significantly worse for Nybyen station where the estimate of wind seems to be more complicated. Finally, the evaluation of the software SNOWPACK is contrasted and depends considerably on the location and results are forced by wind data estimation. Thus, it is difficult to conclude on the usability of SNOWPACK in Svalbard. For future studies, equip every station with anemometers would significantly improve the accuracy of daily simulations provided by SNOWPACK. These simulations could provide valuable information in order to improve avalanche forecasting in Svalbard.

Acknowledgements

Contents

List of Figures

Introduction

The archipelago of Svalbard is located in the Arctic ocean, far in the north. Svalbard is composed of all the islands between 74° and 81° north latitude and 10° to 35° east longitude. Spitsbergen, the largest island, has an area of barely equivalent to Switzerland ($37'673\ km^2$ vs $41'285\ km^2$).

On this island, there are few settlements like Barentsburg, Sveagruva, Ny-Ålesund and as the administrative centre, Longyearbyen, the northernmost urban community of the world. Its population is approaching 2650 inhabitants according to a specific source [1], and more likely 2210 inhabitants according to the website of Statistics Norway [2]. On one side the mining, which was the primary activity on the island with a peak of production during the year 2007, decreases, and on the other side activities linked to research and tourism increase. Thus, the population varies for several years. From 1993, Longyearbyen hosts the University Centre in Svalbard, which is the world's northernmost higher education institution. Students come in and leave as well as the tourists, who are showing growing interest to visit this raw arctic nature [1]. It implies an increase of human activity inside and outside of the town.

Longyearbyen is one of these cities where people need to be armed to go out of the town, to get protection against polar bears. Many people in Svalbard will be only concerned about the danger, which polar bears represent. To the contrary, they should be more concerned about the avalanche danger. The risk is much higher than undergo an attack from a polar bear. Alexander Prokop (2017, [3]) said "It might be interesting for people to know that in the last 15 years, seven people died from avalanches. But in the last 35 years, only three people have died from polar bear attacks. It is more likely that you will die from an avalanche in Svalbard than from a polar bear.". Avalanches in Svalbard also occur inside the town, as in 2015. During December, a terrible event took place, when 11 houses were destroyed in Longyearbyen by an avalanche, causing two casualties. The city is surrounded by mountains and slopes steep enough to have avalanches to be triggered.

The goal of this project is to test the software SNOWPACK, developed by SLF[1] in Switzerland, with data from Svalbard in the high Arctic. In fact, the software is designed for the alpine climate. Nevertheless, it could work for Svalbard climate, as the processes are the same. The main point is to find out if the software can model the snowpack correctly with radiation changes, due to the polar night and polar day, as well as strong winds. This thesis tries to demonstrate it, with data from three weather stations located above buildings that might be endangered by avalanches, at least for two of them, where the wind accumulates snow. The software SNOWPACK is capable of modelling the stratification with a certain amount of inputs and specialised in the layering of the snowpack. Fieldwork is essential to verify the correspondence between the model and the field to assess the concordance. It is important to say, that this software is used every day in Switzerland for avalanche forecasting.

Data are used from five weather stations located around the town since the three weather stations do not measure every required input. After collecting every data, processing is mandatory to clean the data and verify their quality. False, misleading or incomplete data require processing with Matlab. This software also allows the user to create the input file for the software SNOWPACK, taking into account that every station does not record data at the same time step. Several simulations are run, and comparisons are made between snow profiles realised during the spring and the model. Finally, a discussion concludes the report, speaking of the use of SNOWPACK in the high Arctic and the limitations and possible improvements for this project.

Ultimately, in the case where the software works appropriately for those weather stations, one can suppose that the model could be used to improve the actual avalanche forecast. Indeed, this model provides much information for avalanche forecasters, for example, when digging snowpits is not possible, because of the bad weather or of the instability of the snowpack. Furthermore, it can save much time, in comparison to go out on the field. This part is not covered in this thesis, but can serve as a basis for a thorough development of the use of SNOWPACK in Svalbard.

---

[1]Schnee und Lawinen Forschung / Research for Snow and Avalanches

1 Scientific background

Snow is a porous visco-elastic granular media composed of water in its three phases (solid, liquid and vapour), air and trace gases [4]. First of all, to understand the snowpack stratification, it is essential to explain what are the different types of snow that are possible to find within a snowpack. Second, these shapes are created through several processes described in Chapter 1.2, like metamorphism, but this is not the only process involved in the snow crystals transformation. The wind and later precipitations affect the snow by compaction and adding weight at the top of the snowpack.

1.1 Types of crystals

As a reminder, the following subsections describe the grain shape classification according to the International Classification for Seasonal Snow on the Ground (Fierz and al., 2009 [5]). Only the main classes are presented, but it exists many subclasses.

Precipitation particles

Precipitation particles or fresh snow is formed in clouds and fall directly on the ground or the existing snowpack. A low density and small hardness index characterise this snow. In Switzerland, it is common to have big snowflakes with branches. In Svalbard, this kind of large snowflakes is rarer because of the specific super-saturation degree, temperature and relative humidity. These parameters conduct to the formation of every precipitation particle like columns, needles, plates, etc.

Decomposing and fragmented precipitation particles

Decomposing and fragmented precipitation particles have the characteristics of the precipitation particles, even if they might be partly rounded. This kind of snow has been deposited recently and is close to the surface. To reduce the surface free energy, fragmentation occurs to decrease the surface area. The speed of fragmentation is reduced if the temperature or the temperature gradient is decreasing. This decomposition process reduces the strength, but afterwards, it regains cohesion by sintering.

The action of wind on fresh snow is also one process, which leads to the snow fragmentation. When the wind is blowing, grains are mechanically destroyed by rolling, saltation or suspension, and become rounded. Rolling occurs when the gravitational force is larger than the force exerted by the wind. Snow grains keep in contact with the ground, in contrast with saltation and suspension (Jaedicke, 2001 [6]). If the winds are strong enough to lift the grains from the surface, saltation occurs, and snow grains are moving in the air with frequent contact with the surface (Pomeroy and Gray, 1990 [7]. If the winds are even larger, it can transport the grains on long distances and higher heights; it is called suspension (Jaedicke, 2001 [6]). Thus, snow gets wind-packed and becomes denser. Naturally, the destruction of precipitation particles increases with the wind speed, and the strength is increased due to the fast sintering.

Rounded grains

As it is called, this shape is rounded, and its size can be more or less significant. Within the snowpack, a decrease of the surface area occurs by a reduction of the number of grains and an increase of the diameter of the mean grain. With a low-temperature gradient, grain-to-grain vapour diffusion happens. It means that the excess vapour density is below the critical threshold for kinetic growth, which is explained below (Chapter 1.2). On one side, higher temperature increases the growth rate, and on the other side, a high density will slow down the growth rate. This snow is well sintered, which provides good strength. Time, settlement and smaller grains can even increase this strength more.

Faceted crystals

Faceted crystals are usually hexagonal prisms. The primary process is vapour diffusion from one grain to another driven by a large temperature gradient. Large enough, so that the excess vapour density is above the threshold to enable kinematic growth. The solid crystal has sharp edges and corners with smooth faces. The growth rate is increased with temperature and increasing temperature gradient. It is not considered as a stable layer since the strength decreases with increasing growth rate and grain size.

Depth hoar

Depth hoar looks like striated cup-shaped crystals. The same physical process drives the formation of depth hoar as faceted crystals. Again, the vapour diffusion from one grain to another leads to the formation of depth hoar driven by a large temperature gradient. The only difference is that the excess vapour density has to be well above the threshold, which determines if kinematic growth occurs or not. Same as faceted crystals, growth rate increases with temperature, increasing temperature gradient, and decreasing density. A depth hoar layer is considered to be a weak layer in a snowpack. Thus, it is the worst situation regarding avalanches. Still, the strength can increase with the density. Recrystallisation combined with high-temperature gradients can also lead to the formation of depth hoar, but it is facilitated by a recrystallisation rate lasting for a long time and a density being low.

Surface hoar

Similar to depth hoar, surface hoar crystals are striated but usually flat contrary to depth hoar. These specific crystals are formed on the surface, where the snow surface has to be colder than the air temperature. This phenomenon is possible through radiative cooling occurring when there is an excess of emitted longwave radiation over the absorbed energy. The process is a rapid kinetic growth, and it requires a rapid transfer of vapour from the air above the snowpack to the snow surface. The more the snow surface is colder than the air above, the more the growth rate increases. High relative humidity also leads to a higher growth rate. This kind of layer is, and it may remain its weakness even after being buried under new snow. Thus, dangerous situations are predictable as soon as surface hoar appears.

Melt forms

Every different shape described above are considered as dry snow. As soon as air temperature increases and exceed $0°C$, some melt forms will appear. Melt snow used to appear during the spring or rainfalls. This is why melt forms should be wet unless it has melted and then refrozen. It is made of clustered rounded crystals linked with ice-to-ice bonds. Water is present inside these clusters. Melt forms also include slush, which is separated rounded particles surrounded by water. Depending on which category, the water content is very different. For clusters, the water content is low, but still holding free liquid water. Clusters are formed to minimise the surface free energy. For slush, the water content is high, and ice and water are in thermodynamic equilibrium. Clusters can form if there is drainage. As soon as there is an impermeable layer (i.e. ground), the snow will transform into slush. If the temperature is cold enough, the layer can refreeze into rounded polycrystals and more likely in a melt-freeze crust. The strength of the layer depends on the water content, except when it has refrozen, where the strength is high.

Ice formations

Ice formations often appear as horizontal ice layer, but other classes exist like basal ice layer or rain crust. When rain or meltwater percolate through cold snow ($T < 0°C$), it might refreeze and form an ice layer. It depends on the cycle of freezing-melting, but these formations occur more likely when a layer of fine grains exists above a layer of coarse grains. Regarding the strength, it is quite strong, except if the snow is wet, thus the strength decreases.

Table with symbol, code and colour convention

Below, Figure 1 presents the summary of the symbols, codes and colours used for each main grain shape classes. The most important thing regarding this project is the colour code. In fact, the software SNOW-PACK, use the same code, to give the best visual rendering. The colour of precipitation particles is light green, while decomposing and fragmented precipitation particles appear dark green. Rounded grains are light pink, and faceted crystals are light blue. Regarding depth hoar, the colour to look at is blue. Surface hoar appears to be fuchsia, whereas melt forms are red. Finally, the colour of ice formations is cyan.

Class	Symbol	Code	Colour[1]
Precipitation Particles	+	PP	
Machine Made snow	◎	MM	
Decomposing and Fragmented precipitation particles	/	DF	
Rounded Grains	●	RG	
Faceted Crystals	□	FC	
Depth Hoar	∧	DH	
Surface Hoar	∨	SH	
Melt Forms	○	MF	
	∞	MFcr	
Ice Formations	■	IF	

Figure 1: Symbols, codes and colours convention for the main grain shape classes. Source : Fierz and al. (2009, [5])

1.2 Metamorphism

After a snowfall, precipitation particles will transform into the snowpack. This process is called metamorphism. The snow crystals are relatively unstable, looking at the ratio between their high surface area and their light mass, which is the specific surface area. Snow is continuously changing to tend to its thermodynamic equilibrium state. Metamorphism is a significant actor, regarding the layering of a snowpack. Vapour pressure variations drive this phenomenon. Due to temperature gradients and to the presence of ice or water, vapour pressure increases with temperature. Over liquid water, the vapour pressure will always be higher than vapour pressure above ice. The geometry of snow crystals also affects the vapour pressure; above convex surfaces, the vapour pressure is higher than above flat surfaces. Thus, these both characteristics will induce a mass transport of vapour, from warmer snow crystals to colder one and from convex to concave areas (Lehning and al., 2017 [4]). Here is a review of the different types of metamorphism, that modify snow crystals within the snowpack.

Destructive metamorphism

Destructive metamorphism, also called equilibrium or isothermal metamorphism, occurs when the temperature is below 0°C. It is considered as dry snow metamorphism since no liquid water is present. The gradient of temperature has to be small ($< 10 \,°C/m$), which induces a small gradient of vapour pressure ($< 3.5 \, mb/m$). Evaporation will occur at edges, because of the higher vapour pressure around convex areas and vapour will be deposit at roots, the central part of crystals. The result of this process is smoothing of the original grain. Snow crystals become smaller with less complex structure and increase their number. All this leads to a reduction of the total surface area and of the surface free energy. Finally, vapour gradient decrease and tends to equilibrium. By sintering, these small grains can aggregate into a bigger one, to reduce even more the free surface energy. If the temperatures are close to 0°C, the process is faster than with lower temperatures. Following this type of metamorphism, the snowpack becomes more stable from a mechanical point of view (Sommerfeld and LaChapelle, 1970 [8], Lehning and al., 2017 [4]).

Constructive metamorphism

Conversely, constructive metamorphism, also called kinetic or temperature gradient metamorphism, occurs under high-temperature gradient ($>$ 10 $°C/m$) and large vapour pressure gradient ($>$ 3.5 mb/m). It happens when the ground is warmer than air temperature, which is often the case in Svalbard. Then, mass transport of vapour is occurring along the temperature gradient, in the upward direction. New crystals formed will grow towards the vapour source, which creates cup-shaped crystals, vertically oriented. They are called depth hoar. This process makes the snowpack more fragile, as this vertical orientation gives little shear strength to the layer (Sommerfeld and LaChapelle, 1970 [8], Lehning and al., 2017 [4]).

Wet snow metamorphism

The wet snow metamorphism occurs when snow temperature is close to 0°C. Liquid water is present and acts as medium for heat diffusion, instead of air. Enhanced destructive metamorphism occurs, which means that the process is accelerated. It is possible that the temperature drops below 0°C, which induces the refreezing of meltwater. The snowpack can pass through one process to another, depending on the melting-refreezing phase. In the beginning, only the snowpack surface is affected, but it can transform the entire snowpack (Sommerfeld and LaChapelle, 1970 [8], Lehning and al., 2017 [4]).

2 State of the art

Different software is used for modelling snow in different ways across the world. In the Arctic, the combination of wind and snowfall play a particularly important role regarding snow distribution. There are several reasons to have a model simulating the wind redistribution, to assess, for example, avalanche conditions due to wind loading. SnowTran-3D is a software capable of correctly predicting the drift location and the volume of snow transported by wind (Liston and Sturm, 1998 [9]). It is commonly used to give indications when to close threatened roads or railway in the United States of America. In Alaska, this software, working in three dimensions, is also used to understand the modifications brought by snow cover to the different energy transfers between atmosphere, ground and global radiation balance (Liston and Sturm, 2002 [10]). This software has also been used in Svalbard to have a better understanding of the impact of wind in this high Arctic climate for an ecological and hydrological purpose. In fact, snow redistribution has a significant influence on the possibilities of greenhouse gas exchange and the duration of the plant-growing season. This last parameter is relevant for the arctic terrestrial fauna (Bruland and al., 2004 [11]).

Another well-known software is the French snow model CROCUS, developed by CNMR[2] [12]. This model, integrated into SURFEX, which is a platform for surface modelling, is a numerical model, working in one dimension (vertical dimension). Its basis is established on thermodynamics, simulating energy and mass balance of the snowpack. To do so, the model uses a semi-quantitative method of the evolution of snow crystals morphological properties during metamorphism. Several inputs are required: air temperature, specific humidity, wind speed, incoming radiation (shortwave and longwave), precipitation rate (distinction between rain and snow) and atmospheric pressure. The graphical result gives numerous information about the evolution of snowpack throughout the snow season. Height of snow, layer thickness, grain shape, temperature profile are some of the primary results (Vionnet and al., 2012 [13]). Furthermore, they are corresponding entirely to the goal of this project. The reason why CROCUS is not used is that the solid and liquid precipitation data are not available. In fact, SNOWPACK is comparable to CROCUS, although snow depth can be used as primary input for the model. This is the reason why SNOWPACK is preferred to CROCUS.

2.1 SNOWPACK

SNOWPACK is a software developed by SLF[3] in Switzerland. It is mainly used for avalanche forecasting, but some scientists use it for research in different fields like snow sciences, permafrost research, glaciology, etc. [14]. SNOWPACK models snowpack in vertical dimension (1D), using several inputs based on weather data, described in Chapter 2.1.1. Using a finite-element method, the software solves, numerically, the equations governing mass, energy and momentum conservation inside the snowpack (Bartelt and Lehning, 2002 [15]).

As the software has been developed mostly for avalanche forecasting, the model has been constructed to handle specific problems linked with avalanche warning. The model can simulate snow cover for several hours to years; however, the short-term development is the most interesting. Avalanche forecasters are interested in snowpack stratification, as it is made of several layers. One can define the layers by their thickness and their properties at two different scales: macroscopic and microscopic. Macroscopic properties include temperature, mean stress, water content, although the microscopic properties include grain size, bond size, dendricity and sphericity. Using these four primary microstructures parameters, the complex texture of snow is implemented with rate equations, which predict the development in time and depend on the conditions of the surrounding environment (Lehning and Bartelt, 2002 [16]). Focusing on the stratification, the model uses constructive and destructive metamorphism routines (Bartelt and Lehning, 2002 [15]). Relations as creep viscosity governing snow settlement and thermal conductivity governing energy transport are implemented considering both macroscopic and microscopic properties. In SNOWPACK, the three phases (ice, water and vapour) are mass and energy conserving. It means that the processes of melting, refreezing, deposition of vapour (gas to solid) and sublimation (solid to gas) are taken into account. Removal of mass is also included by wind erosion or meltwater runoff (Bartelt and Lehning, 2002 [15]).

---

[2] Centre National de Recherches Météorologiques / National Centre for Meteorological Research
[3] Schnee und Lawinen Forschung / Snow and Avalanches Research

The development of snowpack during winter and spring is simulated, and modelling is possible for every location having required data measured on site. This model provides much information for avalanche forecasters, without going out on the field. This is the reason why SNOWPACK is used every day in Switzerland since it brings valuable information in complement to snow profiles.

2.1.1 Inputs

This section describes the used way to realise this project. Other ways exist but are not presented in this report. To run SNOWPACK ([18], Lehning and al., 2002 [17], Lehning and al., 2017 [4]), two files as input are mandatory : a .SMET file and a .SNO file. The .SMET contains two parts as shown in Figure 2, which is the top of one of a file used: HEADER and DATA. The HEADER includes the name of the station, station id, altitude, location (latitude, longitude, easting, northing), coordinates system (epsg), the value assigned to missing data (nodata) and the list of the fields. They are in the right order : time (timestamp), air temperature (TA), relative humidity (RH), ground temperature (TSG), snow surface temperature (TSS), snow depth (HS), wind speed (VW), wind direction (DW), outgoing shortwave radiation (OSWR), incoming shortwave radiation (ISWR), incoming longwave radiation (ILWR), precipitations (PSUM) and three fields saved for temperatures within the snowpack (TS1, TS2, TS3). Linked with these fields, two rows (units_offset and units_multiplier) allow the user to add an offset or to multiply any column. This is very useful to do a sensitivity analysis, as it is done in this project, without creating a new file. The DATA part lists all the data for every field. The structure has to be respected, for example, for the time column, if the "T" between the date and the time of the day is omitted, the software is not going to run properly. Even if some data are missing, it needs to be filled in with "nodata" value specified in the HEADER. Figure 2 cut the last four columns of the DATA part filled with "-999" values, due to the layout.

```
SMET 1.1 ASCII
[HEADER]
station_name     = Lia
station_id       = Lia
altitude         = 121
latitude         = 78.215400
longitude        = 15.649400
easting          = 514773.000000
northing         = 8682420.000000
epsg             = 32633
nodata           = -999
tz               = 1
fields           = timestamp TA RH TSG TSS HS VW DW OSWR ISWR ILWR PSUM TS1 TS2 TS3
units_offset     = 0 0 0 0 0 0 0 0 0 0 0 0 0 0 0
units_multiplier = 1 1 1 1 1 1 1 1 1 1 1 1 1 1 1
[DATA]
2017-11-11T17:00:00   272.404      0.755    271.846    270.464      0.000      4.805     79.690      0.188     -0.112    298.400
2017-11-11T17:05:00  -999.000   -999.000   -999.000   -999.000   -999.000   -999.000   -999.000      0.207     -0.143    298.300
2017-11-11T17:10:00   272.597      0.728    271.989    270.518   -999.000   -999.000   -999.000      0.179     -0.085    298.100
2017-11-11T17:15:00  -999.000   -999.000   -999.000   -999.000   -999.000   -999.000   -999.000      0.219     -0.152    297.700
2017-11-11T17:20:00   272.931      0.705    272.227    270.669   -999.000   -999.000   -999.000      0.006     -0.052    297.700
```

Figure 2: Example of a .SMET file

The .SNO file is slightly different, but it is also made of a HEADER and a DATA part. The HEADER contains some information, but the most important are coordinates, altitude, coordinates system (epsg), start time of the simulation (ProfileDate), slope (SlopeAngle), azimuth of the slope (SlopeAzi) and fields. The DATA contains information about an existing snowpack, namely the layers thickness, temperature, volume fraction of ice, water and vapour, etc. The software will start with this existing layers as a base, to model new snowpack above it. One has to use it, if, at the beginning of the winter, snow is still covering the area of interest. For this project, an extra input file is used, to correct data related to radiation. More information is given in Chapter 4.4.1.

2.1.2 Configuration file

The configuration file is the general guidelines for SNOWPACK, depending on the user. Necessary information as the height of wind measurement or weather data is set, but also the coordinate system, the boundary condition, etc. This configuration file allows verifying the data, using filters to remove outliers and interpolate possible missing data. One defines the name of the output, to compare results between different simulations. Here are more explanations for the boundary conditions.

Boundary conditions

This setting can be set as TRUE or FALSE. TRUE means that Dirichlet boundary condition (Equation 1) is used and FALSE indicates that Neumann boundary condition (Equation 2) is used.

Dirichlet condition:

$$Upper\ boundary\ \longrightarrow T_s = T_{ss} \tag{1}$$

$$Lower\ boundary\ \longrightarrow T_s = T_G$$

T_s is the snow temperature, T_{ss} is the snow surface temperature and T_G is the ground temperature.

In case in which only reflected shortwave and snow surface temperature are available, using Dirichlet boundary condition (TRUE) is recommended ([18]). One can also set TRUE, for cold temperature and the boundary condition will change as soon as temperature reaches a threshold (THRESH_CHANGE_BC in the configuration file). It means that Dirichlet boundary condition is used until the snow surface temperature reaches the threshold. From there, Neumann condition will be used, unless the temperature drops under the threshold again. Usually, this threshold is set to -1°C.

Neumann condition:

$$Upper\ boundary\ \longrightarrow k_s \cdot \frac{\partial T_s}{\partial z} = q_{lw} + q_{sh} + q_{lh} + q_{rr} \tag{2}$$

$$Lower\ boundary\ \longrightarrow k_s \cdot \frac{\partial T_s}{\partial z} = q_G$$

Upper boundary in Equation 2 equals k_s, the snow thermal conductivity, times the vertical temperature gradient to a sum of terms, where q_{lw} is the net longwave radiation energy, q_{sh} is the sensible heat exchange, q_{lh} is the latent heat exchange and q_{rr} is the heat flux from rain. Lower boundary is similar to upper boundary, except that on the right side there is only one term, the subsurface heat flux (Bartelt and Lehning, 2002 [15]).

In case in which incoming, outgoing shortwave and incoming longwave radiation are all appropriately measured (under ventilated and heated conditions), the best approach is to set FALSE in the configuration file. The software will use Neumann boundary condition. Regarding the energy flux calculations, it seems to be better, according to the documentation of SNOWPACK ([18]).

2.1.3 Command file

Command file is the executable file to run SNOWPACK. The one available in the example downloaded with the software is used. One has to indicate the path to the configuration file wanted and the date and time of the last simulation time step. Figure 3 shows an example of this file.

```
:: Copy and edit this file for your own simulations!
@ECHO OFF
ECHO Running Snowpack for %USERNAME% on %DATE% %TIME%

snowpack -c cfgfiles/io_operLia.ini -s Lia -e 2018-05-24T00:00
:: wait for the user to press a key before closing the window
pause
```

Figure 3: Example of a command file

2.1.4 Outputs

The software creates five outputs: .HAZ, .MET, .PRO, .SNO and a command file. The file .PRO is the most interesting, used to display the snowpack stratification, according to snow temperature, grain shape, grain size, density, liquid water content, sphericity or dendricity. For this project, the focus is on the grain shape and the temperature profile, given the data collected on the field. Profiles can be extracted for any time, to compare with snow profiles realised during winter and spring.

3 The test area

3.1 Situation of Svalbard

Svalbard is a mountainous archipelago located in the high Arctic, and its climate is defined as a polar tundra climate according to Koeppen-Geiger climate classification (Kottek and al., 2006 [19]). The temperatures are freezing during winter, and the annual precipitation is low (200 mm water equivalent [21]). Only during a few months, the temperatures are positive (Eckerstorfer and Christiansen, 2011 [20]). Nevertheless, the climate is less extreme than for other locations at a similar latitude. The mean annual air temperature in 2009, equal to -3.8°C [21], was consequently warmer than other weather stations situated in the high Arctic (between latitude 70° and 82°). For those stations, the mean annual air temperature reaches a range between -9°C and -15°C (Eckerstorfer and Christiansen, 2011 [20]), like Eureka in the high Canadian Arctic. First, the influence of the warm Norwegian current that flows along the west coast of Svalbard and second the location of Svalbard in the main North Atlantic cyclone track make the climate warmer. However, Eckerstorfer and Christiansen (2011, [20]) assume that the snowpack in Svalbard and other high Arctic locations are comparable, with dissimilarities due to warmer temperatures, like rain-on-snow event (Hansen and al. 2014, [22]). According to Humlum (2002, [23]), high fluctuations of air temperature on a daily or weekly basis are typical during winter in Svalbard.

Snow distribution in Svalbard is very heterogeneous. Some places are entirely snow-free on wind exposed slopes, and other places have a thick snowpack, where the wind accumulates snow on lee slopes (Jaedicke and Gauer, 2005 [24]). At the snowpack base, it is widespread to have a layer made of depth hoar. In a research conducted by Eckerstorfer and Christiansen (2010, [20]), 81% of 109 snow pits realised during two snow seasons (2007/2008 and 2008/2009) were constituted with a 10 centimetres depth hoar layer on average at the base. Depth hoar accumulates during autumn and early winter, because of the slow onset of snow cover. Thus, the temperature gradients are great and enable kinetic metamorphism. Later in winter, when the snowpack is thicker after several snowfalls, large temperature gradients still exist in the snowpack, but its base ($\simeq$ 40 centimetres) stays more or less isothermal in contrast to the upper part. One can expect rain crusts due to warm events when rain occurs and percolates through the snowpack until it refreezes on the subzero ice lattice. Close to these ice masses, faceted crystals can often be observed, as ice is relatively impermeable to vapour transport (McClung and Schaerer, 2006 [25]). Thus, near-crust faceting occurs. Rounded grains are mostly the result of the wind in the slab. Almost no destructive metamorphism occurs in comparison with constructive metamorphism, which is much more significant (Eckerstorfer and Christiansen, 2010 [20]).

One can compare the snowpack between Svalbard and Alert, a Canadian scientific station located in the high Arctic, at a latitude of 82°. According to Dominé and al. (2002, [26]), the snowpack has a thickness from 10 to 50 centimetres, and it consists mainly of a depth hoar base layer covered by one or more wind-packed layers. They can be separated by softer layers, made of faceted crystals.

3.2 Weather stations

For this project, five weather stations are used mainly located around the settlement of Longyearbyen: three snow stations, one wind station and one station, which measures the radiation. The region is not equipped with weather stations like the ones used in IMIS[4] network in Switzerland, as explained on the SLF website [27]. These stations are perfectly adapted to the software SNOWPACK, which means every input required for the model are measured at every location. In Svalbard, the stations used do not measure every input required. Data from different stations, which means different locations are used for one simulation. To ensure the best quality, data processing is then mandatory to get data the closest possible to reality. That was one of the main challenges of this project. The processing also allows verifying the data and export graphs to have a better understanding of simulation results. Figure 4 shows the locations of every station and few landmarks around the settlement of Longyearbyen.

---

[4]Intercantonal Measurement and Information System

Figure 4: Map of weather stations with geographical landmarks

3.2.1 Snow stations

Three snow stations are distributed around Longyearbyen strategically placed. As shown in Figure 4, one station is located in Lia, one in Nybyen and the last one in Sverdruphamaren. These stations measure five of the most important inputs to run the model: snow depth, relative humidity, ground temperature, snow surface temperature and air temperature. Data are recorded every ten minutes. As the aim of the project is to model the snowpack at those specific locations, no data processing is needed, except when data is missing and snow depth correction at the beginning of winter. For example, at the end of March, the station in Nybyen was out of order for two days. It will be explained how the missing data were filled below. It is important to notice that Lia station is located on the slope, where an avalanche was triggered naturally in 2015 and has destroyed 11 houses.

The snow depth is measured with an ultrasonic device. Knowing the height between the device and the ground, the instrument measures the distance separating the top of the snowpack and the device itself, $h_{measured}$. A correction factor, k, is applied according to air temperature, as the speed of sound varies with temperature. This corrected height is subtracted from the initial height, h_0, which is the distance from the ground to the device, to get the final snow depth, h_{snow}. Relevant information is that the depth is measured perpendicularly to the horizontal and not perpendicularly to the slope. Equation 3 shows how to get the correct snow depth.

$$h_{snow} = h_0 - h_{measured} \cdot k \tag{3}$$

An infrared camera measures the snow surface temperature. A thermometer measures merely the ground and air temperature. For every measurement, except for ground temperature, the instruments have to be high enough not to be covered by snow. The stations are powered by a battery, rechargeable by a solar panel.

Figure 5: Slope next to Lia station, above the settlement Longyearbyen

Figure 6: Slope where Nybyen station is, located above the small settlement of Nybyen

3.2.2 Radiation station

The next station used for this project is the one located in Adventdalen as presented in Figure 4, east of Longyearbyen. Despite the distance between snow and radiation stations (up to 6 kilometres [28]), this is the only option available to get radiation data. This station recorded data every five minutes. Radiation data required for SNOWPACK are incoming shortwave radiation, outgoing shortwave radiation and incoming longwave radiation. Incoming shortwave radiation is the energy received from the sun, although outgoing shortwave radiation is the reflected fraction of incoming shortwave on the snow. Incoming longwave is the energy received by the snowpack from the atmosphere depending on its temperature and humidity, and so cloud cover. Taking into account the different locations and aspects of the stations, shortwave radiation data has to be processed. In Chapter 4.4.1, it will be explained the way to correct it.

3.2.3 Wind station

The last station used is measuring the wind speed close to the city. It is located in Gruvefjellet as shown in Figure 4. An anemometer measures the wind speed at 3.5 metres high. The station also recorded the wind direction. Data from this station are recorded every hour; this is the reason why the average is used.

Taking into account that this station is located at the top of a plateau, a correction has to be applied to data to fit reality. A sensitivity analysis is developed in Chapter 6.5, to understand the impact of the wind. First, only a percentage is applied as a correction for the entire data set. The wind speeds occurring in the snow stations should follow the same trend as the wind station; there are no major obstacles and the slope are quite homogeneous. The main difference is that the snow stations are protected from winds coming from the opposite direction of the slope orientation. Furthermore, looking at the distances between the stations, wind patterns have to be similar. In fact, the maximum distance is between Lia station and Gruvefjellet station, reaching 1.5 kilometres [28].

As explained above, the wind station also measured the wind direction. It is thereby possible to apply another correction method. Looking at the orientation of the stations, different corrections are applied to wind speed according to wind direction. In fact, the snowpack in the wind station is altered by wind from every direction, as it is at the top of a plateau, and this is not the case for snow stations. The exact way of doing it is developed below in Chapter 4.5.2.

4   Data and methods

Every data is processed with Matlab, and all plots are created with this software. As the different stations do not record the data at the same time step, Matlab was also used to create tables for every input of same length with "nodata" value. The management of time step is essential for SNOWPACK, to work properly.

4.1   Lia station

Lia station was set up on the 11th of November 2017. Unfortunately, the station had to be removed on the 5th of June 2018. It was located where new fences were going to be built, to prevent avalanches to be triggered. Looking at Figure 5 and 8, one can easily imagine that if an avalanche is triggered on this slope, it reaches the town. As a reminder, a slope with a steepness more than 30° can be triggered. As shown in Figure 7, this slope is 32° steep. As works were realised in the area, data are used until the 24th of May 2018. After that, data for snow depth shows gaps made by workers. In the following subsections, data from the 11th of November 2017 until 24th of May 2018 are presented.

Name	Lia
Coordinates north WGS84	78.2154 °
Coordinates east WGS84	15.6499°
Coordinates north UTM Zone 33N	8682420
Coordinates east UTM Zone 33N	514773
Altitude	121 [m]
Slope	32°
Aspect	315°

Figure 7: Information about Lia snow station

Figure 8: Snow station of Lia

4.1.1   Temperature

Figure 9 shows different temperatures needed for the model, specifically air temperature, snow surface temperature and ground temperature. The first observation is their amplitude. In a few days, air temperature can raise from -15°C to 4°C. The same observation is valid for snow surface temperature, with gaps even more significant from -22°C to 0°C at the beginning of February. Snow surface temperature is most of the time colder than air temperature, meaning that the weather should be clear. Unfortunately, data of cloud cover is not available for Svalbard. Nevertheless, looking at Figure 10, one can say when precipitation occurs, air temperature and snow surface temperature are close, due to a cloudy sky. Regarding the ground, it seems logical that its temperature has far less variance, as snow acts as an insulator. From the 20th of November until the beginning of May, ground temperature is quite constant between -5°C to -2°C. Before that, ground temperature was quite similar to air and snow surface temperature, which means there was no snow during that period. Looking more closely to air temperature after November 20th, one can see several events with a temperature higher than 0°C, at least eight major events without the late events during spring. According to Rennert and al. (2009, [29]), these warm and extreme events are likely to become more and more frequent in the Arctic. Ground temperature almost reaches the melting/freezing point on the 18th of January. The extended warm event up to 4 days with a temperature reaching 4.9°C explains it. Relevant information that one might forget is the polar night in Svalbard. The sun is below the horizon from the 26th of October until the 15th of February in Longyearbyen [30]. Regarding this unexpected warm event, the sun is not responsible for it. The global warming is the explanation, as the climate change causes extreme weather events, such as heat waves or heavy rainfall (Hansen and al. 2014, [22]). According to Førland and al. (2011, [31], the effect of climate change is amplified in the Arctic land. Different reasons could explain this over-warming compared to other regions on Earth. Loss of sea ice, changes in atmospheric and oceanic

circulation or a combination of the two are some of them. Moreover, identify and understand these extreme phenomena is one of the most challenging topics in the actual climate research (Stocker and al. 2013, [32]).
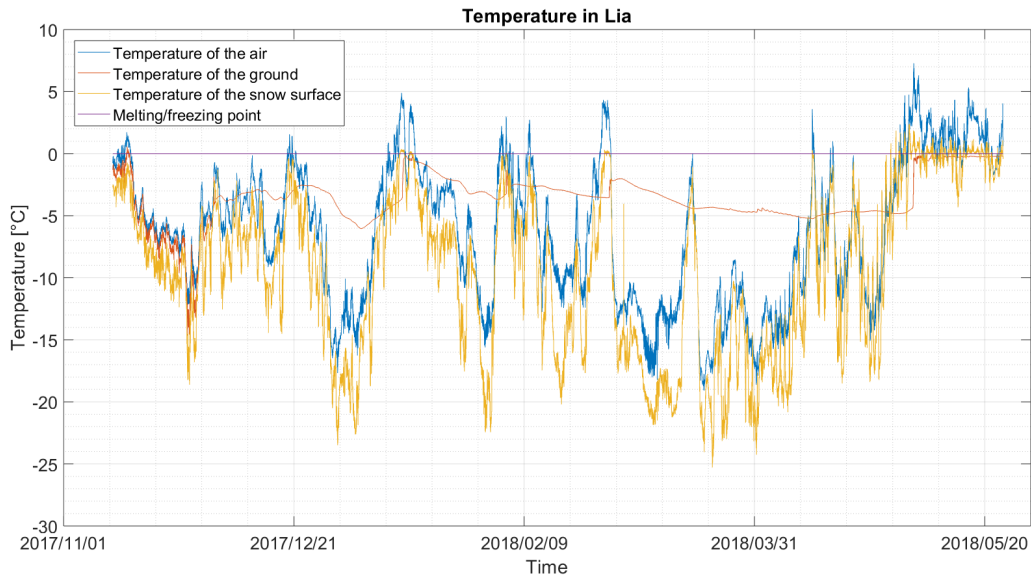
Figure 9: Air temperature, ground temperature and snow surface temperature in Lia from the 11th of November to the 24th of May

4.1.2 Precipitation

Regarding precipitation, these data have to be handled carefully. In fact, the measurements are recorded every 12 hours in Adventdalen, at the same location than radiation station, shown in Figure 4. On the one hand, the purpose of this subsection is to know if precipitation coincides with a warm event. Knowing if it rained or not is useful for results interpretation. On the other hand, snowfall can also be identified. Looking at the event type, these data are interesting, but the quantity is irrelevant as the location is not the same as the snow station. Furthermore, the time step between two records is far too long, and data may include significant errors, taking into account the wind, the water phase (solid or liquid) and the difficulty to get proper precipitation data. Figure 10 represents potential solid or liquid precipitation, using air temperature prevailing in Lia station and precipitation recorded in Adventdalen station. The limit set between snow and rain is 0°C. Thus, the worse situation is considered, as it usually can snow with temperatures up to 2-3°C (Dai, 2008 [35]).

However, three main rainfalls can be identified on the 13th of January, 26th to 27th of February and 12th of April. They will have a significant impact on the snowpack layering. As explained by Rennert and al. (2009, [29]) and Stimberis and Rubin (2011, [34]), these events are called rain-on-snow events (ROS).
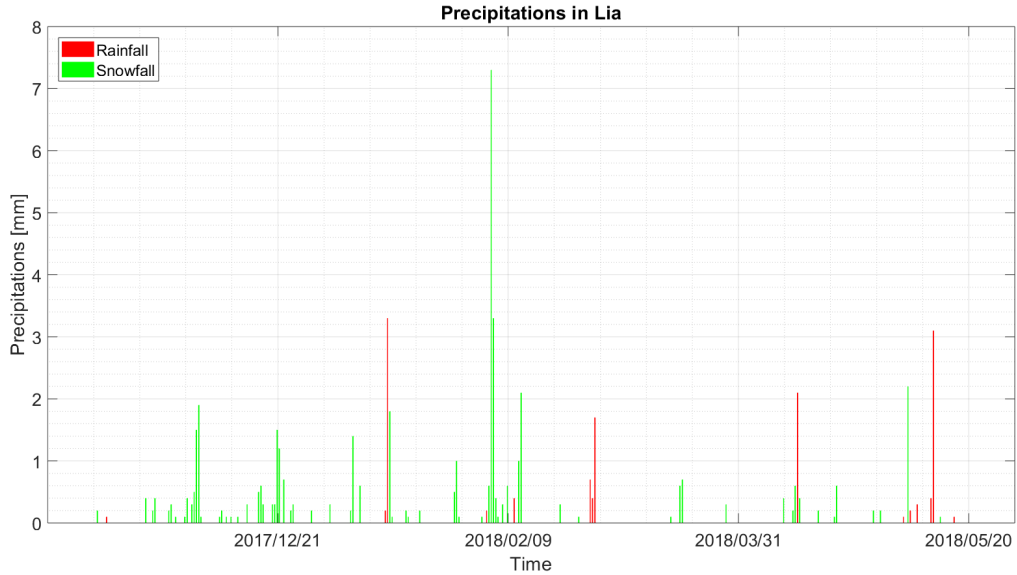
Figure 10: Accumulated precipitation in Adventdalen with air temperature prevailing in Lia from the 11th of November to the 24th of May. The threshold between snow and rain is set to $0°C$. Source `eklima.met.no`

4.1.3 Snow depth

One of the essential inputs for SNOWPACK is the snow depth. The measurements obtained by the station in Lia are presented in Figure 11. The upper plot represents raw data. Some processing is mandatory to get proper data. Even if SNOWPACK has a set of modules, called MeteoIO, which is supposed to handle and filter data, processing with Matlab is still necessary. At the beginning of the winter, snow depth data are very noisy because of the ultrasonic device, which is not accurate with low depth. Besides, it is not obvious when the first snowfall occurs. To clean the data, ground and air temperatures are used. Before they differ, snow depth is set to 0. Looking at Figure 9, one can see that it happens on the 20th of November. Thus, no snow is considered before this date, and it was easier to do it with Matlab.

The initial height from Equation 3, h_0, is given by the all the maximum values in raw data, as measured depth, $h_{measured}$ at those times is equal to 0. One find for h_0 310 centimetres above the ground. This information is required in the configuration file, like the height of meteorological values. To clean the data, there is an offset to remove that is established by comparing data and measurements on the field, equivalent to 25 centimetres. Then, all outliers are removed, namely all negative data and data above two metres. To clean the rest of the data, more manual processing is required to get proper data, usable by SNOWPACK. MeteoIO could clean it, but it has been decided to process everything with Matlab. Figure 10, the different increases or decreases coincide with rainfalls or snowfalls. Still, some increases of snow depth are lagged compared to the actual snowfall. It is due to snow redistribution by wind. Wind erosion can also explain some decreases.
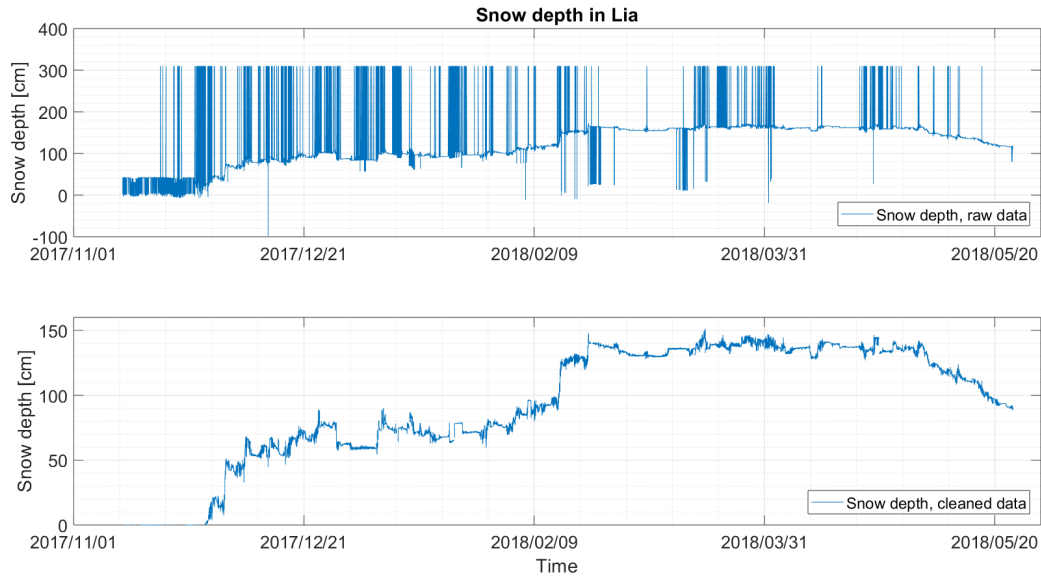
Figure 11: Snow depth in Lia from the 11th of November to the 24th of May. Upper graph represents raw data, lower graph represents processed data

4.1.4 Relative humidity

There is not a lot to say about relative humidity presented in Figure 12, except for the fact that the variance is significant. One can also observe that the values vary very fast. It can drop to 35 % to 100 % in just one day. Precipitation should occur when relative humidity is high, which is the case, looking at Figures 10 and 12.
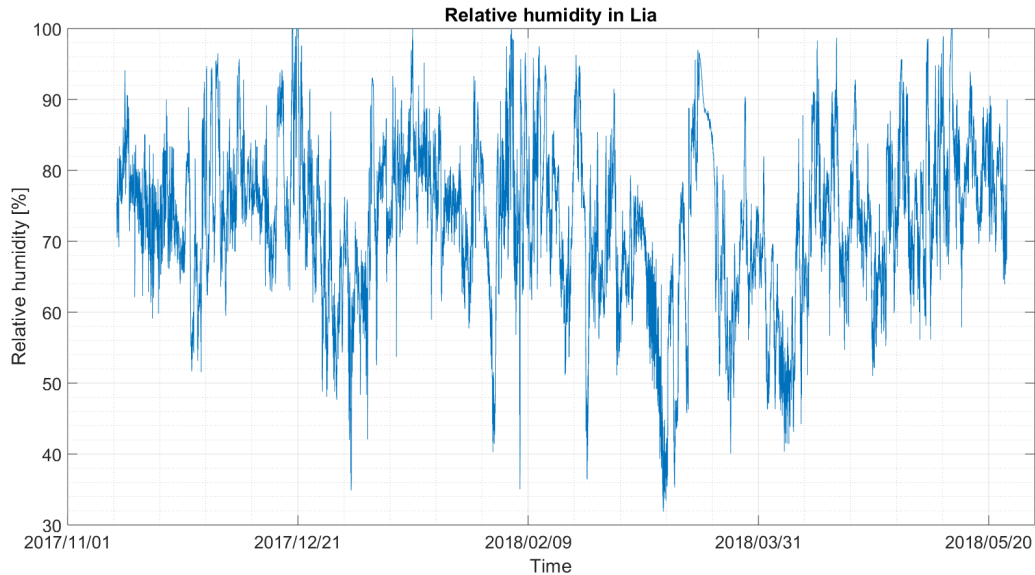
Figure 12: Relative humidity in Lia from the 11th of November to the 24th of May

4.2 Nybyen station

Nybyen station was set up on the 8th of November. It is located above the small settlement of Nybyen in steep terrain, topped by a ridge where quite large cornices form. Looking at Figures 6 and 14, it is evident that several buildings might be endangered if an avalanche is triggered in this slope. Steeper than Lia station, the slope is 34° steep (Figure 13). At the end of March, the station was out of order for two days. The following subsections explain how missing data are completed, and they present data from the 8th of November until the 21th of May.

Name	Nybyen
Coordinates north WGS84	78.1991 °
Coordinates east WGS84	15.6090°
Coordinates north UTM Zone 33N	8680690
Coordinates east UTM Zone 33N	513896
Altitude	352 [m]
Slope	34°
Aspect	300°

Figure 13: Information about Nybyen snow station

Figure 14: Snow station of Nybyen

4.2.1 Temperature

In Figure 15, temperatures for Nybyen station are presented, to know air temperature, ground temperature and snow surface temperature. The same observations as those made for Lia station are feasible. In general, temperatures are colder in Nybyen than in Lia. It is merely due to the altitude, 352 metres for Nybyen versus 121 metres for Lia, as presented in Figures 7 and 13. Figure 15 shows only two warm events during winter.
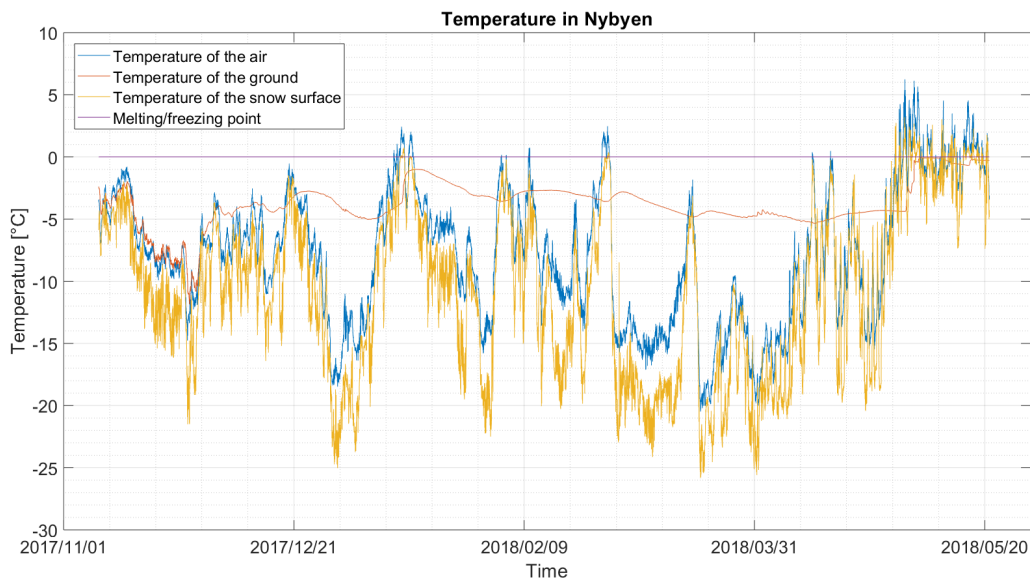
Figure 15: Air temperature, ground temperature and snow surface temperature in Nybyen from the 8th of November to the 21th of May

Data from Lia are used to fill in missing data when the station was out of order. Looking at the temperature before and after the breakdown in both stations, Lia and Nybyen, one can adjust data from Lia to fit Nybyen station. For air temperature, an offset of -1 degree is applied. No modification is needed for ground temperature and snow surface temperature since there is only a very slight difference with Lia.

4.2.2 Precipitation

As explained above, Figure 16 has to be handled carefully, showing the potential precipitation in Nybyen. Only the event type is relevant, either rain or snow. Two rainfalls are significant, on the 13th of January and the 26th of February. It will modify the snowpack considerably at those dates.
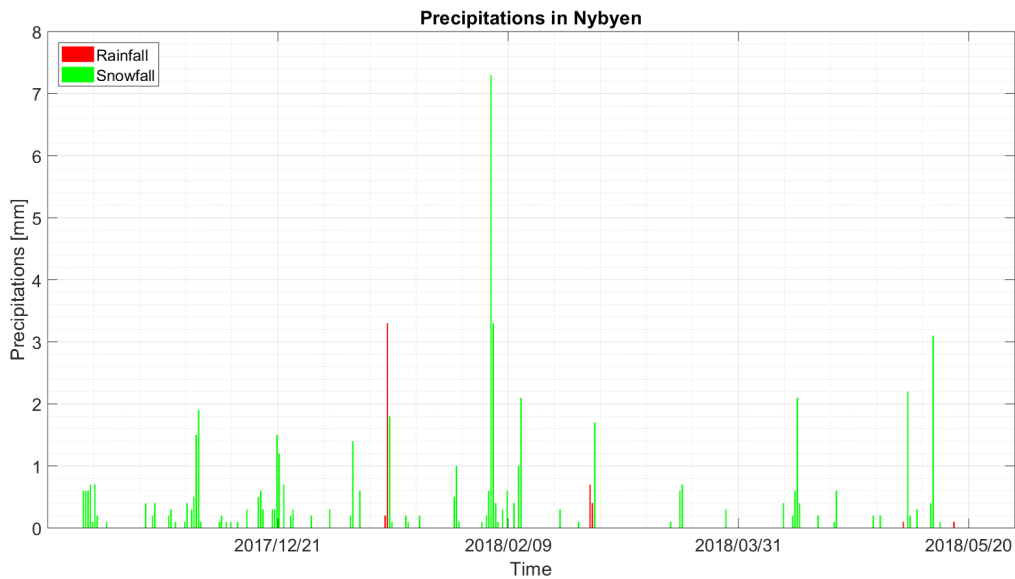
Figure 16: Accumulated precipitation in Adventdalen with air temperature prevailing in Nybyen from the 8th of November to the 24th of May. The threshold between snow and rain is set to $0°$C. Source `eklima.met.no`

4.2.3 Snow depth

Figure 17 represents both raw data and cleaned data. Processing is also mandatory to get usable data. The initial height described in Equation 3, h_0, is equal to 230 centimetres above the ground. Again, the outliers are removed and every data above 210 centimetres and below zero as well. The same method as explained above is used. Looking at Figure 16 previously presented, one can see that increases in depth are correlated with precipitation and sometimes correlated with a time lag due to snow redistribution by wind. The same process is valid for snow erosion.
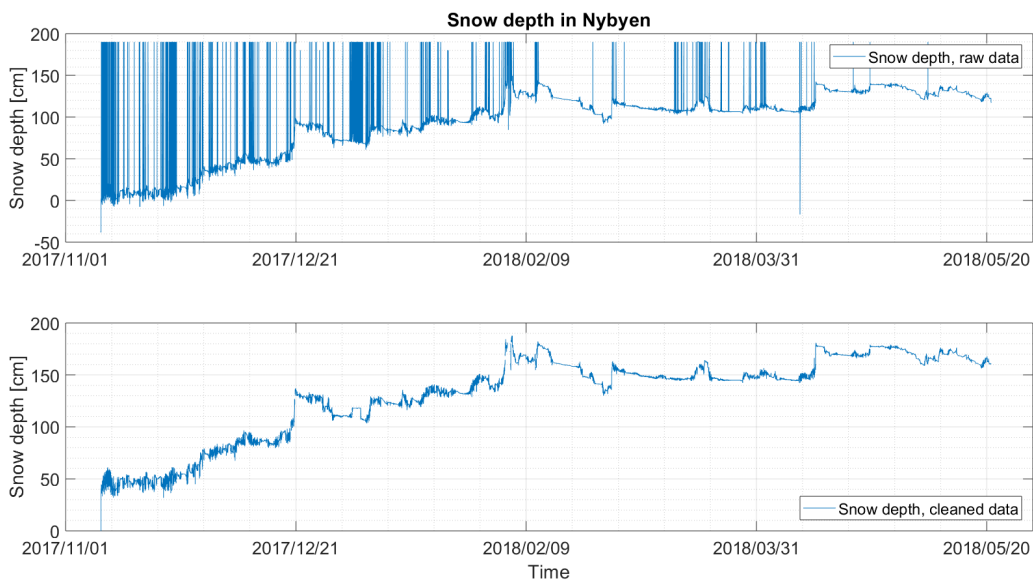
Figure 17: Snow depth in Nybyen from the 8th of November to the 21th of May. Upper graph represents raw data, lower graph represents processed data

Fortunately, no precipitation occurs during the period when the station was out of order. A constant is used to fill in the gap, which makes sense with the value before and after the breakdown.

4.2.4 Relative humidity

Figure 18 represents relative humidity measured in Nybyen, with significant variations. Looking at Figures 16 and 18, precipitation and high relative humidity events coincide. In fact, relative humidity is close to 100 % when precipitation occurs. To fill the missing data, Lia station is used, finding no other method. However, it is not wrong to use these data, as only two kilometres separates the stations [28].
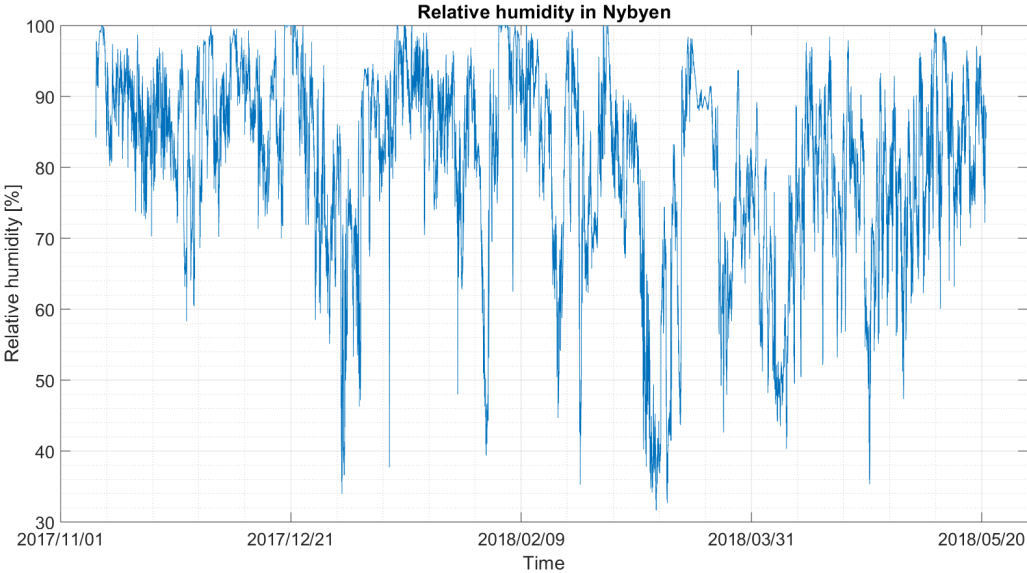
Figure 18: Relative humidity in Nybyen from the 8th of November to the 21th of May

4.3 Sverdruphamaren station

The last snow station used is located close to Sverdruphamaren, a prominent plateau, southwest of Longyearbyen. The station is in a 39° slope, as shown in Figure 19. Its access is complicated, and it is not possible to go there at any time, to dig a snowpit for example (Figure 20). The interesting point with this station is its orientation. Regarding Lia and Nybyen stations, their orientations are towards northwest, although the station in Sverdruphamaren is facing east. However, data presented below show some issues. It seems that the station was not working correctly, especially the ultrasonic device measuring snow depth (Figure 23). In addition, as only one snowpit is available for comparing with the model, everything related to Sverdruphamaren station is not as relevant as the two other stations, Lia and Nybyen. The station was set on the 12th of November. In the following subsections, data from the 12th of November until the 16th of May are presented.

Name	Sverdrup-hamaren
Coordinates north WGS84	78.2102 °
Coordinates east WGS84	15.5665°
Coordinates north UTM Zone 33N	8681896
Coordinates east UTM Zone 33N	512923
Altitude	450 [m]
Slope	39°
Aspect	90°

Figure 19: Information about Sverdruphamaren snow station

Figure 20: Snow station of Sverdruphamaren

4.3.1 Temperature

Temperatures in Sverdruphamaren, presented in Figure 21, are similar to temperatures in Nybyen. In general, air temperature is a bit colder, due to the altitude of 450 metres, which is about 100 metres higher than Nybyen. Only two small warm events are notable, without those of May. Looking at ground temperature, it is much colder than the one measured in Nybyen. The snow depth in Sverdruphamaren (Figure 23) is less thick than in Nybyen, which means less insulation. Thus, the ground is colder.
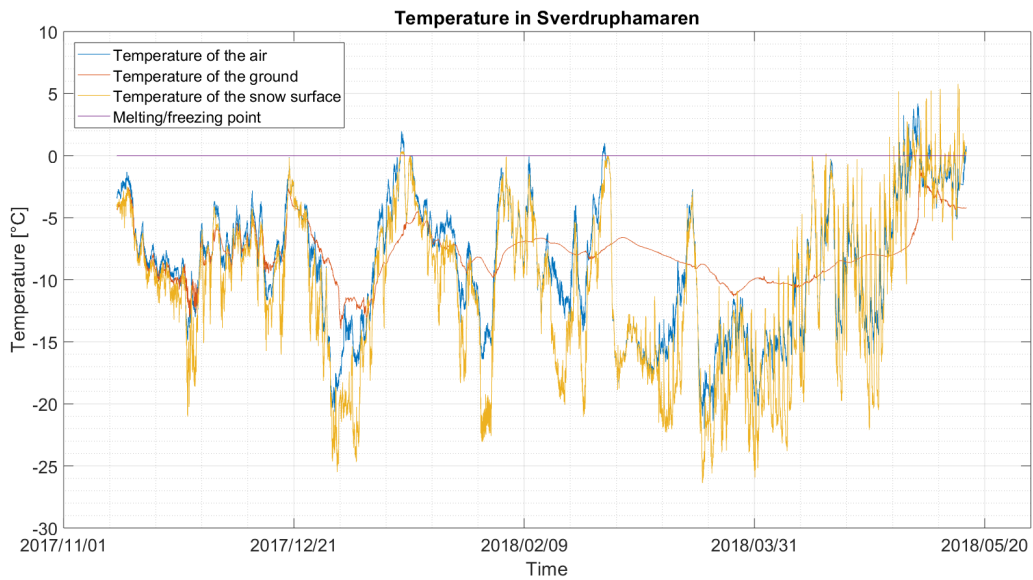
Figure 21: Air temperature, ground temperature and snow surface temperature in Sverdruphamaren from the 12th of November to the 16th of May

4.3.2 Precipitation

Looking at the precipitation type shown in Figure 22 and not at the quantity, no rainfall has occurred in Sverdruphamaren from the 12th of November until the 16th of May.
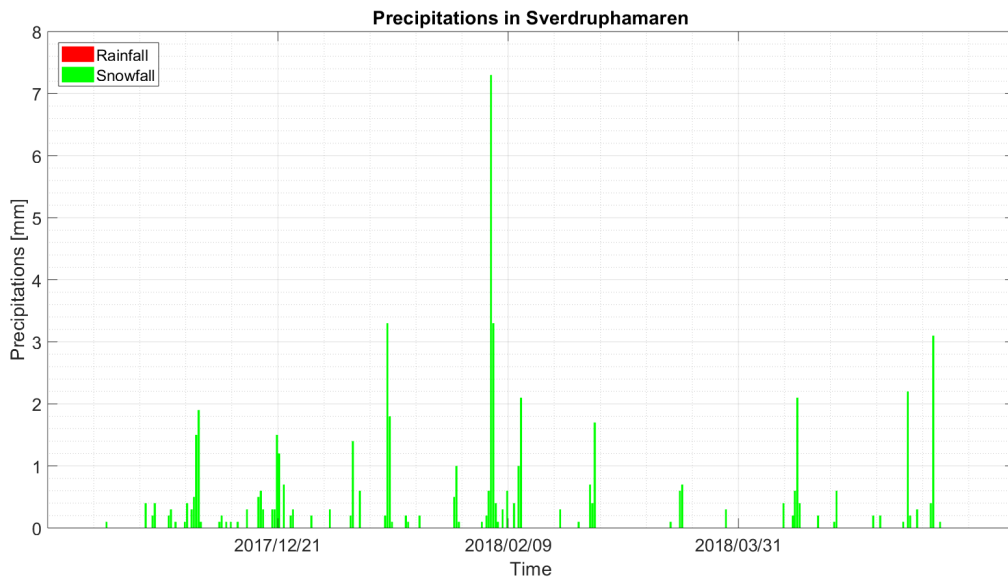
Figure 22: Accumulated precipitation in Adventdalen with air temperature prevailing in Sverdruphamaren from the 12th of November to the 24th of May. The threshold between snow and rain is set to 0°C. Source `eklima.met.no`

4.3.3 Snow depth

In Figure 23, raw snow depth and processed data are presented. The same methodology than explained above is used. The first observation one can make, is the small amount of snow in this area. Even if this station is situated at the highest altitude in comparison with the other two, the snow depth reaches barely 80 centimetres. One can easily understand that the wind is responsible for that. Until the massive snowfall that took place on the 5th of February, less than 20 centimetres were recorded at this station. After this main event, a lot of snow accumulates, probably due to wind coming from the southwest. Knowing that the station is facing east (Figure 19), one can understand the significant snow accumulation. Indeed, the average wind was equal to 18 m/s during this period. The snowpack depth rises to 60 centimetres. Thus, the wind plays a primary role for this station. The processing for snow depth data is the same than the two other, but smoothing was needed, to reduce noise.
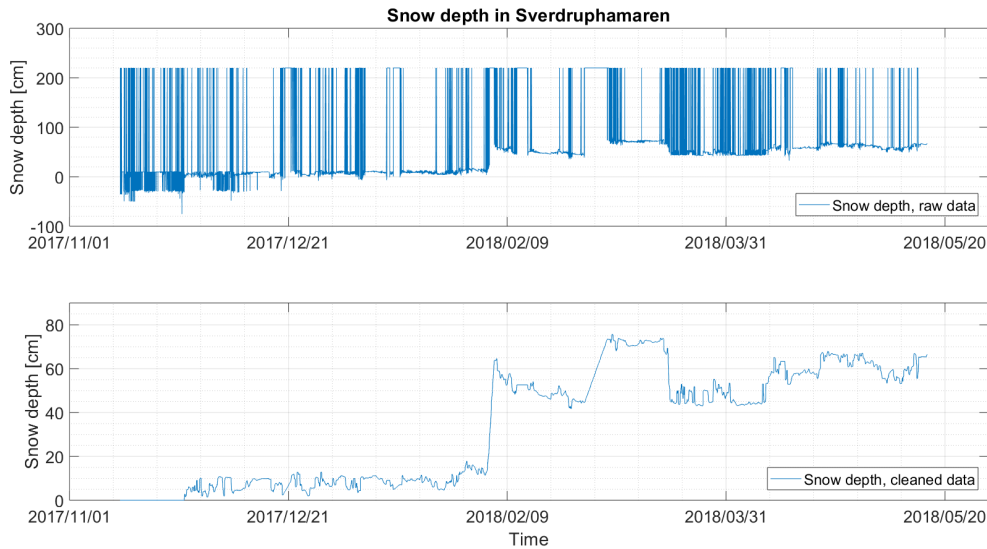
Figure 23: Snow depth in Sverdruphamaren from the 12th of November to the 16th of May. Upper graph represents raw data, lower graph represents processed data

4.3.4 Relative humidity

Relative humidity for Sverdruphamaren is shown in Figure 24. Even if the distance between the station, which recorded the precipitation (Adventdalen station), and Sverdruphamaren station is considerable (6 kilometres), precipitation and relative humidity stay correlated, as one can see in Figures 22 and 24.
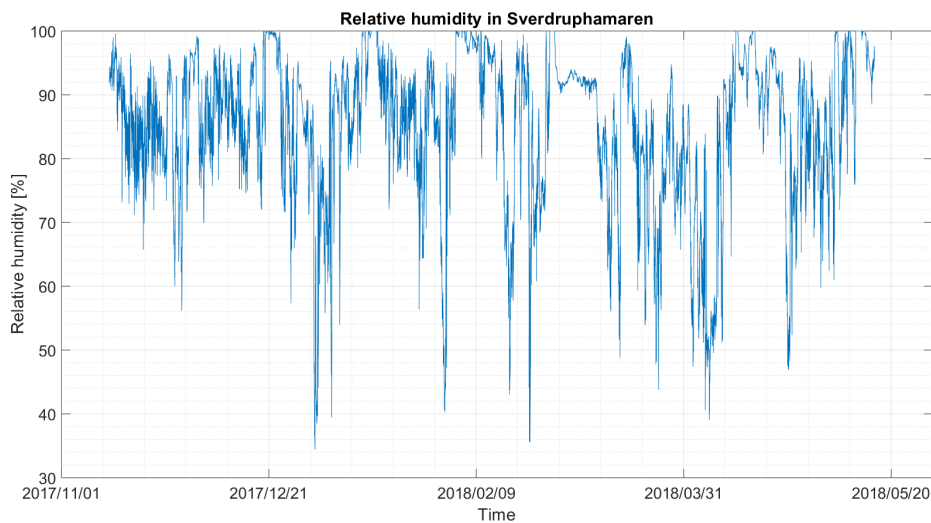
Figure 24: Relative humidity in Sverdruphamaren from the 12th of November to the 16th of May

4.4 Radiation data

4.4.1 Shortwave radiation

Incoming and outgoing shortwave radiation are presented in Figure 25. Until the end of the polar night (i.e. 15th of February), the values for both incoming and outgoing shortwave are null. After this date, it increases linearly until the 20th of April, five days after the beginning of the polar day. Afterwards, the average seems to be constant, depending on cloud cover.
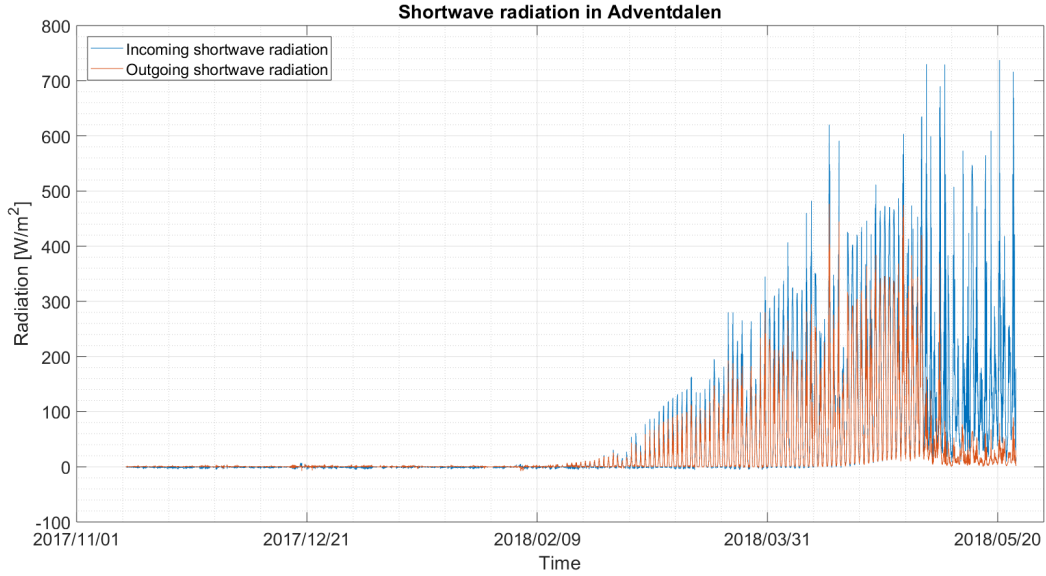
Figure 25: Incoming and outgoing shortwave radiation in Adventdalen from the 8th of November to the 24th of May

At the end of the considered period, outgoing shortwave radiation present issues from the 2nd of May. The explanation is straightforward: no more snow covers the ground in Adventdalen. Thus, a correction has to be applied. Albedo is calculated and shown in Figure 26. The start date for this plot is February 15th, the date on which the polar night ends. In the beginning, the values of incoming and outgoing shortwave are so small, that the albedo is irrelevant. Since it seems to be valid, from the 25th of February to the 2nd of May, the mean is computed and is equal to 0.74. This value is used to correct outgoing shortwave radiation from the 2nd of May until the dataset end, which is the 24th of May, with Equation 4.

$$Albedo = \frac{Outgoing\ shortwave}{Incoming\ shortwave} \implies Outgoing\ shortwave = Albedo \cdot Incoming\ shortwave \qquad (4)$$

The upper graph in Figure 27 represents raw data, and the lower graph shows corrected data for shortwave radiation. Even if the correction is simplistically, one can see that corrected data are suitable compared to data before the 2nd of May. A comparison of results is conducted in Chapter 6 with and without correction.
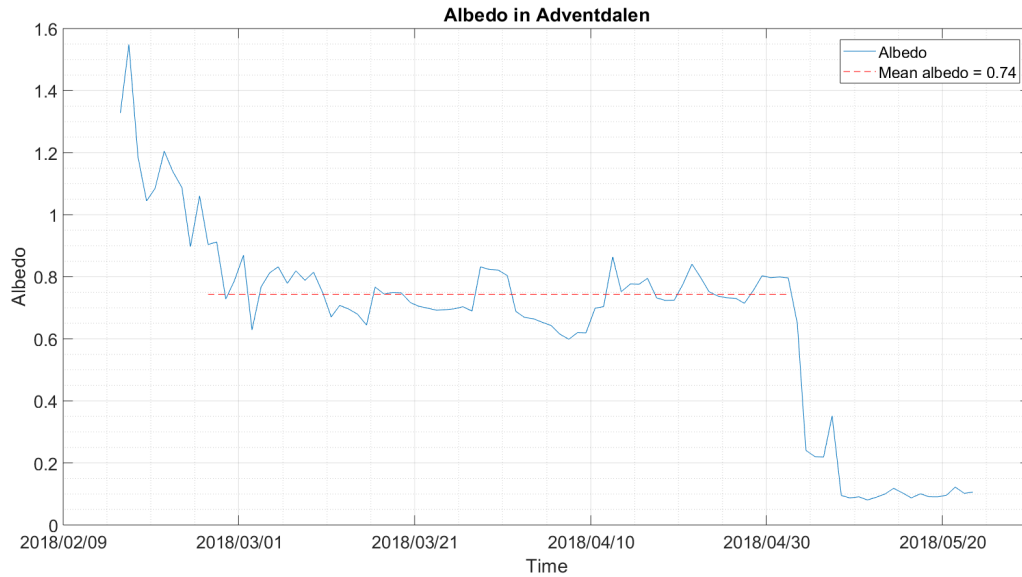
Figure 26: Albedo in Adventdalen from the 15th of February to the 24th of May at 11:30
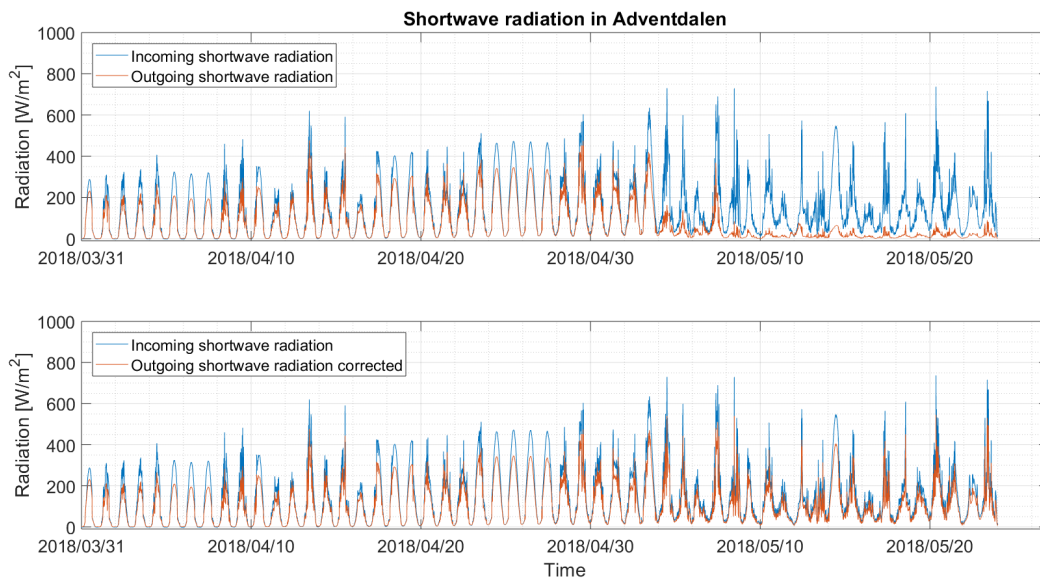
Figure 27: Incoming and outgoing shortwave radiation in Adventdalen from the 31th of March to the 24th of May. Upper graph represents raw data, lower graph represents corrected data

Another aspect to take into account linked with shortwave radiation is the difference of topography for every station. Shortwave radiation in Adventdalen situated in a large valley is not the same as for snow stations situated on steep slopes. From ArcGIS, one can extract the horizon seen from every snow stations location. Then, with MeteoIO, these horizons are used as masks to produce the right amount of shading. They are integrated into the model to simulate the relief. The mask file is a two-column text file including in the first column the azimuth (every degree, from the north, clockwise) and the elevation angle from the ground in the second column. In Figure 28 to 33, the horizon created with ArcGIS are presented from the different snow stations. The left column is the horizon on a plane, and the right column represents the hemispherical view.
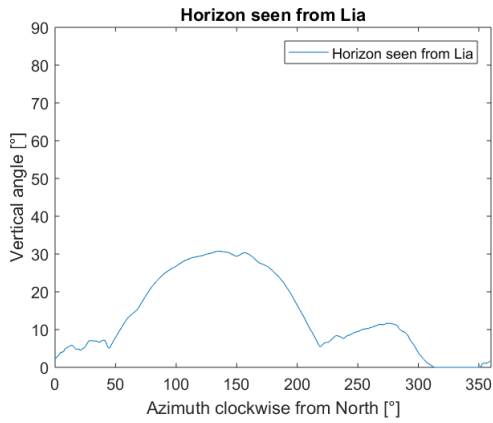
Figure 28: Horizon seen from Lia station
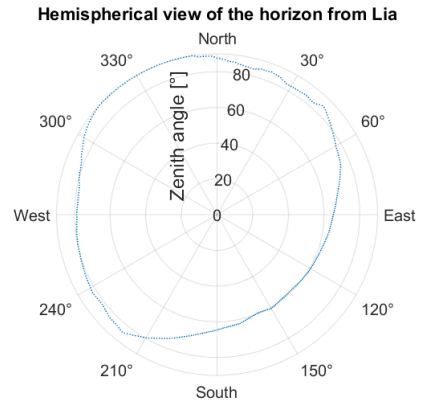
Figure 29: Hemispherical view from Lia station
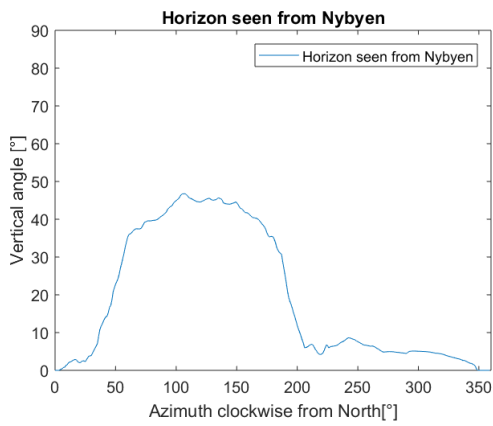
Figure 30: Horizon seen from Nybyen station
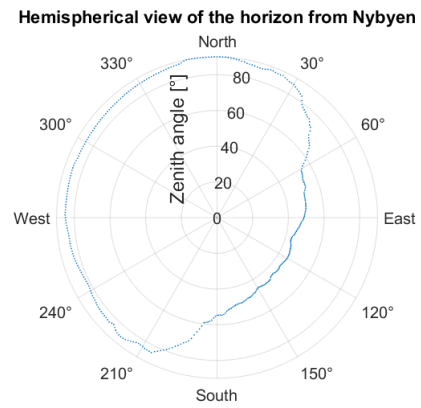
Figure 31: Hemispherical view from Nybyen station
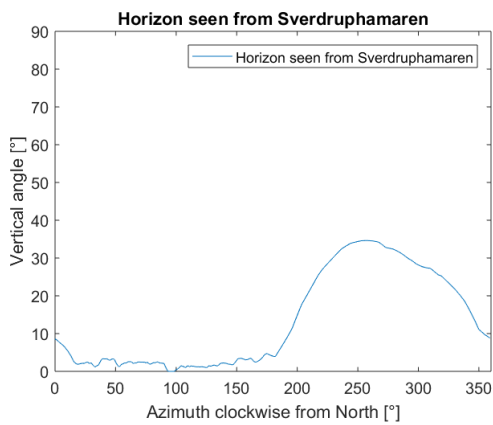
Figure 32: Horizon seen from Sverdruphamaren station
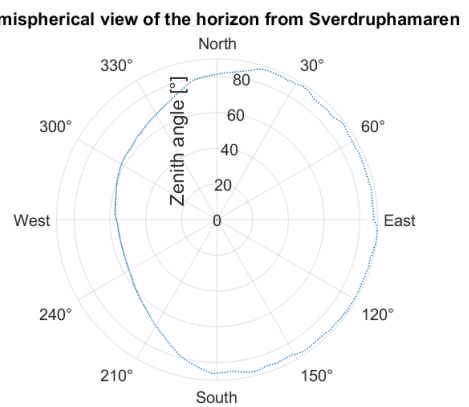
Figure 33: Hemispherical view from Sverdruphamaren station

4.4.2 Longwave radiation

Incoming longwave radiation is shown in Figure 34. The atmosphere emits longwave radiation, and they are positively correlated with cloud cover as well as humidity. Looking at precipitation presented in Figure 10, one can say that they coincide with periods with high incoming longwave radiation. Low longwave radiation means clear sky and good weather as it was the case during most of March and April, unlike May, when the sky was mostly cloudy. Even if the measurements are not taken at the same location as snow stations, these data are used in a raw way. Relatively low distances between the stations would not affect that much the values.
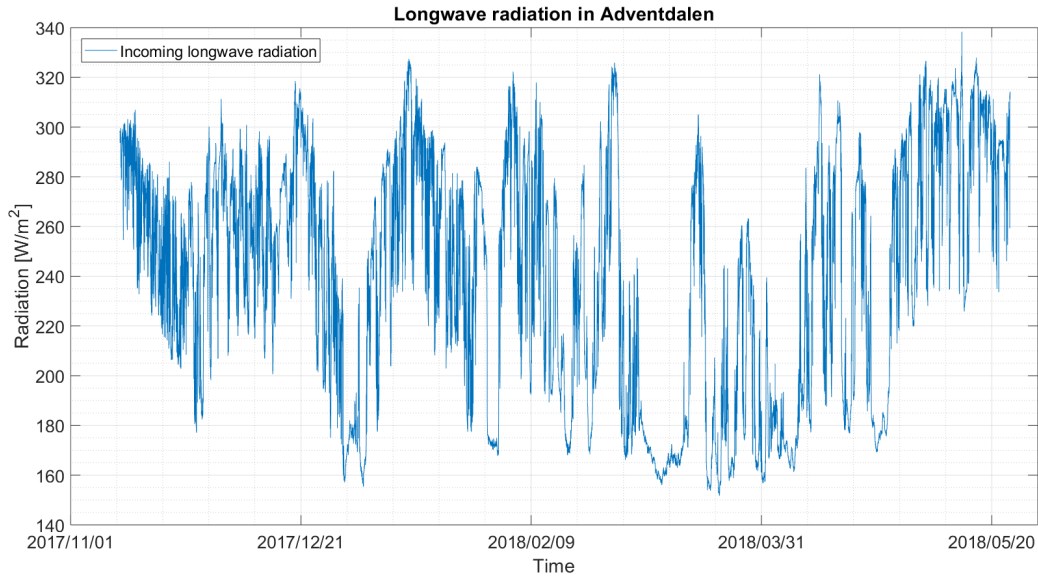
Figure 34: Incoming longwave radiation in Adventdalen from the 8th of November to the 24th of May

4.5 Wind data

4.5.1 Wind speed

Figure 35 represents wind speed during the considered period. Variations are very fast, with a maximum wind speed of 18 $\left[\frac{m}{s}\right]$. As a reminder, every data is the hourly average. One can also say, that wind is almost omnipresent. The wind is one of the leading actors regarding the snowpack stratification. In fact, the wind impacts only on top layers (10 to 20 centimetres). Still, the layers created can remain until the end of snow season.
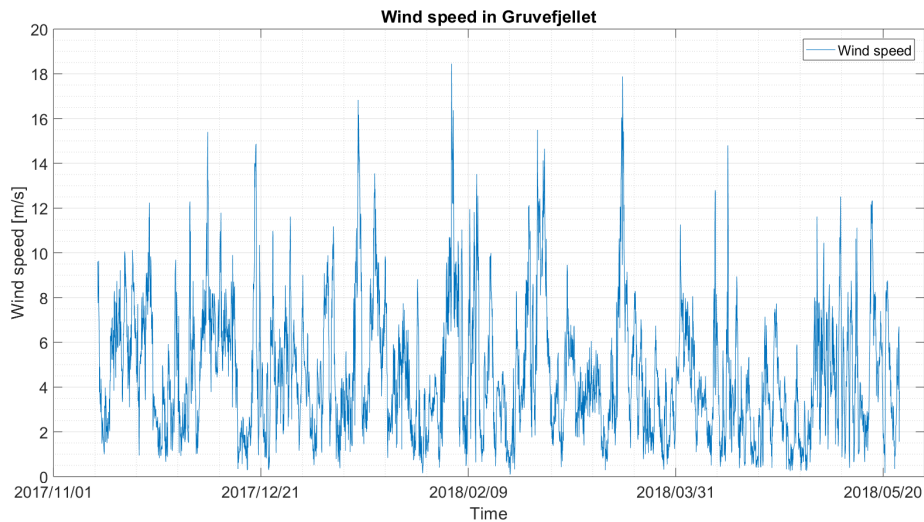
Figure 35: Wind speed in Gruvefjellet from the 8th of November to the 24th of May

Figure 35 shows raw data in Gruvefjellet. As explained above (Chapter 3.2.3), data need corrections because of the topography between the wind station and the three snow stations. Their situation, considerably different from each other, require a sensitivity analysis, to observe changes undergone by the snowpack. First, corrections are applied to wind coming from every direction. A sensitivity analysis is made in Chapter 6.5 with correcting factors from 25 % to 100 % every 25 %. Afterwards, according to the aspect and the location of every snow stations, specific correcting factors are used in function of wind direction.

4.5.2 Wind direction

Figure 36 presents the wind direction. This Figure is useful for results interpretation, to know when the wind is blowing in a specific direction. Wind speed is shown according to wind direction in Figure 37, which is more useful to establish the correcting factors. Often wind comes from west, southwest and south up to $5 \frac{m}{s}$, but the strongest and most predominant winds come from east or southeast up to $10 \frac{m}{s}$. At least, these observations are valid for most points represented in Figure 37. Occasionally, strong winds up to $15 \frac{m}{s}$ blow from southwest, south and east. Winds from north are less frequent and weaker, although winds up to $10 \frac{m}{s}$ can come from east-northeast and west-northwest.
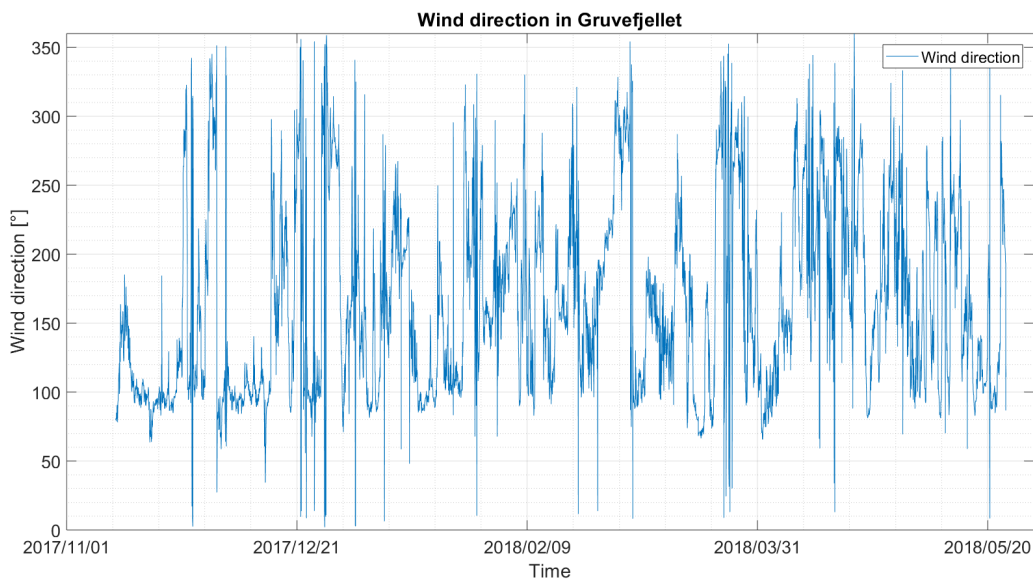
Figure 36: Timeline of wind direction in Gruvefjellet from the 8th of November to the 24th of May

With these first observations, one can suppose the impact of the wind on different snow stations. After running numerous trials that are shown in Chapter 6.5, knowing the topography around snow stations and using common sense, here is a summary of correcting factors. Correcting factors for facing winds are set as a 90° sector centred on the orientation of each station. Winds from northwest are facing Lia station and Nybyen station, while winds from southwest are blowing perpendicularly to these stations. For Lia, it is decided to set to 75 %, the factor for facing winds. For winds that are blowing along the slope, the factor is fixed to 62.5 %. Only 25 % of raw data are used for winds coming from elsewhere, as this station is well-protected from wind coming from east to east-southeast. Correcting factors for Nybyen station are approximately the same, except for winds blowing alongside. The factor is reduced to 50 %, as it is more protected than in Lia. The interval is also a bit shifted, as the azimuth of the slope is orientated in a slightly different direction.

Regarding Sverdruphamaren station, it will be impacted by strong east winds facing the station; thus the factor is set to 75 %. Winds coming from south-southeast and north-northeast will also have an influence, although weaker and the factor is fixed to 50 %. Winds coming from elsewhere are less relevant for Sverdruphamaren station, as it is well-protected from westward winds, which explains the 25 % factor. Figure 38 presents the different corrections applied to raw data according to wind direction for every snow stations. Thumbnails of the map (Figure 4) are also displayed to understand the chosen intervals.
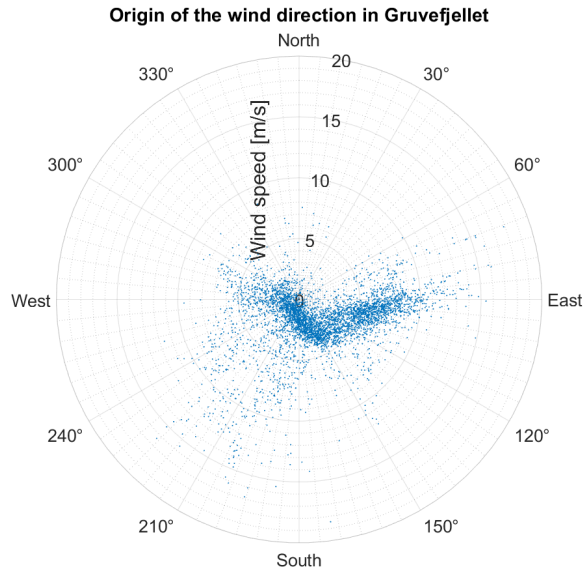
Figure 37: Wind speed in function of wind direction in Gruvefjellet from the 8th of November to the 24th of May
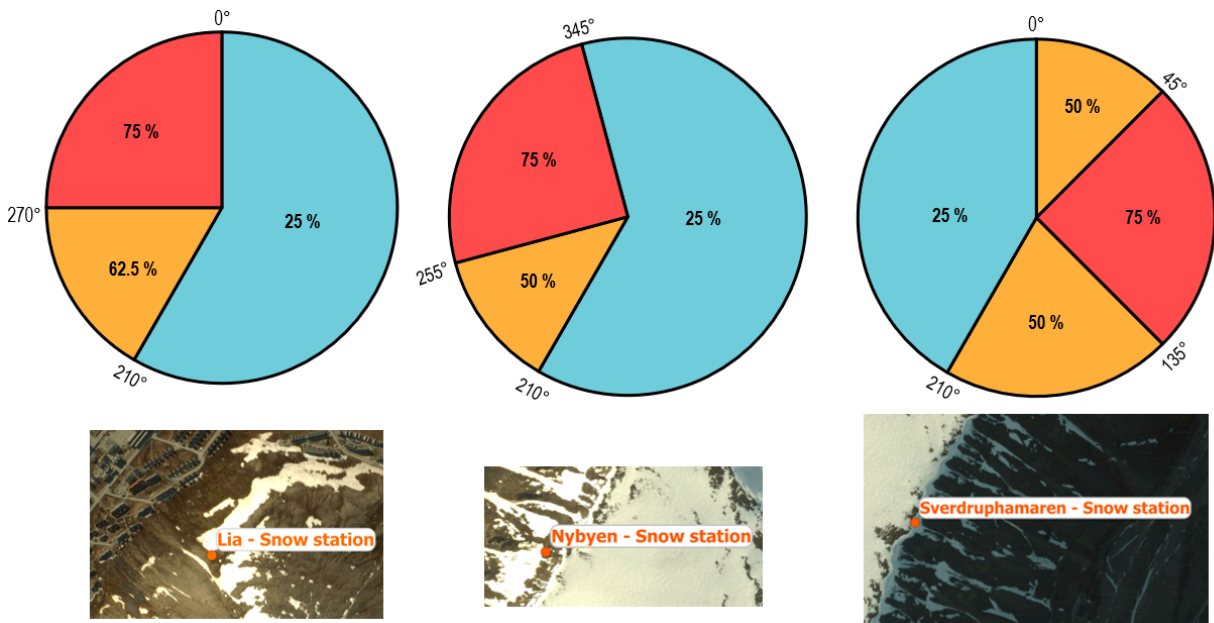
Figure 38: Wind data correction for Lia, Nybyen and Sverdruphamaren according to wind direction and topography

5 Fieldwork

Fieldwork consisted of digging snow pits nearby the three snow stations. It was also necessary to measure the snow depth manually with a probe at four spots under the ultrasonic device, responsible for snow depth measurements. In fact, this device has quite a large footprint, which explains why four measurements were required. Searching for a place close to the stations with the same snow depth was the next step. A range of $\pm 15 - 20$ centimetres was considered, due to the very irregular and rocky terrain. After finding the right spot, a pit was dug, large enough to have space to work. Snow profiles were realised according to the classification system of Fierz and al. (2009, [5]). The first step was to identify the different layers coarsely. Then, more precisely, from top to bottom, the snow profile was made. It includes different measurements: thickness of each layer, snow crystals type, size of crystals, hardness and temperature profile with measurements every 10 centimetres. Snow crystals types are presented in Chapter 1.1 and hardness is assessed according to Fierz and al. (2009, [5]). Hardness scale is from 1 to 5, by testing the layers hardness with a fist (1), four fingers (2), one finger (3), a pencil (4) and a knife (5). It should not be tough to puncture the layers. An indication if snow is wet or not, verified with the temperature profile, is taken. In total, seven snowpits were realised, three for Lia station, three for Nybyen station and one for Sverdruphamaren station. Unfortunately, this last station was quite dangerous to reach, which explains why there is only one snowpit. Below, an example of a profile realised in Nybyen on the 27th of March is presented (Figure 39). Every profile can be seen in Appendices (A, C, E, G, I, K and M).

5.1 Snow profiles in Lia

The first snow profile realised in Lia station was on the 28th of March and is presented in Appendix A. Some fresh snow had fallen (7 centimetres) at that time over a thin fragmented snow layer of about 3 centimetres. Beneath these soft layers (fist to one finger), a very hard layer (knife), 40 centimetres thick of melt forms, laid over a softer layer (pen) also made of melt forms. Below, there was an ice layer of 2 centimetres. Underneath, there were two layers of melt forms with a decreasing hardness (pen to one finger), of 10 centimetres each. Underneath 70 centimetres from the ground, there was an alternation between crusts and faceted crystals layers. Crusts were very hard (knife), although faceted layers were quite soft (one finger). About twenty centimetres was made of three shifts between those layers. From 49 to 32 centimetres, another very hard (knife) layer made of melt forms laid over a softer layer also made of melt forms, about 10 centimetres thick. Right beneath this layer, rounded grains were found, with a high hardness (pen). It remained over the last layer, made of faceted crystals, which constituted the snowpack basis. Temperature profile remained almost constant above the ice layer (between -12.2 and -12.7°C) with an air temperature of -12°C. Underneath the ice layer, temperature increased relatively fast (+0.6-0.7°C every 10 centimetres on average), to reach a temperature of -5.7°C on the ground.

On the 17th of April, the second snow profile in Lia station was made, shown in Appendix C. The snowpack was complex with several thin crusts linked to faceted crystals or depth hoar layers. A thin crust was at the surface, probably due to humidity deposition, laying on a thin fragmented precipitation particles layer. Underneath a thin layer of a mix between faceted and rounded crystals topped another thin crust. Melt forms, faceted crystals, crusts formed the next 20 centimetres. A thick layer of rounded grains was right beneath of about 20 centimetres. Underneath, melt forms, faceted crystals, depth hoar and three crusts formed the next 50 centimetres. Crusts and melt form layers are very hard (pen to knife), although faceted and depth hoar layers are softer (one finger to 4 fingers). A last faceted layer constituted the snowpack from 39 centimetres to 8 centimetres. At the basis, depth hoar crystals were present with the last crust separating the depth hoar layer from the faceted crystals layer. This snowpack was hard in general, with several weak layers between those hard layers. Temperature profile was almost isothermal since only 2°C separated the top from the bottom.

The last profile for Lia station was made on the 3rd of May, and it is presented in Appendix E. The total depth was 160 centimetres, and the air temperature was 3.5°C. The snowpack was mainly made of melt form layers relatively hard (one finger to pen) except for two very hard crusts (pen-knife and knife), right beneath the snowpack surface and at 127 centimetres above ground and a basal layer made of large depth hoar up to 3 millimetres. Temperature profile proved that the snowpack was still not wet. Linearly decreasing until the last 50 centimetres, the temperature reached a minimum of -6.2 at 20 and 30 centimetres above ground. For the last 50 centimetres, the temperature fluctuated around -6°C.

5.2 Snow profiles in Nybyen

Figure 39 shows the snow profile realised with the help of Prof. Alexander Prokop on the 27th of March. Without wind, the cloud cover was low and the air temperature at around -15°C. The first layer of 5 centimetres consisted of a mix between precipitation particles and fragmented snow, very soft (fist). Right beneath, another layer of precipitation particles was more compact (four fingers), with a thickness of 23 centimetres. A very hard crust (knife) of one centimetre laid just under this new snow, formed by a melt-freeze process. Another one-centimetre layer was underneath the crust and formed by faceted crystals. This layer seemed to be a weak layer, as Figure 39 shows a fracture after the 20th step of a Column Test (CT20)[5]. Beneath this weak layer, the snowpack was made of a significant layer of melt forms refrozen, hard (one finger to pen), 72 centimetres thick. Below this layer, laid a large crust of 25 centimetres, made of melt forms and very hard (pen to knife). Underneath, a layer of faceted crystals quite soft (one finger) of 18 centimetres remained on the last layer made of depth hoar. They were big, up to 3 millimetres, and formed the last 25 centimetres of the profile. Looking at the temperature profile (red line in Figure 39), one can see that the snow surface temperature was 5.0°C colder than air (-15.0°C for air and -20.0°C for snow surface). Within the snowpack, it increased quite fast until the first crust, 28 centimetres below the surface, where the temperature was -13.0°C. Underneath, the temperature increased linearly until the 20 last centimetres to reach 5.9°C. To the ground, temperature was constant with tiny variations of 0.1°C.

Appendix I presents the snow profile realised on the 24th of April. Snow depth was 45 centimetres higher than a month before. At the top, ten centimetres of fragmented snow laid on a thick, wind-packed (one finger) rounded crystals layer, of 37 centimetres. Underneath, a hard melt form layer (pen) was 17 centimetres thick. Right beneath, a layer formed by faceted crystals is trapped between one crust and melt form layer, which had refrozen. The layer was soft (four fingers) and 16 centimetres thick. Regarding the crust, it was already there one month earlier. Very hard (knife), it laid over a thick layer of melt forms (64 centimetres), similar to the one discovered a month earlier. Below, three very hard crusts (knife) are mixed with melt forms (pen and pen-knife) and together formed a very compact layer of 49 centimetres. At the basis, two layers of depth hoar, 8 centimetres thick each, are separated by a melt form layer of 10 centimetres. The temperature profile showed a similar trend, which was a fast temperature increase the first 35 centimetres (-15.8°C to -9.9°C) and below, temperature increased linearly until the last 20 centimetres (+ 0.2-0.3°C every 10 centimetres), where it stayed almost constant to the ground. The overview is quite close in comparison to the profile made a month earlier.

The last profile for Nybyen station is presented in Appendix K, made on the 19th of May. At that moment, the snowpack was almost isothermal. The upper part was wet from top to 90 centimetres above ground. In fact, there was no more freezing due mostly to polar day. A thin layer (3 centimetres) of fragmented snow laid on snowpack top. Otherwise, except for two regions where one already identified crusts and basal depth hoar layer, the snowpack is mostly made of melt forms. The crust location and their thickness are a bit different due probably to the snow pit location, but they matched with those found in the other two profiles. The last 90 centimetres had a temperature below zero and reached a minimum of -0.6°C at 20 centimetres above ground.

5.3 Snow profile in Sverdruphamaren

Appendix M shows the only snow profile realised in Sverdruphamaren station, on the 14th of May. There is much less snow (95 centimetres) at this station, due to the slope orientation, windward. As a reminder, the main wind direction is towards north-west and west. As the station is facing east, erosion occurs significantly. On top, there was a thin crust of 1 centimetre due to humidity deposition. As temperature was below 0°C, it had frozen. Underneath, a thin melt form layer reached 90 centimetres above ground. Below, several layers of melt forms with increasing hardness with depth (four fingers to pen) were noticeable. At 55 centimetres, a large and soft (four fingers) layer of melt forms was present. It laid over a thin rounded layer of 5 centimetres quite soft (four fingers). A last hard melt forms layer (pen) was above a very hard crust of two centimetres. Finally, the soft (four fingers) basis of this snowpack was made of 12 centimetres of depth hoar. The temperature profile shows a singularity at 90 centimetres, where the temperature was the warmest and equalled 0°C (-2.3°C for the surface). Below, the temperature decreased until reaching a minimum at 30 centimetres with a temperature of -3.7°C. To the ground, it stayed constant with a temperature of -3.5°C.

---

[5]A column test consists of digging around a rectangle of 90 centimetres long and 30 centimetres wide to the ground. With a shovel placed upside-down at one edge of this rectangle, one hits the shovel with increasing strength to assess the snowpack stability. First, ten hits with fixed wrist, then ten hits with fixed elbow and at the end ten more hits from the shoulder.

Figure 39: Snow profile in Nybyen on the 27th of March 2018

6 Results

This section gathers all simulation results obtained with SNOWPACK for the three snow stations described in Chapter 3.2.1. First, optimal simulations are displayed and discussed. Then, results with different settings are analysed, as the mask effect and a little sensitivity analysis concerning the wind effect. All these secondary results have led to optimal simulations presented below in Chapter 6.1.

6.1 Optimal simulations

Figures 41, 44 and 47 show simulations with the "best" set of parameters. It means that reflected shortwave radiation are corrected according to the methodology presented in Chapter 4.4.1, to know, use a mean albedo and apply it to incoming shortwave radiation after the 2nd of May to get outgoing shortwave radiation. The masks presented in the same section (Chapter 4.4.1) are used to adjust the incoming shortwave radiation amount. Regarding the boundary condition, Dirichlet equation (1) is preferred since snow surface temperature is measured on-site. As a reminder, Neumann equation (2) is based on radiation fluxes. As they are not measured on-site, but recorded in a station distant of several kilometres, the results would be better with Dirichlet condition. Finally, the most important input, the wind, is set according to Figure 38. After numerous trials with different adjustments for wind, the trend was always the same. Changes in thickness of each layer, especially for melt forms layers. As strong winds bring more energy to the snowpack; more melting occurs, and it creates larger melt forms layers. Strong winds also induce fewer precipitation particles because they transform rapidly into fragmented precipitation particles and rounded grains. Fieldwork revealed that fresh snow layers were not thick at all. It also includes fragmented precipitation particles.

Correcting factors presented in Figure 38 have been set taking into account results obtained in Chapter 6.5. They are showing that relatively high correcting factors have to be used because of the small number of precipitation particles found on the field. Still, lower values than raw data seem to be appropriate considering the topography. One also fixes the percentages presented in Figure 38 based on wind direction and common sense. Facing winds will have a bigger impact than winds blowing along the slope. It seems correct that Nybyen station is more protected than Lia station. For Sverdruphamaren, looking at snow depth (Figure 23) helps to find appropriate correcting factors set. Obviously, this methodology is too simplistic, but common sense dictates the choices made.

6.1.1 Lia station

Figure 40 shows air temperature, and wind speed corrected according to Figure 38 to have clues to understand how the snowpack developed throughout the snow season. Figure 41 and 42 present simulation results for Lia station, respectively representing grain shape and temperature. Snow comes on the 20th of November according to temperature data presented in Chapter 4.1.1. In the beginning, the snowpack is mostly made of precipitation particles and then fragmented precipitation particles appear underneath the fresh snow since the snowpack got thicker. After December 10th, rounded grains appear at the bottom of the snowpack, formed by destructive metamorphism, as the temperature gradient is low. At the end of December, snow depth reaches 80 centimetres and a thick layer ($\simeq$ 40 centimetres) of faceted crystals formed in the upper part. Looking at temperatures inside the snowpack, one can observe a large difference between the surface, close to -20°C and underneath where it is -10°C. At least, the temperature gradient condition is fulfilled; thus constructive metamorphism might occur. In fact, these faceted crystals might be "near-surface faceted particles", that develop directly from precipitation particles or fragmented particles caused by high near-surface temperature gradients. According to Fierz and al. (2009, [5]), this kinetic growth occurs at an early stage of development. This subclass is a part of faceted crystals. After another snowfall of weak accumulation (10 centimetres), the first warm event combined with rain occurs (see Figure 10). The snowpack becomes wet down to the middle, but the entire snowpack is heated by rain as shown in Figure 42. Release of latent heat can explain this warming. Furthermore, high winds were measured, up to 7 m/s, which further increases the snowpack warming. A thick layer of melt forms ($\simeq$ 30 centimetres) is then created and will last until the end. It will refreeze, due to freezing temperatures occurring after that. Afterwards, other snowfalls increase the depth with fresh snow, which topped fragmented snow and rounded or faceted crystals below. A small warm event is notable on the 4th of February, with an air temperature of approximately 2-3°C. According to Dai (2008, [35]), the phase transition between snowfall and rainfall occurs over a relatively wide range of temperature from -2°C to +4°C, over low elevation land[6]. This assumed rain might be in fact snow, and it explains why this event has not a significant impact on the snowpack. In contrast, the rainfall on the 26th and 27th of February has a much more significant impact since air temperature reaches almost 5°C. The snowpack gets wet down to a depth of 70 centimetres above ground. Again, the entire snowpack is heated to the bottom, with strong winds up to 9 m/s. This layer is lasting until the end since it gets very hard after it has refrozen. To notice that the layer between these melt forms layers is made of faceted crystals. Until the 15th of March, the basal layer is made of rounded grains. From there, faceted crystals are formed to fill the space up to the crust, which is the first melt forms layer. Curiously the temperature gradient condition seems not to be met. At the top, more kinetic growth occurs to create more near-surface faceted crystals. From the 5th of May, the snowpack begins to melt from the top, accentuated by the polar day. In contrary to the Alps, no night-refreezing is happening. Finally on the 17th of May, the whole snowpack is made of melt forms and the snow depth decreases relatively rapidly.
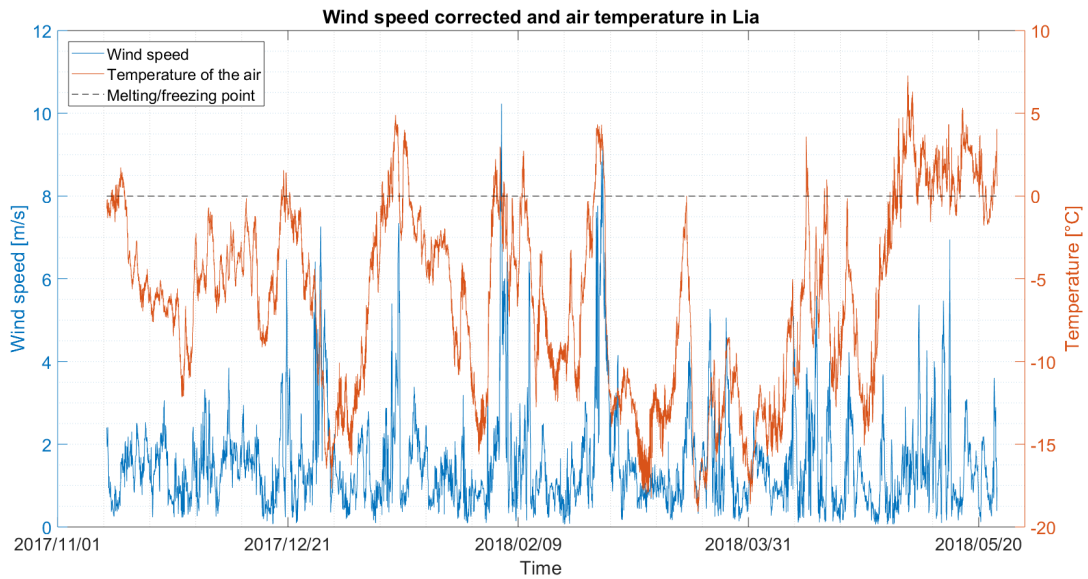
Figure 40: Wind speed and air temperature in **Lia** from the 11th of November until the 24th of May

---

[6]Here it is considered that the three stations are located at low elevation level since high elevation level, according to Dai (2008, [35]), have a pressure below 750 hPa, which is not the case for this study area.
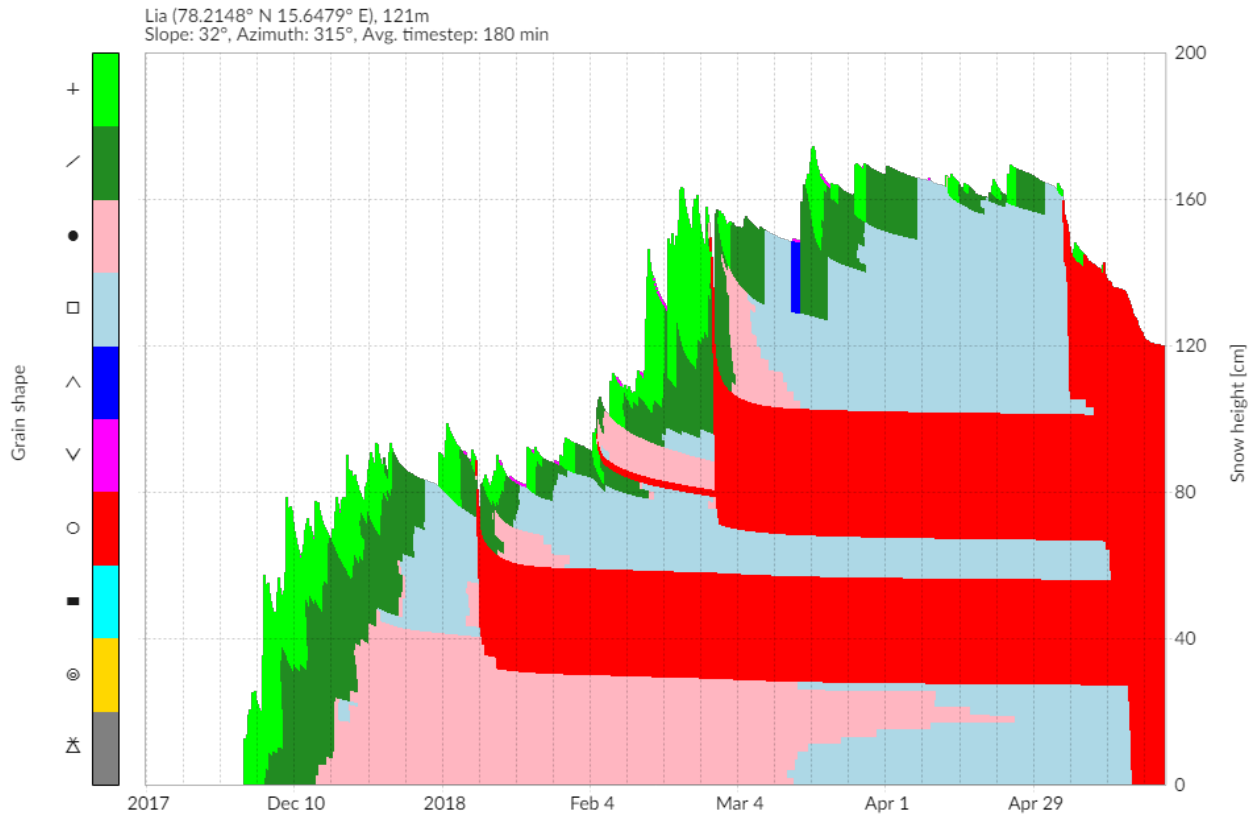
Figure 41: Simulation of grain shape in **Lia** from the 11th of November until the 24th of May, with shortwave radiation correction, with mask and with wind speed according to Figure 38
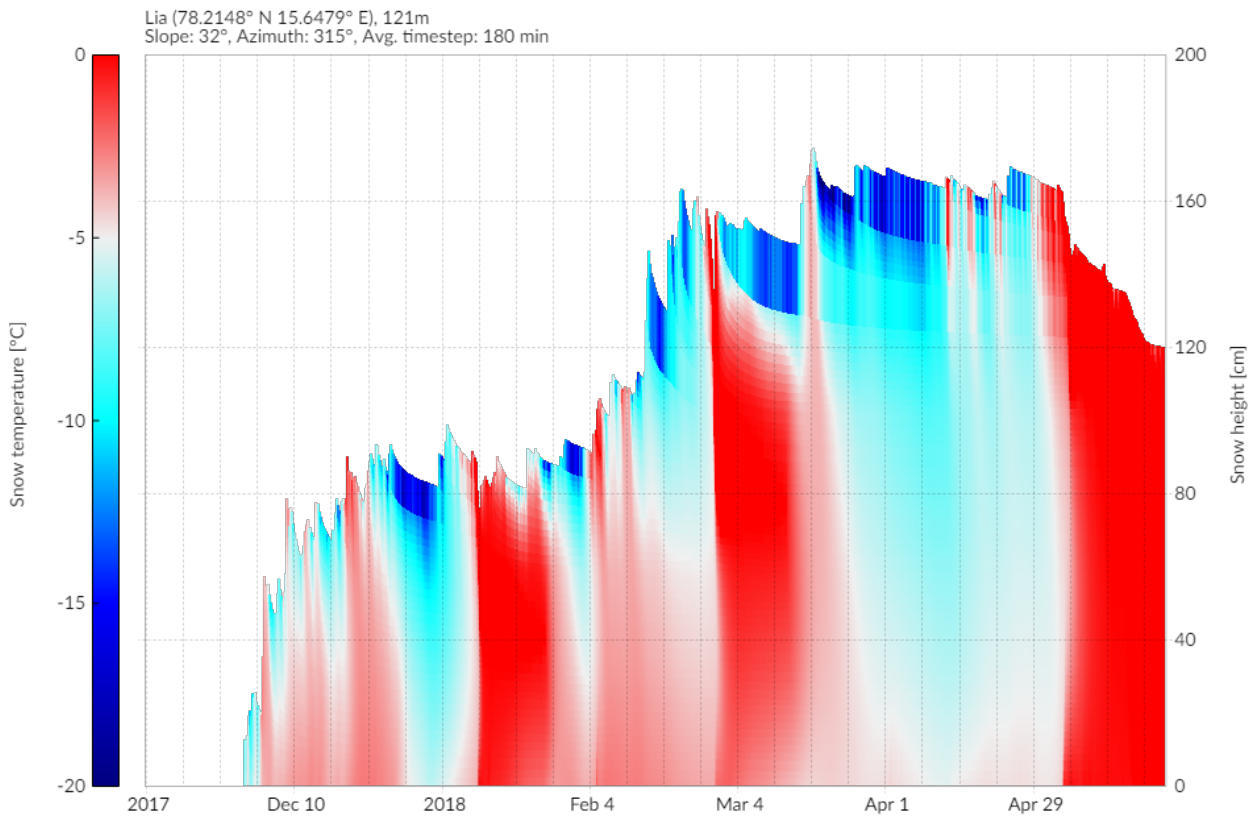
Figure 42: Simulation of temperature in **Lia** from the 11th of November until the 24th of May, with shortwave radiation correction, with mask and with wind speed according to Figure 38

6.1.2 Nybyen station

Figure 43 shows air temperature and wind speed corrected according to Figure 38 in Nybyen. Figures 44 and 45 present simulation results for grain shape and temperature for Nybyen. One finds the same attributes as Lia station. At the beginning of winter, snowpack is mainly made of precipitation particles followed by fragmented snow when the snowpack gets thicker. Some rounded grains appear at the bottom of the snowpack formed by destructive metamorphism. A thin layer of faceted also appear at a depth of 40 centimetres at the beginning of December, more likely near-surface faceted crystals, as fragmented particles are directly transformed into faceted particles. Later on, these faceted particles tend to transform into rounded grains. These different processes occur until the first warm event combined with rain on the 13th of January. At that moment a melt forms layer is created, and the snowpack is heated all the way down to the ground due to latent heat release. High winds are also measured at that time, with wind speed up to 6 m/s. This melt forms layer is not as thick as the one got in Lia station. This is due to the altitude and colder temperature prevailing in Nybyen. Looking at Figure 45 and 42, one can easily understand the less significant impact during this warm event. For Lia, temperatures reach almost 0°C in contrast with Nybyen, where temperatures reach -3°C at most underneath the melt forms layer. Afterwards, this melt forms layer will refreeze due to freezing temperatures and last until the end. From here, faceted crystals remain above the crust, as it acts as a barrier to vapour transport (McClung and Schaerer, 2006 [25]). To note that surface hoar crystals are sometimes created, and remain within the snowpack. They tend to disappear by transforming into faceted crystals. From the 4th of February, faceted crystals are created at the bottom of the snowpack and the layer increases in thickness with time to reach $\simeq$ 35 centimetres at the end of the simulation on the 21st of May. On the 26th and 27th of February, the significant rainfall creates a thin melt forms layer ($\simeq$ 10 centimetres). Once again, strong winds occur at the same time with wind speeds up to 7 m/s. It is less relevant for Nybyen than for Lia since Nybyen is located 250 metres higher. Around the 15th of March, a depth hoar layer appear at the top of the snowpack. This layer may seem not correct, but looking at the temperature within the snowpack, one can assess great temperature gradient. From the beginning of May, the snowpack starts to melt, including the first crust. At the end of the simulation, $\simeq$ 70 centimetres of the upper part is made of melt forms.
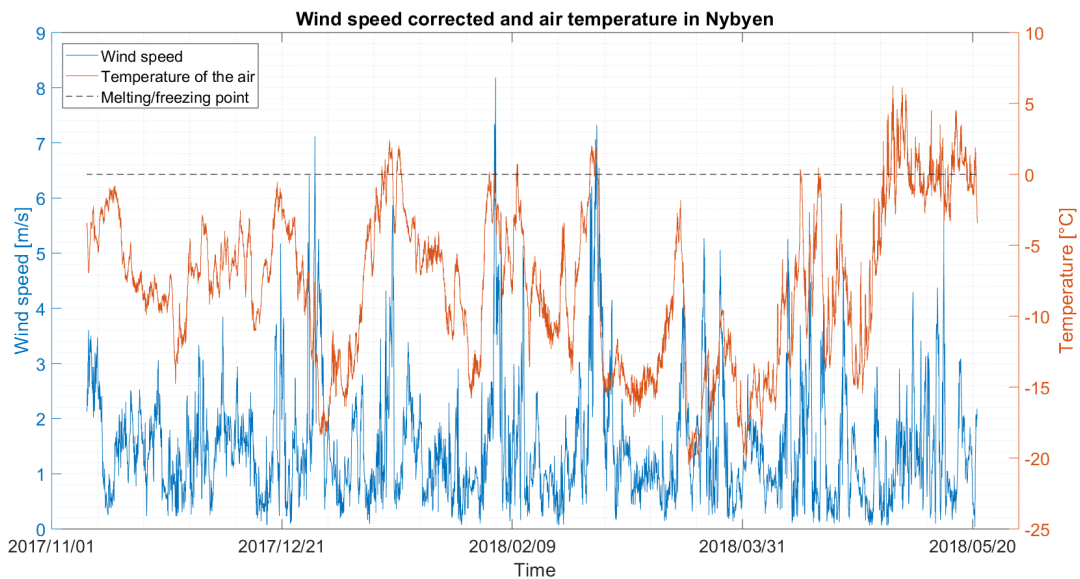
Figure 43: Wind speed and air temperature in **Nybyen** from the 8th of November until the 21th of May

Figure 44: Simulation of grain shape in **Nybyen** from the 8th of November until the 21th of May, with shortwave radiation correction, with mask and with wind speed with wind speed according to Figure 38

Figure 45: Simulation of temperature in **Nybyen** from the 11th of November until the 24th of May, with shortwave radiation correction, with mask and with wind speed according to Figure 38

6.1.3 Sverdruphamaren station

Figure 46 presents air temperature and wind speed, followed by the simulation results, in Figures 47 and 48, respectively representing grain shape and temperature of the snowpack. For this station, the snowpack modelled is considerably different from the other two (Lia and Nybyen). Until the beginning of February, snow depth is quite low, with mostly the same processes as those presented for Lia and Nybyen. Only a bit of fresh snow transformed quickly into fragmented particles and then transformed into mainly near-surface faceted crystals and a small fraction into rounded grains. Later on, the warm event of the 13th of January occurs and has a different effect. First, the entire snowpack is melted ($\simeq 10-15$ centimetres) and right after it refreezes. The melt forms layer, resulting from this heating last until the end. As the depth is shallow, temperature gradient is considerable and sufficient to enable kinematic metamorphism. Thus, depth hoar are created below this crust, at the base of the snowpack. This weak layer will remain until the end of the simulation. It was expected to get this configuration for almost every simulation, as it is frequent to get this kind of basal layer (Eckerstorfer and Christiansen, 2011 [20]). After the snowfall on the 5th of February, a relatively thick layer of fresh snow is deposed after a snowstorm. Usually, the slope where the station is located is windward, but during that event, the trend was reversed, and the slope became leeward. The two primary processes occurring from there are the transformation from precipitation particles to fragmented and finally rounded grains, and kinetic metamorphism. A thick layer of faceted topped a rounded grains layer. Underneath a thin layer of faceted crystals formed right after the warm event and persists to the end of May. From the 6th of May a thick layer of melt forms develops at the surface due to warmer temperatures in May. Situated at 450 metres above the sea, colder temperatures prevailing allows having new snowfall after the onset of the snowpack melting.
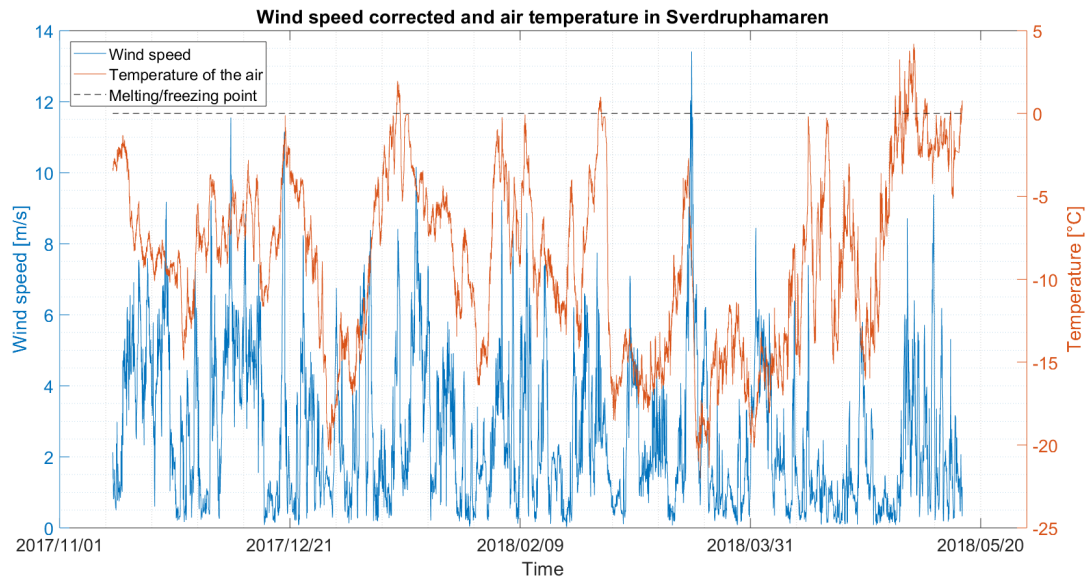
Figure 46: Wind speed and air temperature in **Sverdruphamaren** from the 12th of November until the 16th of May

Figure 47: Simulation of grain shape in **Sverdruphamaren** from the 12th of November until the 16th of May, with shortwave radiation correction, with mask and with wind speed with wind speed according to Figure 38
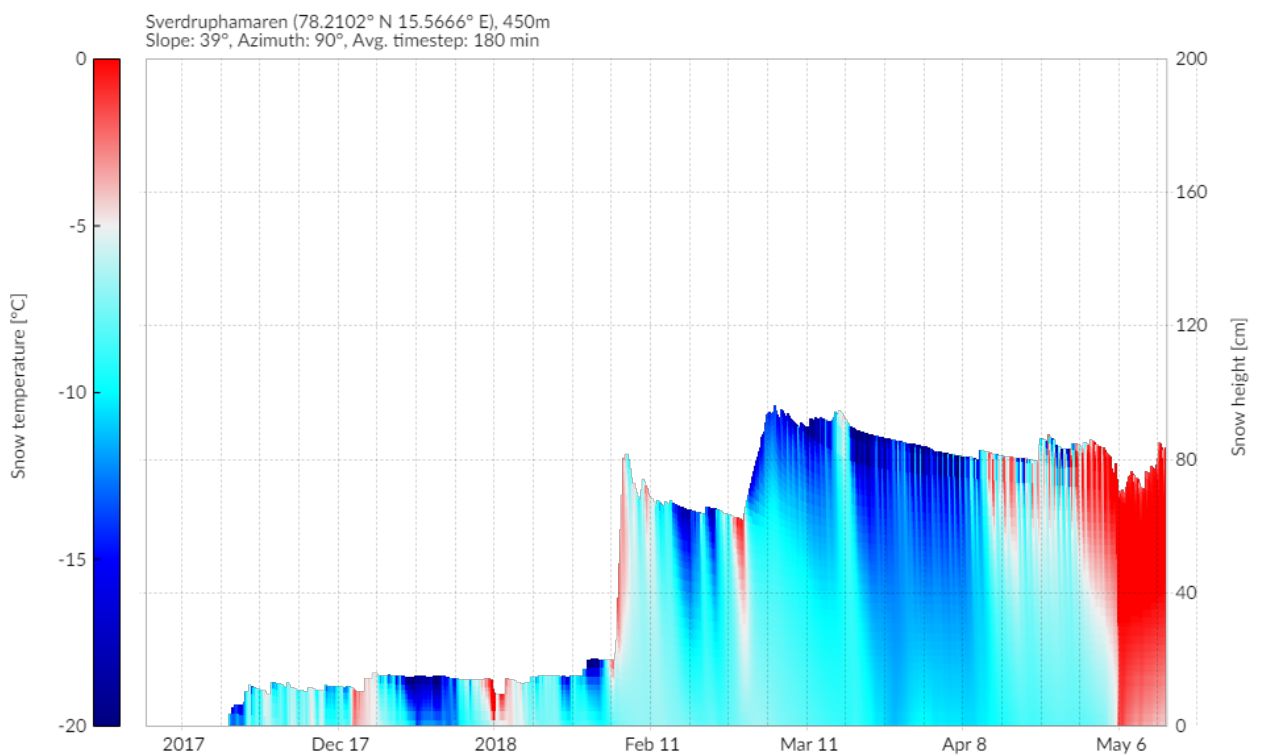
Figure 48: Simulation of temperature in **Sverdruphamaren** from the 11th of November until the 24th of May, with shortwave radiation correction, with mask and with wind speed according to Figure 38

6.2 Effect of the reflected shortwave correction

In Chapter 4.4.1, the issue with outgoing shortwave radiation is mentioned and explained. Figures 49 and 50 present the simulation results for Sverdruphamaren, respectively, without shortwave correction and with correction. One can notice that the snowpack receives more energy with correction, which induces a thicker layer of melt forms. For Lia and Nybyen, no change is notable since the upper part of the snowpack from the beginning of May is already made of a thick layer of melt forms. Those simulations are displayed in Appendix O.

Figure 49: Simulation of grain shape in **Sverdruphamaren** from the 12th of November until the 16th of May, **without shortwave radiation correction**, without mask and with wind speed equal to 50 % of raw data
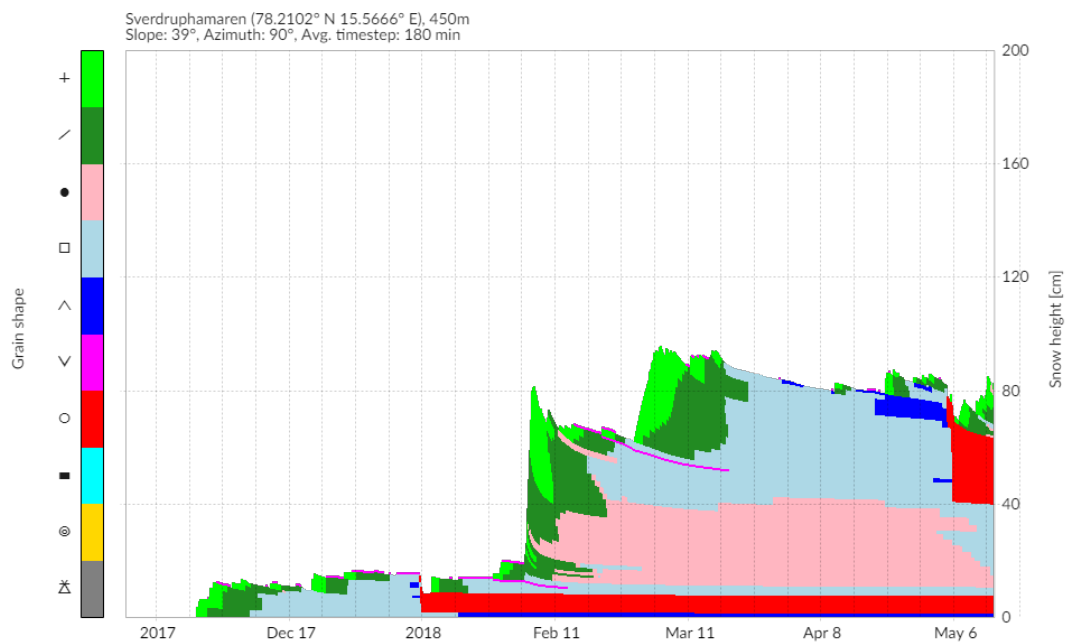
Figure 50: Simulation of grain shape in **Sverdruphamaren** from the 12th of November until the 16th of May, **with shortwave radiation correction**, without mask and with wind speed equal to 50 % of raw data

6.3 Effect of the mask

Figures 51 and 52 show the influence of the mask, producing the right amount of shading and so, decreasing the amount of sunlight (incoming shortwave radiation) received by the snowpack. One can see that the mask does not affect at all even if the amount of shortwave radiation obtained in the output is much lower with mask than without, as shown in Figure 53. Same Figures for Nybyen and Sverdruphamaren are visible in Appendix P. In Sverdruphamaren, the topography impacts less incoming shortwave radiation due to its location, high in altitude.
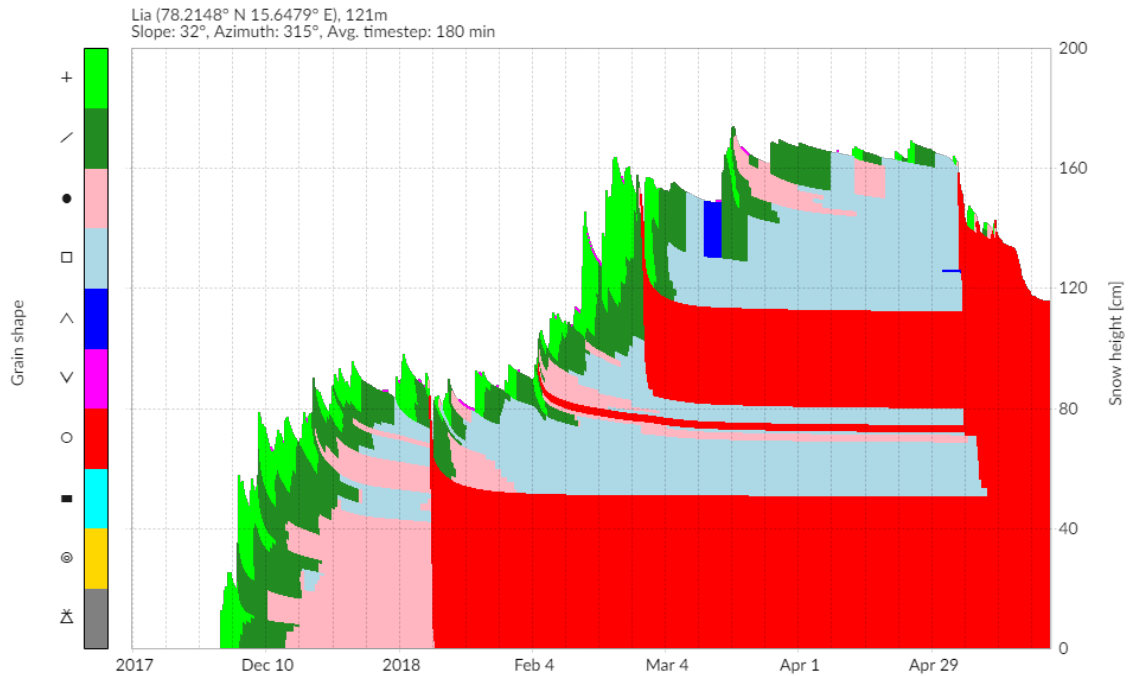
Figure 51: Simulation of grain shape in **Lia** from the 11th of November until the 24th of May, with shortwave radiation correction, **without mask** and with wind speed equal to 50 % of raw data
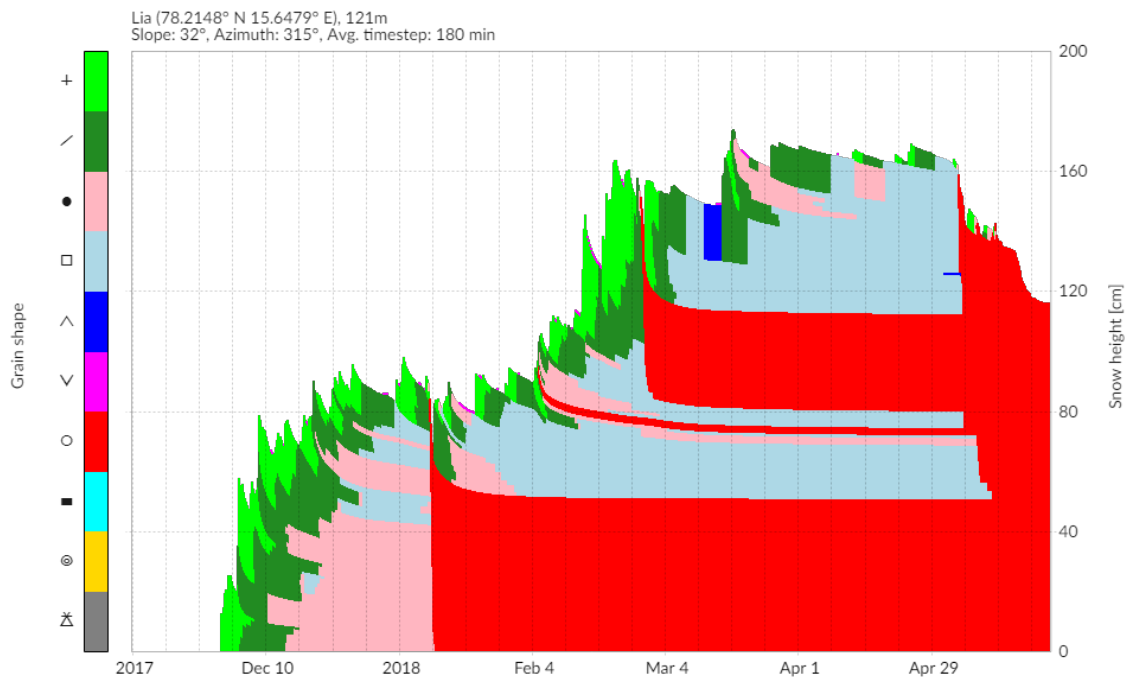
Figure 52: Simulation of grain shape in **Lia** from the 11th of November until the 24th of May, with shortwave radiation correction, **with mask** and with wind speed equal to 50 % of raw data
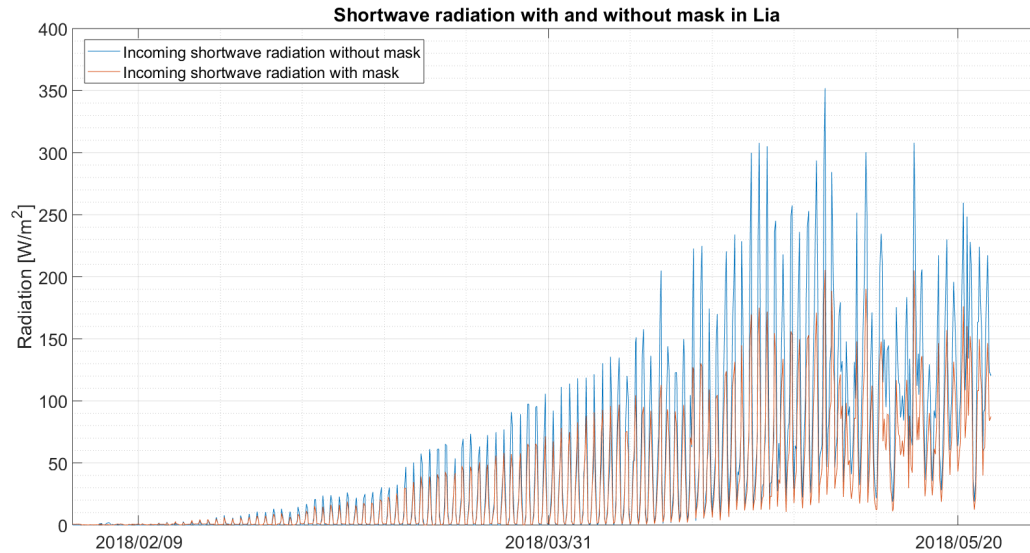
Figure 53: Shortwave radiation from output file in **Lia** from the 15th of February until the 24th of May, with mask and without

6.4 Effect of boundary conditions

Figures 54 and 55 show the differences between the use of the two possible boundary conditions: Dirichlet condition (Equation 1) and Neumann condition (Equation 2). One can observe that no major changes occur, if not alternation between rounded and faceted crystals, but nothing relevant. At the height of 130 centimetres above ground, a thin depth hoar layer developed with Dirichlet condition, although with Neumann condition, it does not. In fact, this is the right depth for an avalanche to be triggered. Having a weak layer there can inform of the danger. Moreover, as Dirichlet condition is used for the final simulations (Figure 44), it is a good point to see that weak layers develop easily with this condition. It is better to have the worse scenario, rather than not, even if this weak layer does not show off in the final simulation. During May, the upper part made of melt forms is thicker with Dirichlet condition.

For Lia station (Appendix Q), results show that melt forms layers are thicker with Neumann condition. Some rounded crystals become faceted crystals, but the differences are irrelevant. In Sverdruphamaren (Appendix Q), more depth hoar layers develop with Neumann condition, which is the opposite observation than the one made for Lia. In any case, it is more accurate to use Dirichlet condition since the values needed in Equation 1 (Dirichlet) are measured on-site.
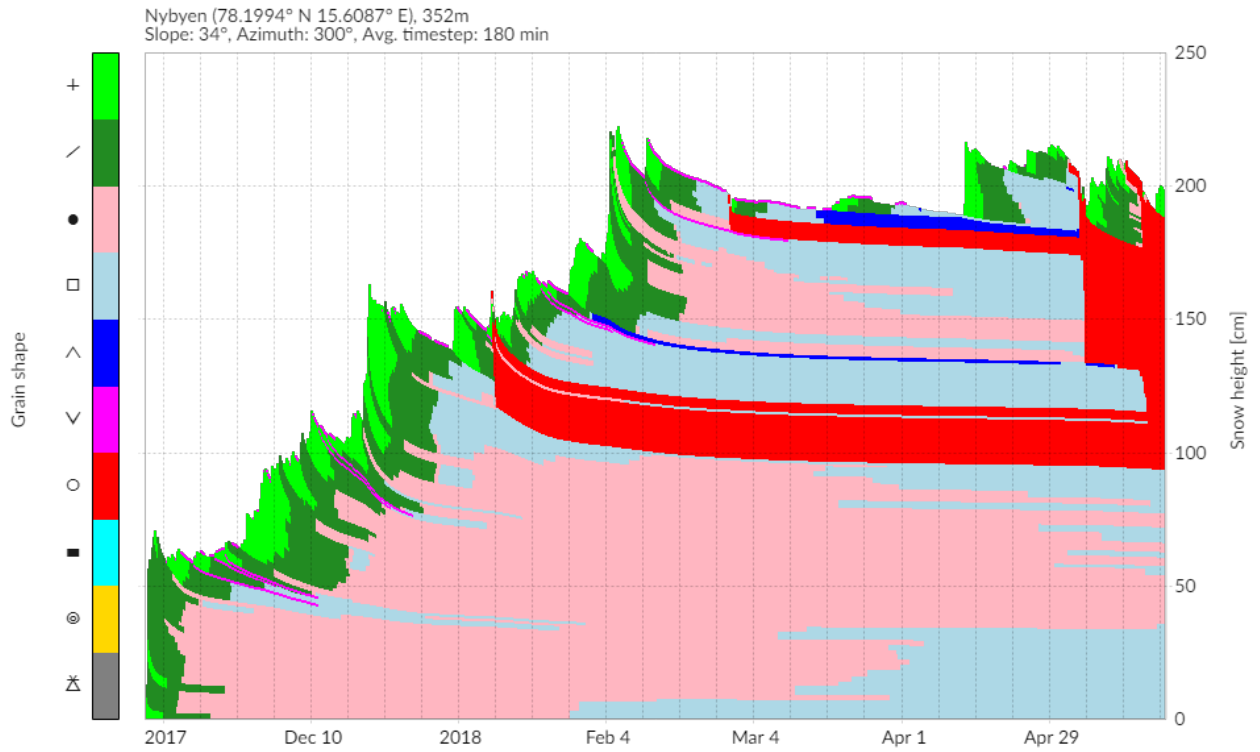
Figure 54: Simulation of grain shape in **Nybyen** from the 8th of November until the 21th of May, with shortwave radiation correction, with mask, with wind speed equal to 50 % of raw data and using **Dirichlet boundary condition**
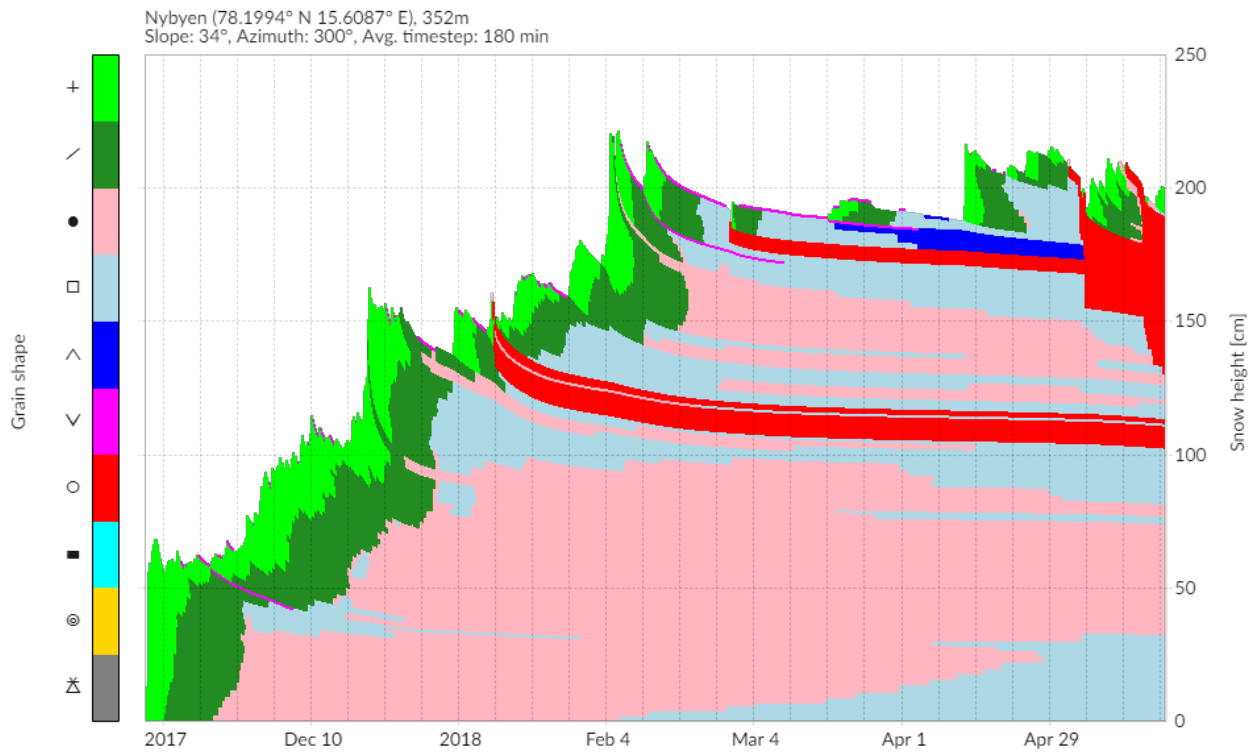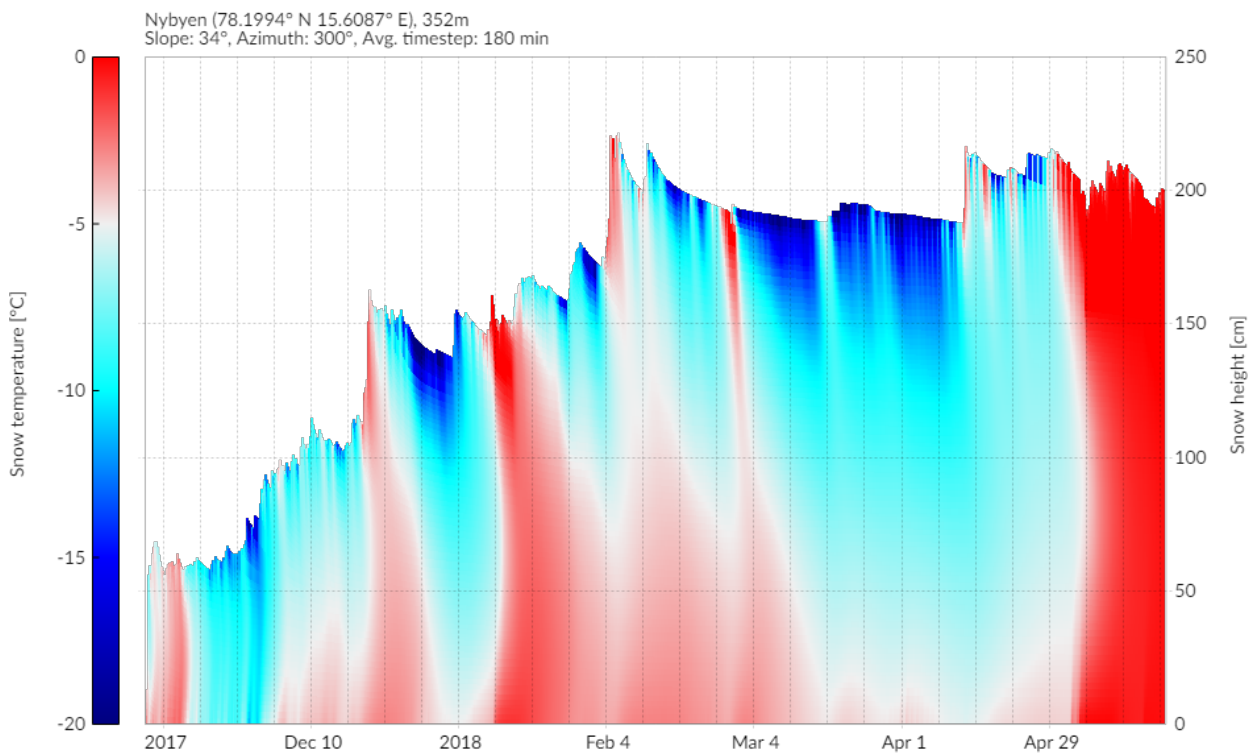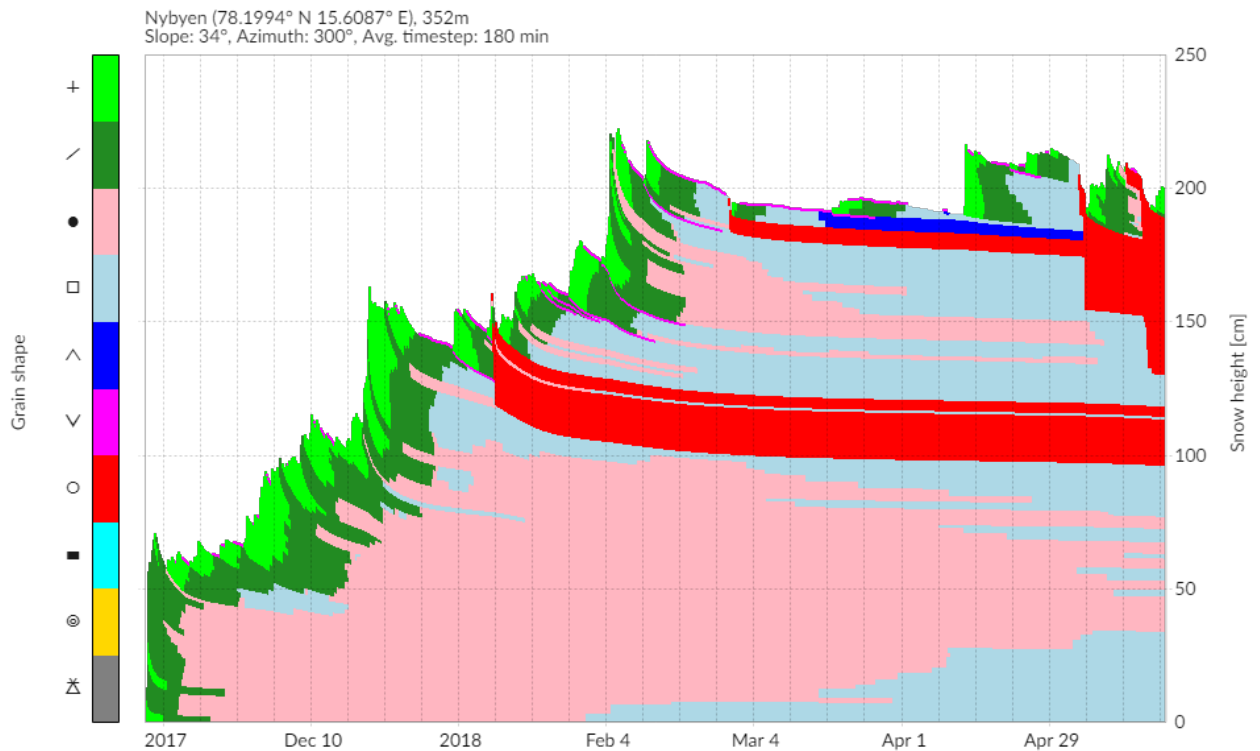

Figure 55: Simulation of grain shape in **Nybyen** from the 8th of November until the 21th of May, with shortwave radiation correction, with mask, with wind speed equal to 50 % of raw data and using **Neumann boundary condition**

6.5 Effect of wind

The input causing most changes is the wind. Unfortunately, wind data are not measured on-site, which leads to apply corrections to raw data as explained previously in Chapter 4.5. Figure 56 to 59 present the simulation results for Nybyen with, respectively, these correction factor applied to raw data: 25 %, 50 %, 75 % and 100%. The correction is applied to wind coming from every direction. The first observation is the thickness of melt forms layers, increasing with wind speed. Giving more energy to snowpack by wind allows more melting. The second observation is about the number of precipitation particles and fragmented particles. With low wind, 25 % of raw data, precipitation particles remain at the top of the snowpack until the beginning of March, in large amount. Underneath, there is a relatively important layer of fragmented snow, even during snowfalls during April and May. When a higher correction factor is used, fresh snow layer gets thinner and almost disappeared in Figure 59. The fragmented particles layer also decreases in thickness and crystals transform into rounded grains more rapidly with increasing wind speed. Wind-packed slabs are typically what one can find on the field in Svalbard. These observations are considered to get the best set of parameters proposed in Figure 38, used in the optimal simulation (Figure 44). Obviously, these corrections are not accurate, but with results presented below, one can at least understand what the snowpack undergo with different wind speeds.

Similar Figures are shown for Lia and Sverdruphamaren in Appendices R and S. Every simulation with a correction factor used for final simulations (Figures 41 and 47) are displayed. Same observations can be made for these stations.
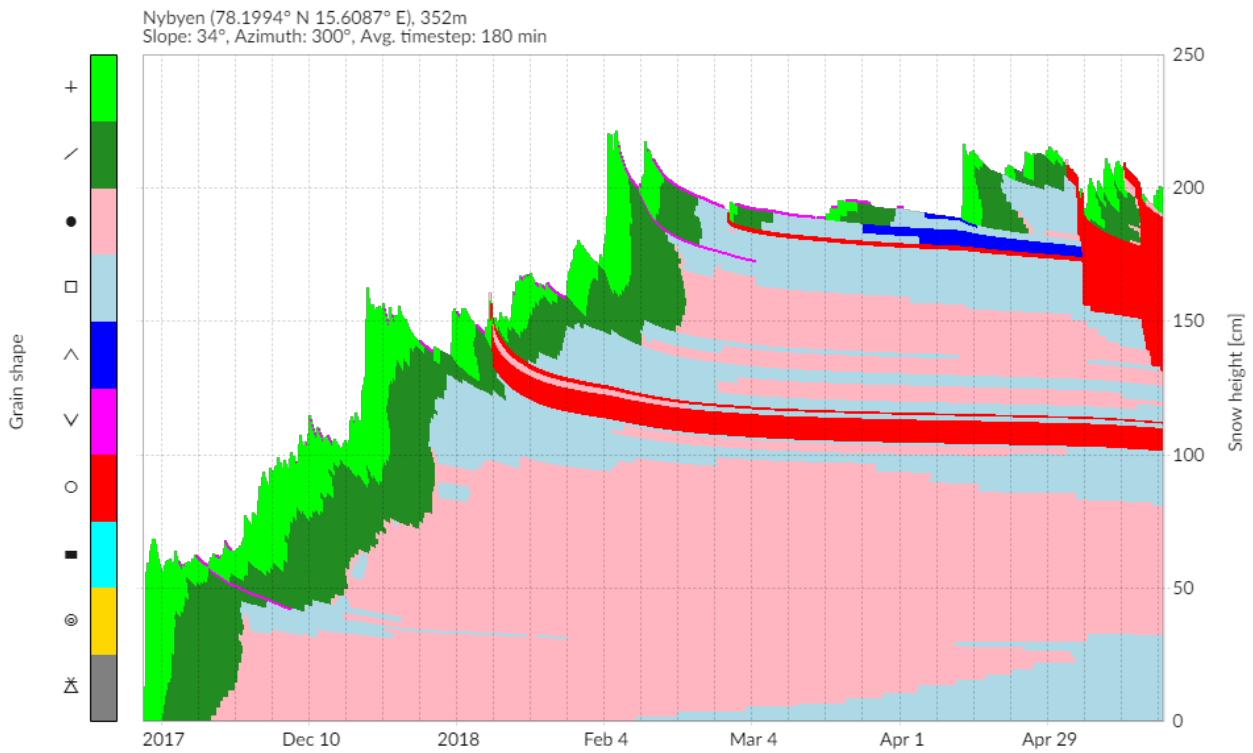
Figure 56: Simulation of grain shape in **Nybyen** from the 8th of November until the 21th of May, with shortwave radiation correction, with mask, with wind speed equal to **25 %** of raw data
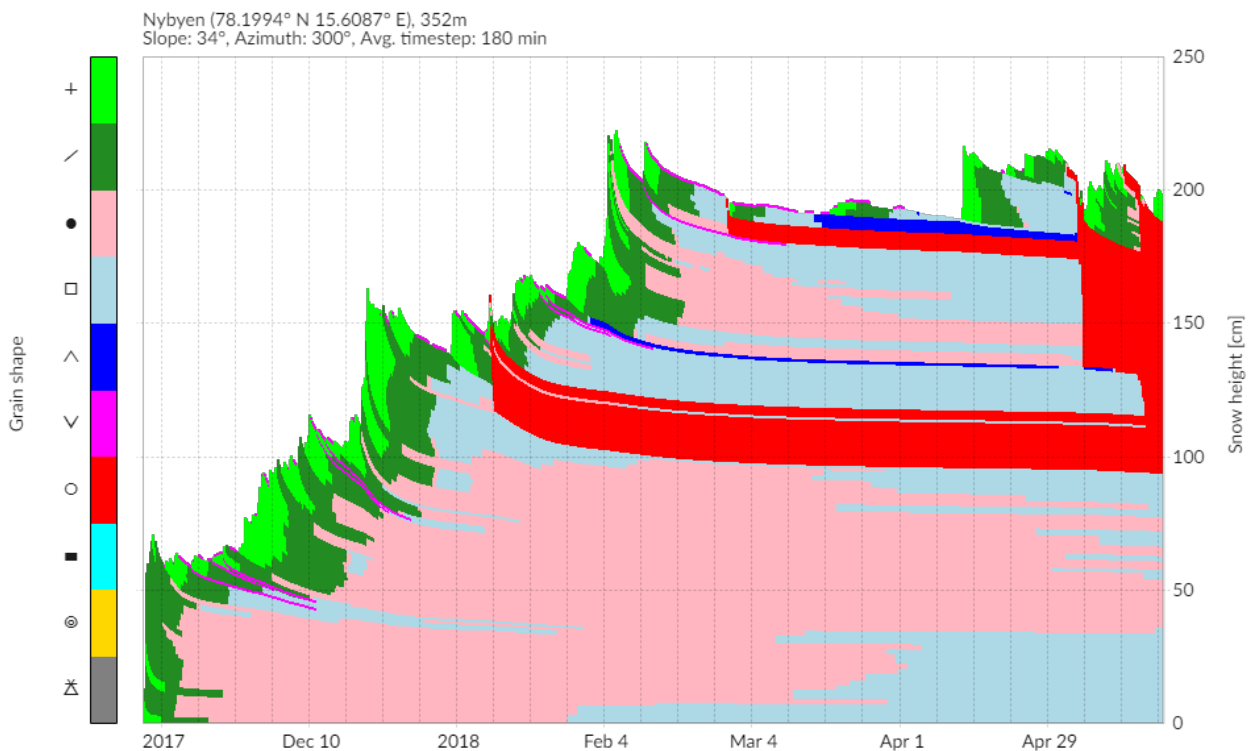
Figure 57: Simulation of grain shape in **Nybyen** from the 8th of November until the 21th of May, with shortwave radiation correction, with mask, with wind speed equal to **50 %** of raw data
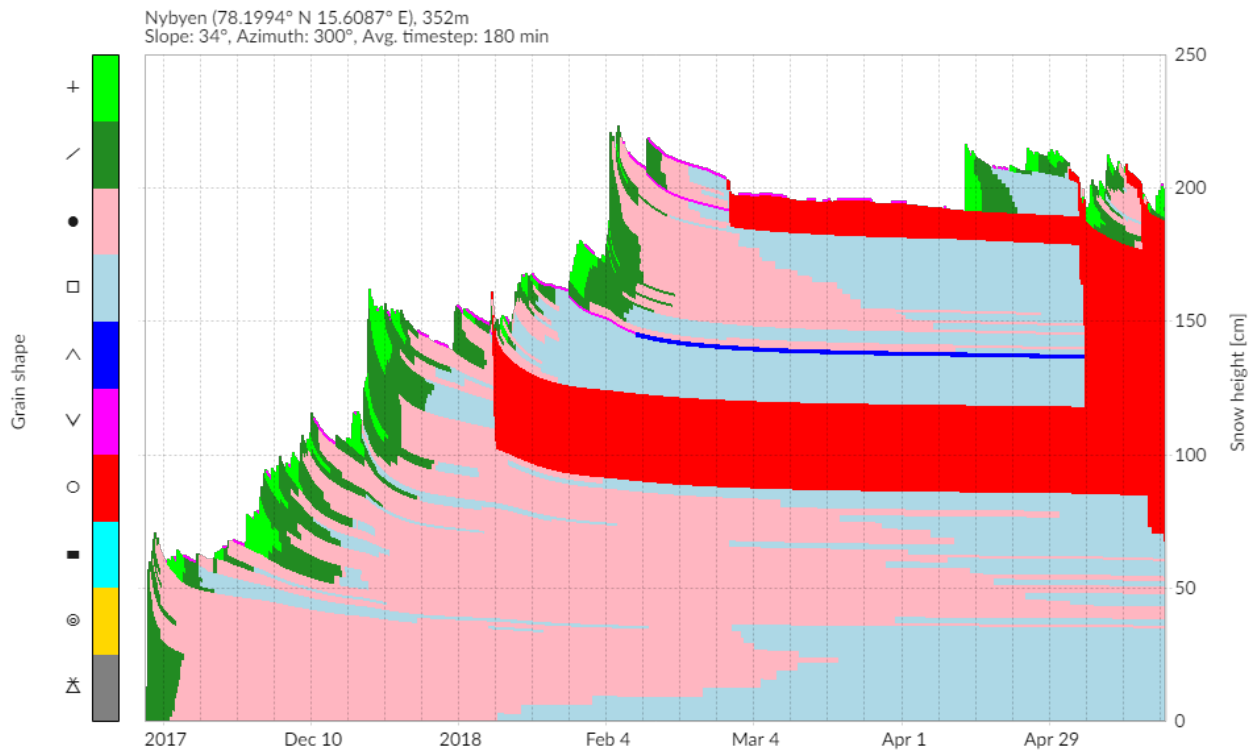
Figure 58: Simulation of grain shape in **Nybyen** from the 8th of November until the 21th of May, with shortwave radiation correction, with mask, with wind speed equal to **75 %** of raw data
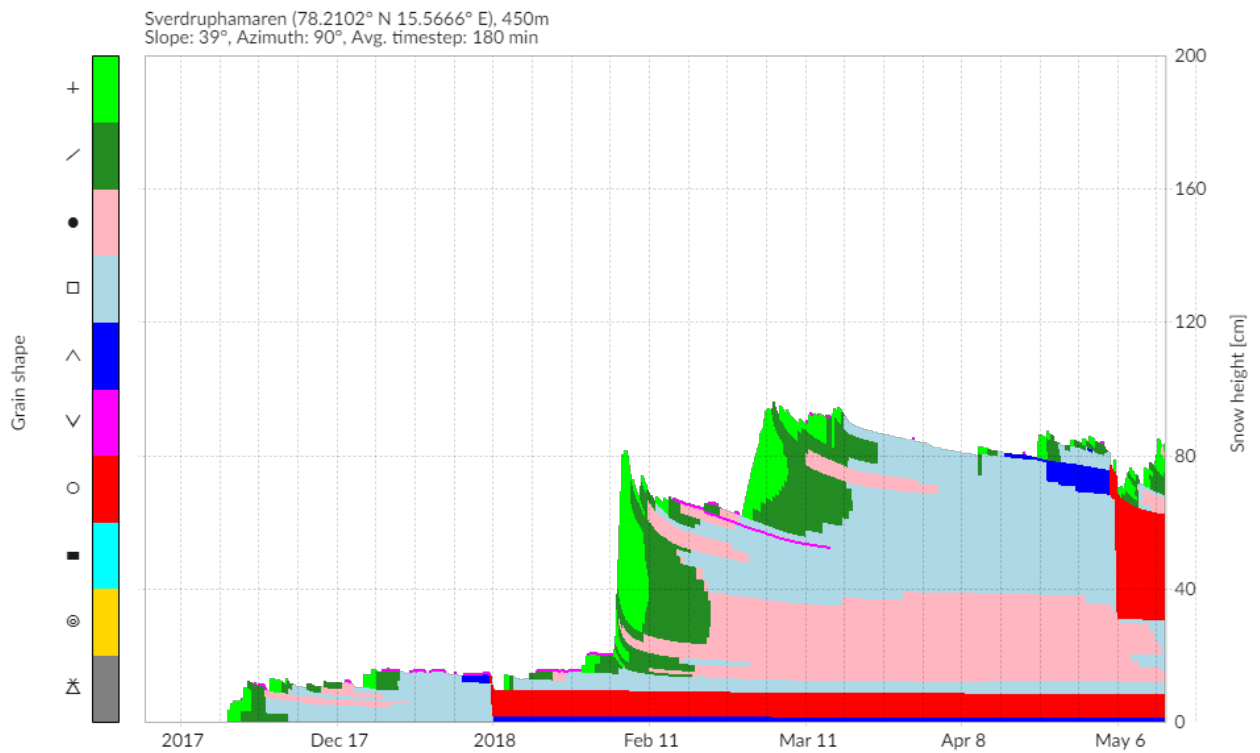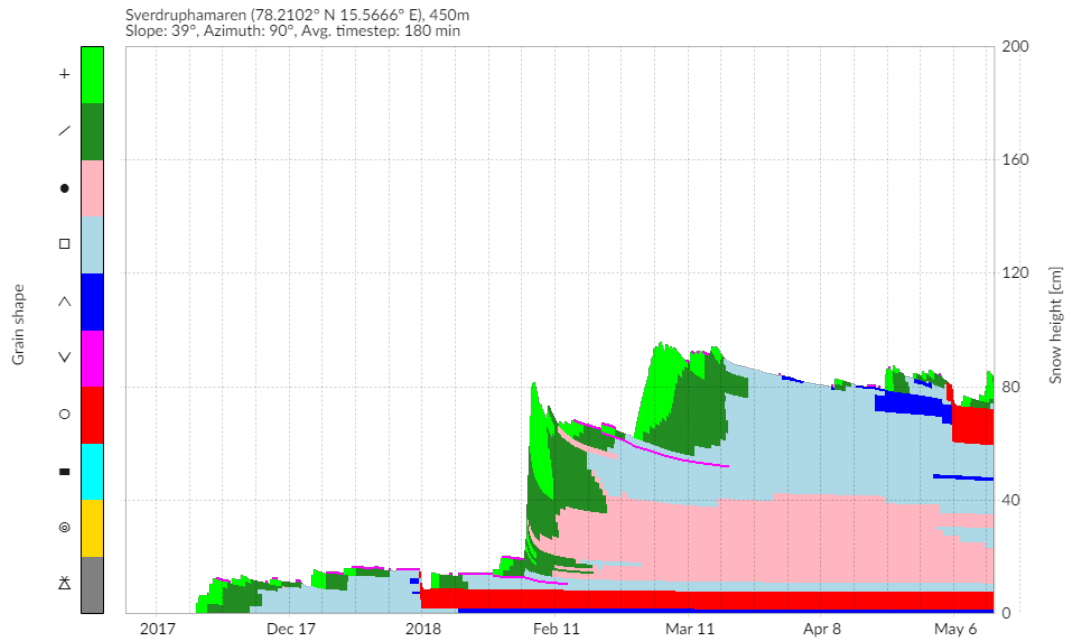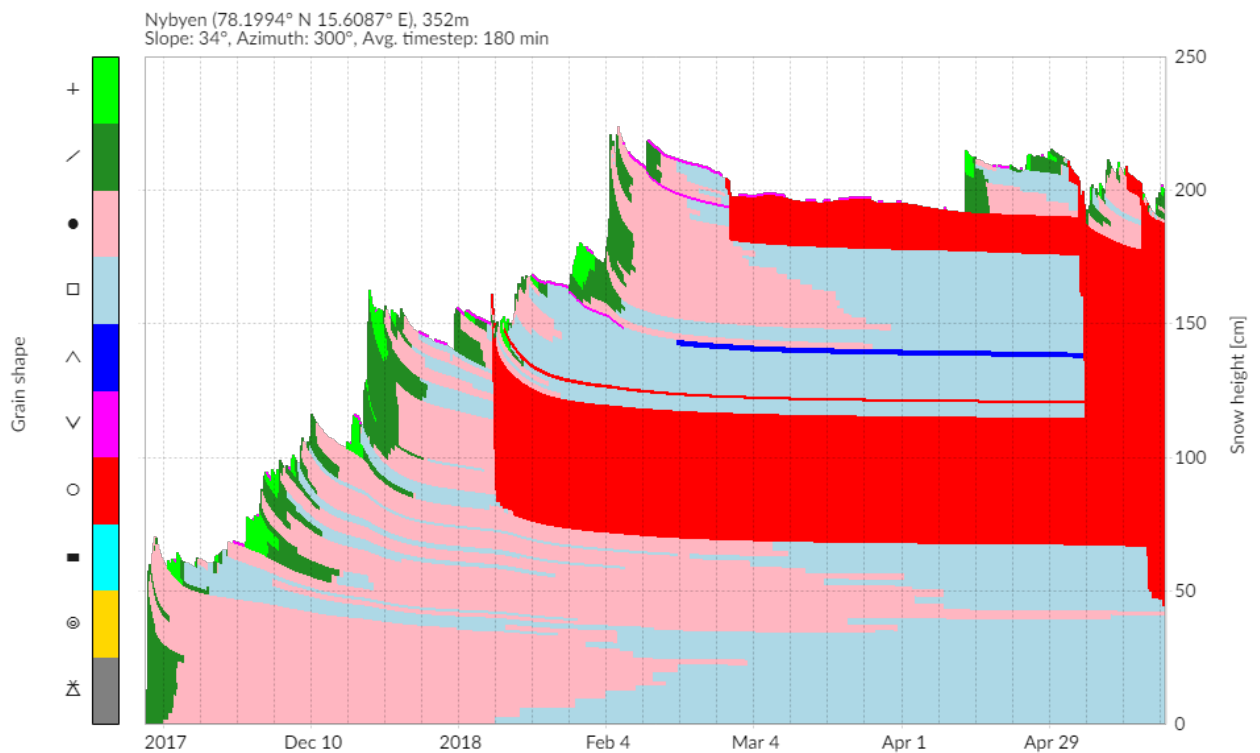

Figure 59: Simulation of grain shape in **Nybyen** from the 8th of November until the 21th of May, with shortwave radiation correction, with mask, with wind speed equal to **100 %** of raw data

7 Discussion

7.1 Comparisons between the field and the model

The goal of this project is to assess the applicability and performances of the numerical model SNOWPACK, for its use in Svalbard. Appendices B, D, F, H, J, L and N show comparisons between profiles made on the field and modelled profiles. Some of them are displayed in the followings subsections. One can observe, good similarities for the first station, Lia (Appendices B, D and F), but also for the station located in Sverdruphamaren (Appendix N). The station in Nybyen (Appendices H, J and L) has less similarities, but many differences. Here are the main observations between the field and the model, from the bottom to the top of the snowpack for every station.

7.1.1 Lia station

Figure 60 presents the comparison between the field and the model on the 28th of March. The base is correctly modelled for the first three layers, without taking into account errors for thicknesses of each layer. Above, the three thin crusts found out on the field do not appear in the model, but between them, faceted crystals are correctly calculated in the simulation. The most significant melt forms layer is not thick enough in the model. On the field, this layer was $\simeq$ 70 centimetres thick, and in the model, one got only $\simeq$ 35 centimetres. As discussed previously, the wind was the predominant input regarding the thickness of melt forms layers. Nevertheless, more wind increases the size of melt forms layers from the lower border. The upper border stays almost at the same depth, which should not be the case according to fieldwork. Correcting this thickness, and one gets something close to reality since the top of the snowpack, was made of rounded crystals, topped by fragmented particles and precipitation particles. The model does not create a layer of precipitation particles, which is not so relevant but creates faceted crystals instead of rounded crystals. Another issue is the temperature gradient. Its shape is the opposite of what field measurements indicate. Most of the snowpack is warmer with the model than in reality. It can be explained either by false data (model) or wrong measurements (field). Another possible explanation is the presence of ice on the field. Above it, the snowpack is almost isothermal and below, the temperature rises. The model did not detect this ice formation, and automatically, it follows a different temperature profile.
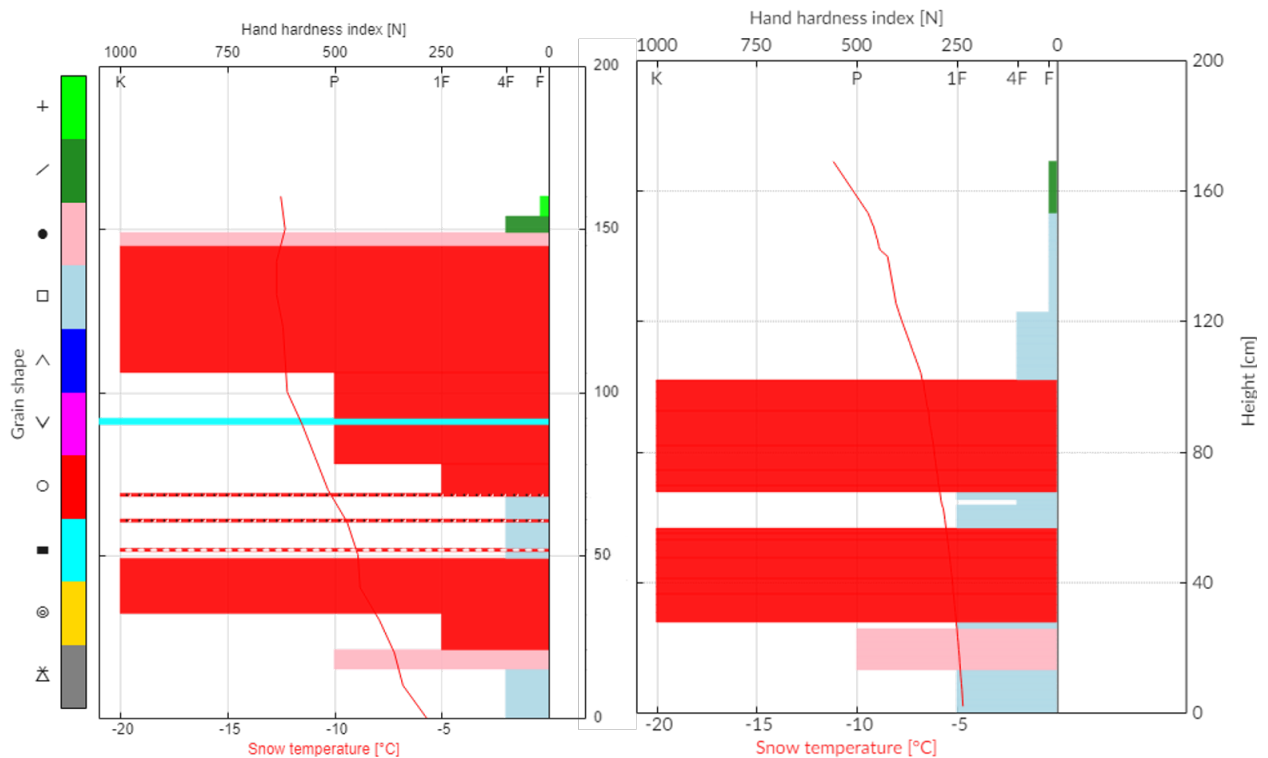
Figure 60: Comparison between the **field** on left side and the **model** on right side in **Lia** on the 28th of March

The comparison between the field and the model on the 17th of April is presented in Appendix D. The second modelled profile differs only a bit from the first one. In contrast, the profile got on the field is considerably different. From the bottom, the depth hoar layer and the first crust is not simulated but modelled as faceted together with the thick faceted layer above. The process between faceted and depth hoar is not so different; this is why it is considered acceptable. On top of that, a sequence of depth hoar and crust is modelled only as a large layer of melt forms. It is followed by a faceted crystals layer, which is correctly modelled. In the model, above that layer, a significant melt forms layer is topped by an enormous faceted crystals layer (50 centimetres), which is most likely not possible. Looking at the real profile, one can see that the second melt forms layer should be bigger, with the upper border located higher. There is even a rounded grains layer in the middle of it not modelled at all. At the top, the model is correct to predict faceted crystals, but with a layer much thinner. The temperature profile is quite close to reality.

On the 3rd of May, the fieldwork reveals that the snowpack is mostly made of melt forms with depth hoar at the base. The simulation has nearly not evolved and still presents the same stratification. The wind data are partly responsible for that, as the temperature profile seems to be correct. Perhaps, the correcting factors underestimate wind speed occurring at this station. The link between this issue and wind data is not guaranteed because higher winds would create much thicker melt forms layers earlier, during the rain events and it should not be the case according to fieldwork. This is the reason why radiation data can also be responsible or other parameters like the roughness length or the atmospheric stability. For every simulation, the roughness length was set to 2 millimetres, and the neutral stability condition is used. These settings were set by default. In any case, these results do not allow to conclude easily.

7.1.2 Nybyen station

The model is not performing well for Nybyen station, especially for melt forms layers. Their thickness should be much larger. As explained above in Chapter 6.5, the wind is mainly responsible for their size. In this subsection, a new simulation is run with a new set of wind speed data. Overestimated correcting factors are used, while the Nybyen station is relatively well-protected from wind, especially east wind. In fact, the station is located close to the foot of a cliff facing west. New correcting factors are: from 0° to 210° and from 345° to 360° → 1.25, from 210° to 255° → 0.75 and from 255° to 345° → 1.
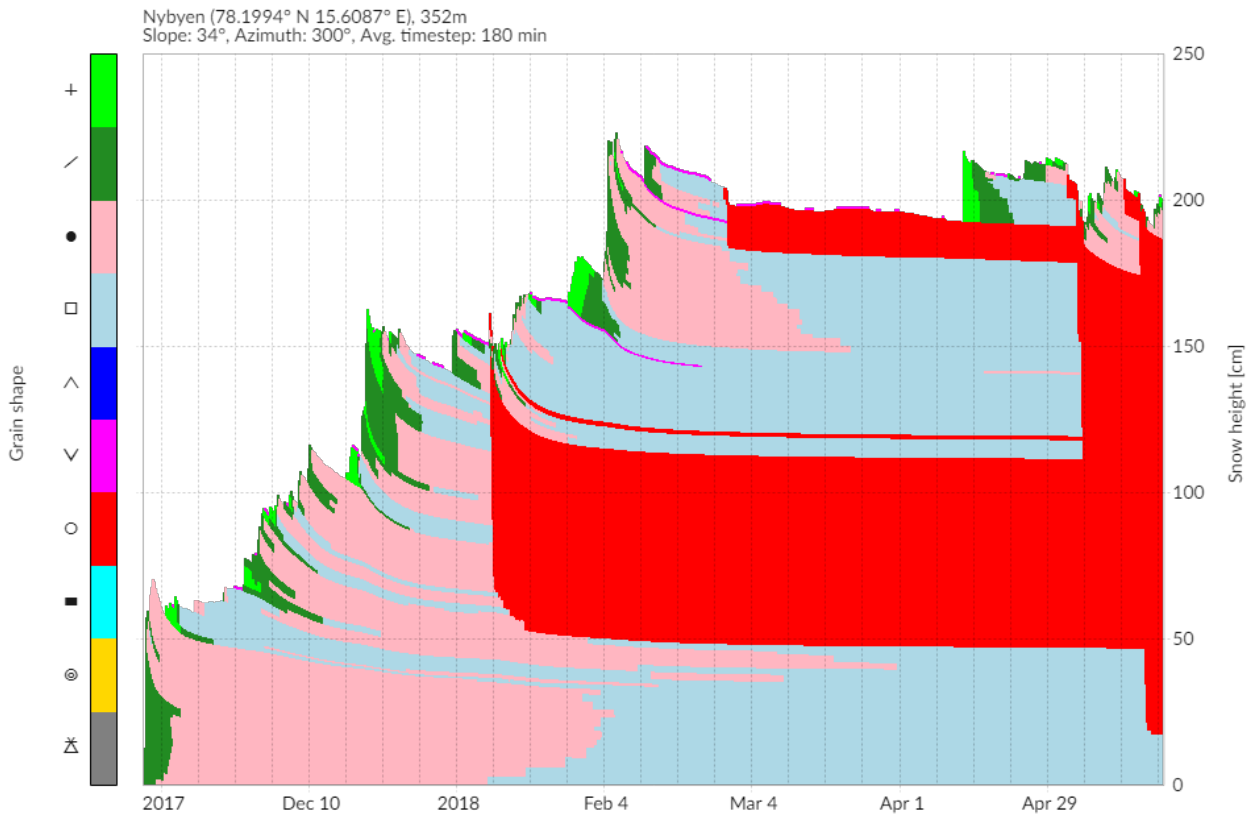
Figure 61: Simulation of grain shape in **Nybyen** from the 8th of November until the 21th of May, with shortwave radiation correction, with mask, with wind data overestimation

Higher wind speeds than on top of the plateau are used, which is not possible, but it is required to get something close to reality regarding the snow profile. Furthermore, the largest coefficient (i.e. 1.25) is senseless because it is attributed to east winds. The main issue is linked with melt forms layers created during rainfalls, and at those times, the wind was blowing from east. This is the reason for this exaggerated correction regarding east winds to understand how it evolves. Figure 61 presents grain shape throughout the snow season with these overestimated correcting factors.

One can see that the precipitation particles transformed into fragmented crystals very rapidly. In comparison with the "optimal" simulation presented above (Figure 44), the proportion of faceted crystals is much more significant with higher winds. It is most likely due to the near-crust faceting process. The goal to get thicker melt forms layer is achieved with two layers of $\simeq$ 60 and $\simeq$ 20 centimetres respectively from the bottom. At the end of the simulation, almost all of the snowpack is made of melt forms, which is expected according to the snow profile realised on the 19th of May. In Appendices H, J and L, one can compare the profiles between the field, the optimal simulation and the simulation with overestimated wind speed.

On the 27th of March (Appendix H), the base of the snowpack modelled with overestimation is closer than the optimal simulation to reality. The bottom has to be made of depth hoar and faceted crystals. As explained, the process for these two types is very close. It is already a good point to detect one of these types. The issue with the overestimated data is the top of the simulation. On the field, layers of precipitation and fragmented particles were found out, which do not appear at all. However, the optimal simulation gives a better layering of the top, which includes fresh snow laying on a crust with near-crust faceted crystals underneath. Even with the overestimated factors, the model cannot detect the melt forms layer supposed to be one metre thick. In contrast, the temperature profile corresponds well to reality.

Comparison for the second profile made in Nybyen was realised on the 24th of April (Figure 62). The result is not good for many reasons. First, the base should be made of two depth hoar layers separated by melt forms. Both simulations show faceted crystals instead. Above, a large layer of melt forms with four thin crusts constituted the main part of the snowpack, modelled as rounded and faceted crystals with a melt forms layer in the optimal simulation and faceted and melt forms in the simulation with overestimated wind data. Again, the wind is probably partly responsible for these errors. Above, faceted crystals are trapped under another melt forms layer. The optimal simulation shows rounded grains, in contrast with the second simulation, which models this part correctly. On top, a thick layer of rounded grains topped by fragmented crystals should appear, which is not the case in any simulations. Instead, several layers of faceted, rounded crystals and even depth hoar are detected in the first simulation. In the second one, the melt forms layer is thicker, and near-crust and near-surface faceted crystals are represented. There are many inconsistencies, even if the temperature gradient is close to reality.
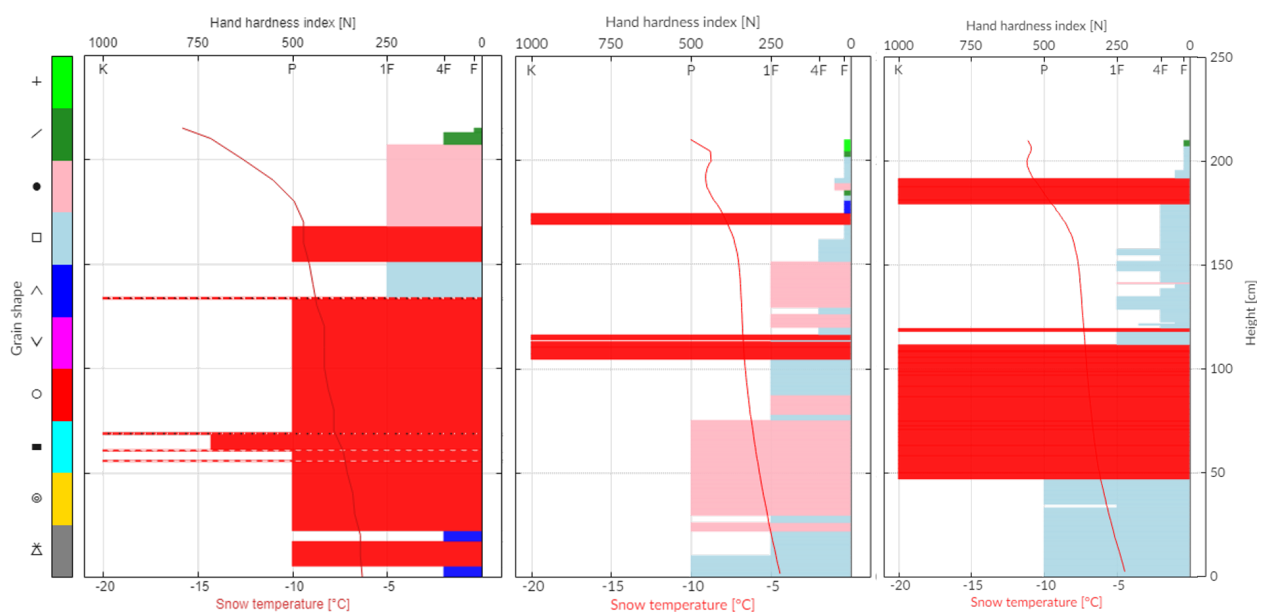
Figure 62: Comparison between the **field** on left side, the **model** in the middle and the **model with wind data overestimation** on right side in **Nybyen** on the 24th of April

The last profile for Nybyen was made on the 19th of May, and the comparison can be seen in Appendix L. It was expected to get exclusively melt forms except for the basal depth hoar layer and a thin layer of fragmented particles at the top. The optimal simulation gives something completely different with several layers of faceted and rounded grains. By contrast with the simulation with overestimated wind data, the result is very close to reality except for rounded grains instead of fragmented particles at the top, but still, it is very close. The model does not detect depth hoar layer at the base, but faceted crystals.

7.1.3 Sverdruphamaren station

The software has relatively well modelled the snowpack in Sverdruphamaren as one can see in Figure 63. The model has detected depth hoar at the base of the snowpack. However, the layer should be thicker (12 centimetres versus 3 centimetres). Above, the first melt forms layer is well represented, with still errors concerning thickness. Although the upper layer should be a sizeable layer of melt forms, the model shows faceted and a thin rounded grains layer in the middle of it. This difference is most likely due to wind data. The second melt forms layer modelled corresponds to reality, but it should be thicker and reach the surface. The upper part of the snowpack is less good because it is supposed to be made only of melt forms and the model detected rounded, fragmented and precipitation particles. Again, wind data is probably responsible for these errors. The temperature profile is too warm, especially for the upper part. Only at 90 centimetres above ground, temperature should reach 0°C. The model calculated that a large part of the snowpack has a temperature of 0°C. Even if, the model shows similarities, it is barely impossible to conclude for this station with only one profile. As a reminder, the station was relatively dangerous to reach with a slope close to 40°.
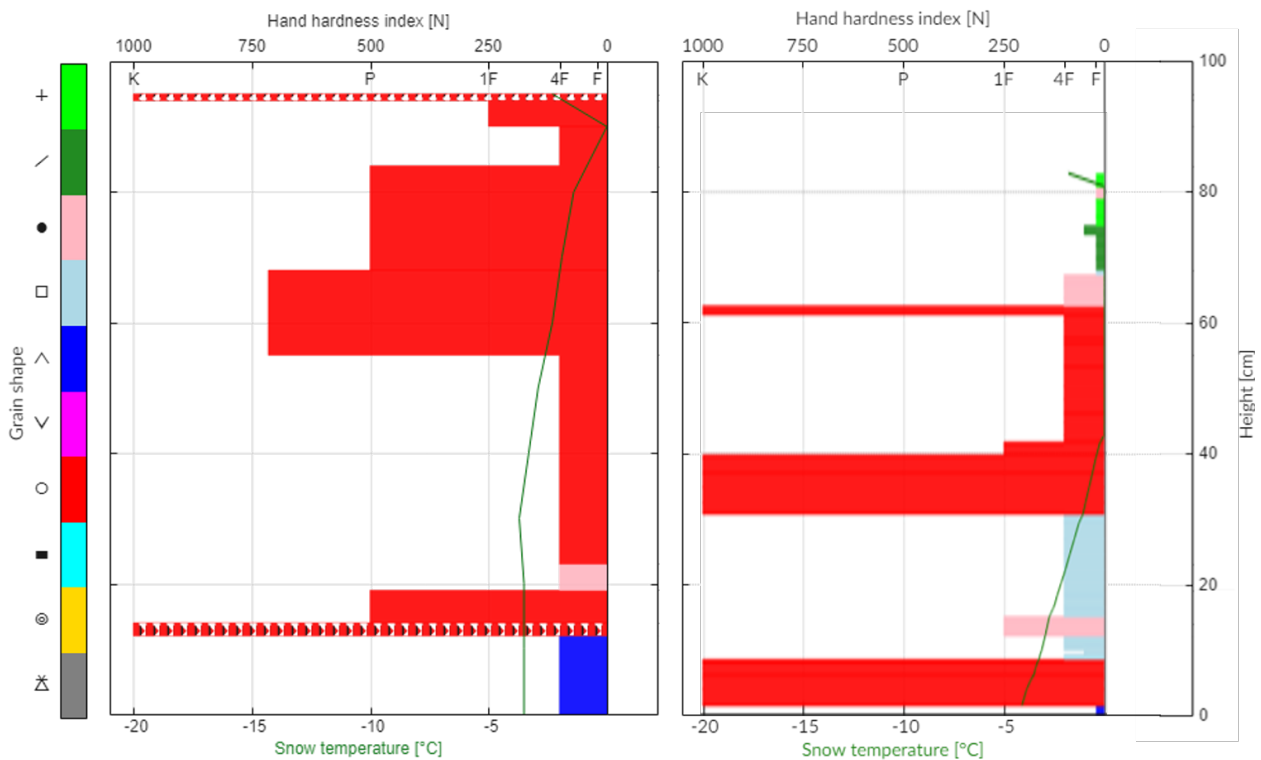
Figure 63: Comparison between the **field** on left side and the **model** on right side in **Sverdruphamaren** on the 14th of May

7.1.4 Summary of comparison

The model detects melt forms layers or crusts created during rainfall. Regarding faceted crystals, they are quite well modelled especially for near-crust and near-surface faceted crystals. The problem is positioning as well as thicknesses simulated of the different layers. The positioning of melt forms layers might be linked with the drop of snow depth during and right after the rainfalls. Looking at Figure 41, just before the 4th of March, one can observe a significant drop in snow depth because of rain. Right after that, snow depth rises again with a supply of fragmented crystals. Instead of fragmented particles, if one replaces by melt forms, the profile becomes much closer to reality. More investigations are required to understand what is the issue. Comparisons have shown that during March, the model works better than later. It is perhaps

a clue to show that radiation data might be a problem in the end. During March radiation data are low and would not affect the snowpack, in contrast with April and May, when the polar day occurs. Radiation amount becomes significant and might have an impact on the snowpack. Nevertheless, first results obtained with SNOWPACK in Svalbard are relatively good and encouraging for the prospect of more common use.

7.2 Limitations of the project - Improvements

The number of the snow pits realised during spring is a limitation. Taking into account weather, avalanche conditions and that two persons had to go on the field, doing more snow pits would have been complicated. The first snow pit was dug on the 27rd of March, after having the right to carry a rifle, one month after the beginning of this project. In any case, it is complicated to do fieldwork before that time, because of the polar night. Still, more snow pits would have been worthwhile, especially at the beginning of the winter. Furthermore, it is essential to consider that I have only a bit of experience with digging snow pits and making snow profiles. Sometimes, crystals look similar and are difficult to differentiate. Thus, the fieldwork might be not so accurate.

This study is limited by the reliability of the data sets used and by the uncertainties of the meteorological measurements. Without IMIS stations, like in Switzerland, a mix of data from at least three stations was required. We have found out that the radiation was not so relevant to model the snowpack in Svalbard. To the contrary, the wind has one of the most significant impacts on the stratification. The adaptation of wind data to other locations with an entirely different aspect and topography is very complex. Getting something close to reality for this particular data, especially in Svalbard, where the weather changes rapidly, is relatively complicated.

In SNOWPACK, a module takes into account snow erosion and snow redistribution. These functions were disabled for this project because few simulations were run with it, and it changed the snow depth entirely throughout the snow season. As the input is the snow depth instead of precipitation, that was not usable since the input should set the snow depth. Furthermore, some phenomena appeared, which were not understandable in the time allowed for this project (i.e. five months). These phenomena consisted in, for example, a high erosion with low winds and a massive snow accumulation with high winds. Besides, the primary parameter for these two functions is the wind. Hence, it is very sensitive to use it since wind data have been adjusted from another station. It exists a variant in SNOWPACK, called Antarctic variant. It could be interesting in a future project to test this option, which is modelling the formation of wind slabs. Unfortunately, it was not possible to use it in this project for reasons of time. More analysis can also be conducted with testing parameters like roughness length and atmospheric stability. Then, more comparison could be made to refine at most the set of parameters.

As shown in Chapter 6.1, there is only a basal layer of depth hoar in Sverdruphamaren while it should be one in every station. This problem is most likely due to snow depth data, especially at the beginning. Eckerstorfer and Christiansen (2011, [20]) assume that the onset of snow cover is very slow in Svalbard, and looking at snow depth data in Lia and Nybyen (Figures 11 and 17), one can see that depths get quite thick rapidly. It can be one reason why temperature gradients are not sufficient to allow the creation of a depth hoar layer at the basis of the snowpack. Indeed, large temperature gradients enable kinematic metamorphism, responsible for the creation of depth hoar. That might also be correct data if the wind was strong enough to bring a lot of snow in a short period.

Finally, to use SNOWPACK efficiently, equipping an anemometer in every snow stations will be very worthwhile. The price is not excessive, and it would bring valuable information to the model. Indeed, the correction used in this project are too simplistic. According to Lonardi (2018, [37]), there is a channelling effect on the wind. It means that the wind changes its direction (going down the valley, from south-southwest). It means that for the three snow stations, located in Longyeardalen, most of the wind should come from south and southwest. Without an anemometer to measure it, it is impossible to guess the wind patterns in the valley. Moreover, it is complicated to know if this effect affects the slopes where snow stations are. Having anemometers would definitively help a lot with the development of SNOWPACK use in Svalbard.

8 Conclusion

Growing interest for Svalbard attracts many people either for scientific research, but also many tourists interested by this Arctic raw nature. The mountainous terrain is favourable for avalanches even close to Longyearbyen, the largest settlement. Hence, more people are exposed to avalanches without knowing the risks.

The primary aim of this project was to test the applicability and the performances of the software SNOW-PACK in Svalbard. First, a description of snow shapes and metamorphism has been made to have a theoretical background of the subject. Then, SNOWPACK and other snow numerical models are studied to be aware of possibilities and requirements to run these softwares. The study area is described in details, especially the weather stations necessary for the simulations. Data from those stations are processed and graphically analysed with Matlab. First indications allow guessing to what the snowpack will look like. Matlab also allows creating the input files in SMET format. Simulations for three stations are run to assess SNOWPACK from November to May.

Radiation and wind data are not measured on test sites. Thus, they are collected on two additional stations. Because of the different location, sensitivity analyses are conducted. Results show that radiation data do not impact that much, but minor corrections are still applied. The use of a mask, which produce the right amount of shading is created with ArcGIS. The horizons seen from every test sites are integrated into the model to reduce the amount of sunlight. Regarding wind data, results show that adjustments have to be done, as it impacts significantly on the snowpack stratification. The challenge was to find the best way to adjust them, taking into account the available resources and the time allowed for this project. To do so, results are compared with snow profiles realised during spring.

Seven snow profiles were realised and compared to simulations results. Even if the modelled profiles do not fit perfectly reality, information about the layering is still valuable. Nevertheless, satisfactory and encouraging results were obtained with the prospect of more widespread use in Svalbard. One of the main issues is that wind data force the results. Without proper wind measurements on every test sites, improve the results quality seems to be compromised. To overcome this issue, adding an anemometer in every snow station would bring much more accuracy to results. In reality, the wind undergoes a channelling effect, without knowing its limitations. Moreover, having more snow stations facing other directions than east and northwest would be excellent additional information. The ultimate goal of this project would be to integrate all the provided information by the model into the actual avalanche forecast. It would allow saving much time, especially when going out on the field is not recommended because of the weather or avalanche conditions.

Snowprofile: Lia Snow Station

Name: Michael Lonardi and Martin Pra...	**e-mail:** martin.praz@epfl.ch	**Observation date:** 28. Mar. 2018 17:00
Location: Lia Snow Station	**Elevation:** 100 m	**Air temperature:** -12.0°C
Subregion: [n/def]	**Incline [°]:** 32°	**Precipitation:** No precipitation
Region: Other	**Aspect:** NW	**Intensity:**
Country: Other	**Wind speed:** Gentle (< 20 km/h)	**Sky condition:** Broken (5/8 - 7/8)
Lat/Long : 78.2154° / 15.6494°	**Wind direction:** NE	**Profile-class:** not classified

+ Precip. particles   ● Rounded grains   ∧ Depth hoar   ○ Melt forms   ⊟ Faceted, rounded   ◎ Melt-freeze crust
╱ Decomp. / fragm.   □ Faceted crystals   ∨ Surface hoar   ■ Ice formations   ⋈ Graupel

Comments:
CT 31: no break

H (cm)	Ø	F¹	F²	D (mm)	K	Lemon	Test
160	1	+	+	1.0 - 1.5	1		
	1	╱	╱	0.5 - 0.75	2	000	
150	1	●	□	0.25 - 0.75	5	00	
140	1	○	○	0.25 - 0.75	5	0	
120	1	○	○	0.25 - 0.75	4	0	
100	1	○	○	0.25 - 0.5	4	00	
90	1	○	○	0.25 - 0.5	3	0	
80	1	◎		0.25 - 0.75	5	00	
	1	□	□	0.75 - 1.0	2	000	
70	1	◎		0.5 - 0.75	5	000	
	1	□	□	0.75 - 1.0	2	000	
60	1	◎		0.5 - 0.75	5	00	
	1	□	□	1.0 - 2.0	2	000	
40	1	○	□	0.5 - 1.0	5	000	
30	1	○	□	1.0 - 1.5	3	00	
20	1	●	□	0.25 - 0.5	4	0	
10	1	□	●	0.5 - 1.0	2	00	

Temperature readings: -12.0°C, -12.5°C, -12.3°C, -12.7°C, -12.7°C, -12.4°C, -12.3°C, -12.2°C, -11.5°C, -10.9°C, -10.3°C, -9.4°C, -8.9°C, -8.8°C, -7.9°C, -7.2°C, -6.8°C, -5.7°C

T(°C): -22 -20 -18 -16 -14 -12 -10 -8 -6 -4 -2 0
R(N): 1100 1000 900 800 700 600 500 400 300 200 100 0
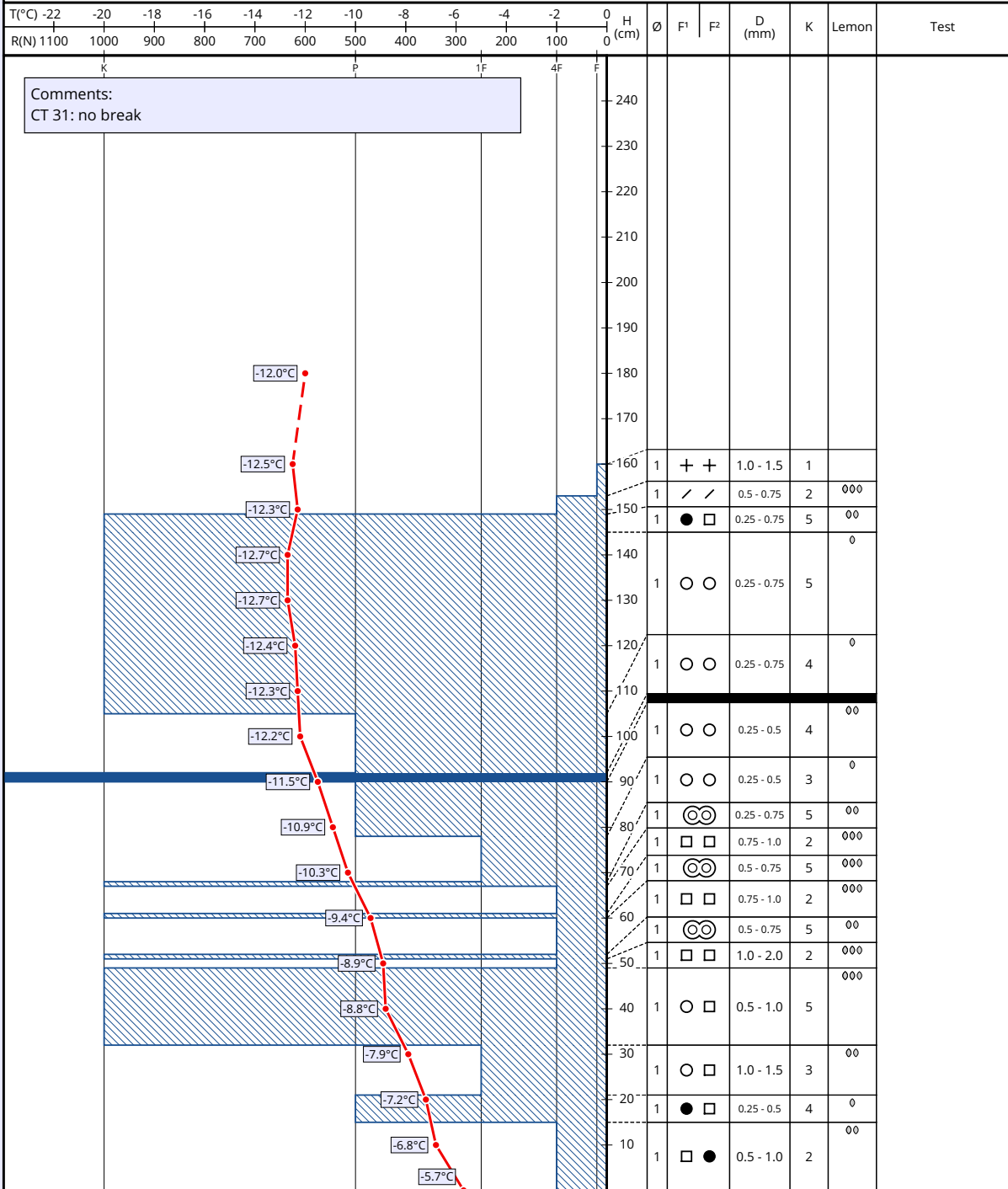
Appendix B   Comparison in Lia on the 28th of March

Figure 64: Comparison between the **field** on left side and the **model** on right side in **Lia** on the 28th of March

Appendix C   Snow profile : Lia station on the 17th of April

Snowprofile: Lia Snow Station

Name: Martin Praz	**e-mail:** martin.praz@epfl.ch	**Observation date:** 17. Apr. 2018 15:00

Location: Lia Snow Station	**Elevation:** 100 m	**Air temperature:** -7.3°C
Subregion: [n/def]	**Incline [°]:** 32°	**Precipitation:** No precipitation
Region: Other	**Aspect:** NW	**Intensity:**
Country: Other	**Wind speed:** Moderate (20 - 40 km/h)	**Sky condition:** Few (1/8 - 2/8)
Lat/Long : 78.2154° / 15.6494°	**Wind direction:** SW	**Profile-class:** not classified

Legend:
+ Precip. particles   ● Rounded grains   ∧ Depth hoar   O Melt forms   ⊡ Faceted, rounded   ◉◯ Melt-freeze crust
╱ Decomp. / fragm.   □ Faceted crystals   ∨ Surface hoar   ■ Ice formations   ⨉ Graupel

H (cm)	Ø	F¹ F²	D (mm)	K	Lemon	T(°C)
~185	1	◉◯	0.25 - 0.5	3 - 4		
~180	1	╱ ╱	0.25 - 0.5	1	000	
~175	1	⊓ ⊓	0.25 - 0.5	4	000	
~170	1	◉◯	0.5	5	0	
~163	1	O □	0.5 - 0.75	5	0	
~157	1	□ □	0.25 - 0.75	2	000	-7.3°C
~150	1	◉◯	0.5	5	000	
~145	1	□ □	0.5 - 0.75	2	000	
~140	1	O □	0.25 - 0.75	4 - 5	000	-7.2°C
~125	1	● ●	0.25 - 0.5	4	0	-6.2°C
~112	1	O □	0.25 - 0.5	4 - 5	0	
~107	1	◉◯	0.5	5	0	-5.7°C
~100	1	∧ ∧	1.0 - 3.0	2	00000	-5.7°C
~90	1	□ □	0.25 - 0.5	4	00000	-6.0°C
~80	1	◉◯	0.5	5	00	-6.1°C
~75	1	∧ ∧	1.0 - 3.0	2 - 3	00000	
~70	1	◉◯	0.5	5	00000	-6.1°C
~63	1	∧ ∧	1.0 - 1.5	3	0000	
~60	1	O □	0.5 - 0.75	5	0000	-5.9°C
~53	1	∧ ∧	1.0 - 3.0	2 - 3	00000	
~47	1	O □	0.5 - 1.0	4 - 5	00000	
~43	1	∧ ∧	1.0 - 3.0	2	00000	
~25	1	□ □	0.25 - 0.75	3	0000	-5.7°C / -5.3°C
~10	1	◉◯	0.5	5	00	-5.3°C
~3	1	∧ ∧	1.0 - 3.0	2	0000	-5.2°C

Appendix D Comparison in Lia on the 17th of April
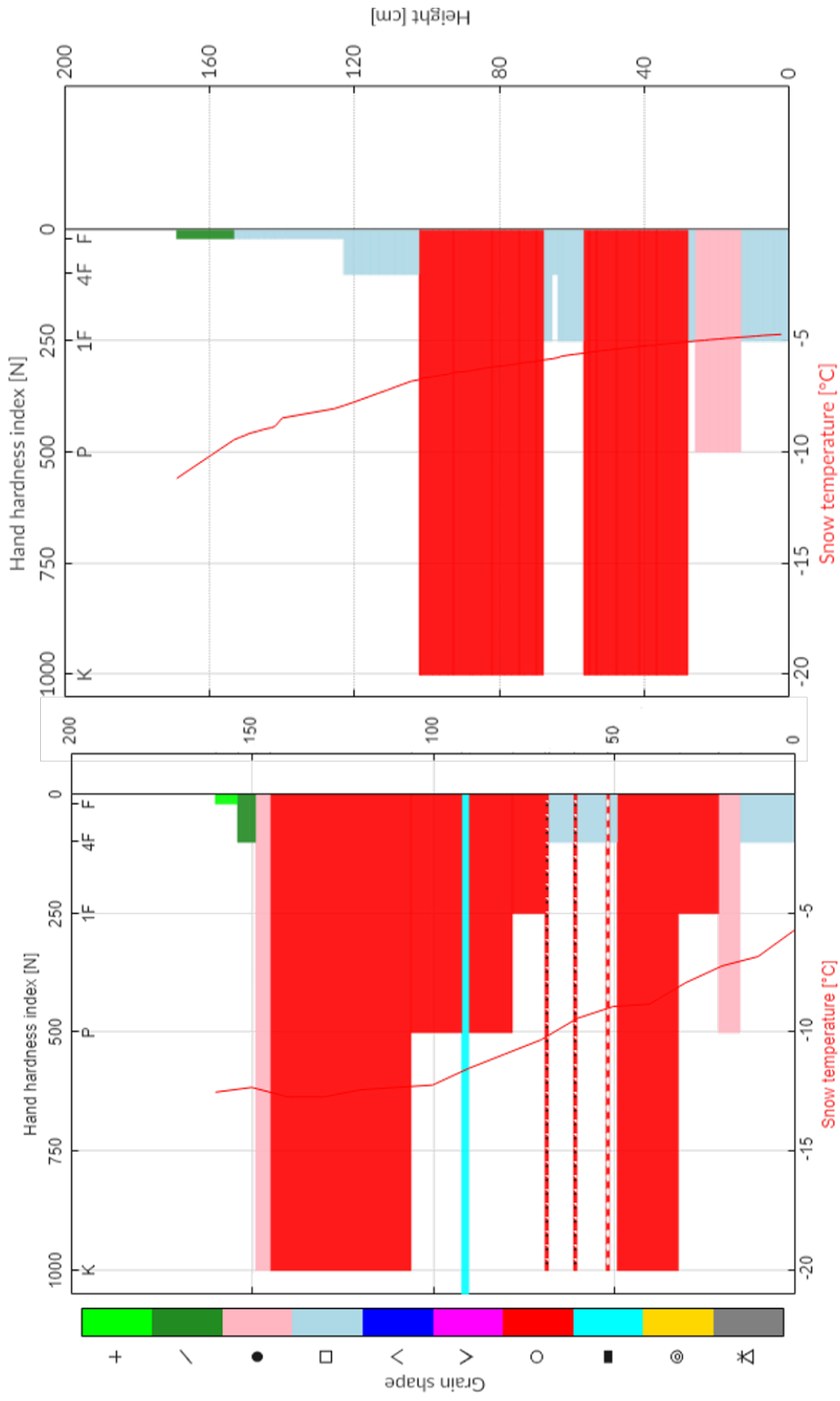

Figure 65: Comparison between the **field** on left side and the **model** on right side in **Lia** on the 17th of April

Appendix E   Snow profile : Lia station on the 3rd of May

Snowprofile: Lia Snow Station

Name: Martin Praz	**e-mail:** prazmartin@gmail.com	**Observation date:** 03. May. 2018 14:00

Location: Lia Snow Station	**Elevation:** 121 m	**Air temperature:** 3.5°C
Subregion: [n/def]	**Incline:** 32°	**Precipitation:** No precipitation
Region: Other	**Aspect:** NW	**Intensity:**
Country: Other	**Wind speed:** Gentle (< 20 km/h)	**Sky condition:** Scattered (3/8 - 4/8)
Lat/Long : 78.2154° / 15.6494°	**Wind direction:** S	**Profile-class:** not classified

Legend:
+ Precip. particles   ● Rounded grains   ∧ Depth hoar   O Melt forms   ⌂ Faceted, rounded   Melt-freeze crust
╱ Decomp. / fragm.   □ Faceted crystals   ∨ Surface hoar   ■ Ice formations   ⋈ Graupel

T(°C) -22 -20 -18 -16 -14 -12 -10 -8 -6 -4 -2 0
R(N) 1100 1000 900 800 700 600 500 400 300 200 100 0

H (cm)	Ø	F¹	F²	D (mm)	K	Lemon	kg/m³	Test
160	3	O O		0.25 - 0.5	2 - 3			
160	2	⊙⊙		0.5	4 - 5	oo		
	2	O O		0.25 - 0.5	4	o		
130	1	⊙⊙		0.5	5	o		
	1	O O		0.25 - 0.75	4	o		
40	1	O O		0.5 - 1.0	3			
30	1	O O		0.5 - 1.5	4	o		
10	1	∧ ∧		1.0 - 3.0	2	oooo		

Temperature readings: 3.5°C, -0.3°C, -1.4°C, -1.9°C, -2.8°C, -3.3°C, -3.7°C, -4.2°C, -4.6°C, -5.2°C, -5.7°C, -6.0°C, -6.2°C, -6.2°C, -6.2°C, -6.0°C, -5.9°C
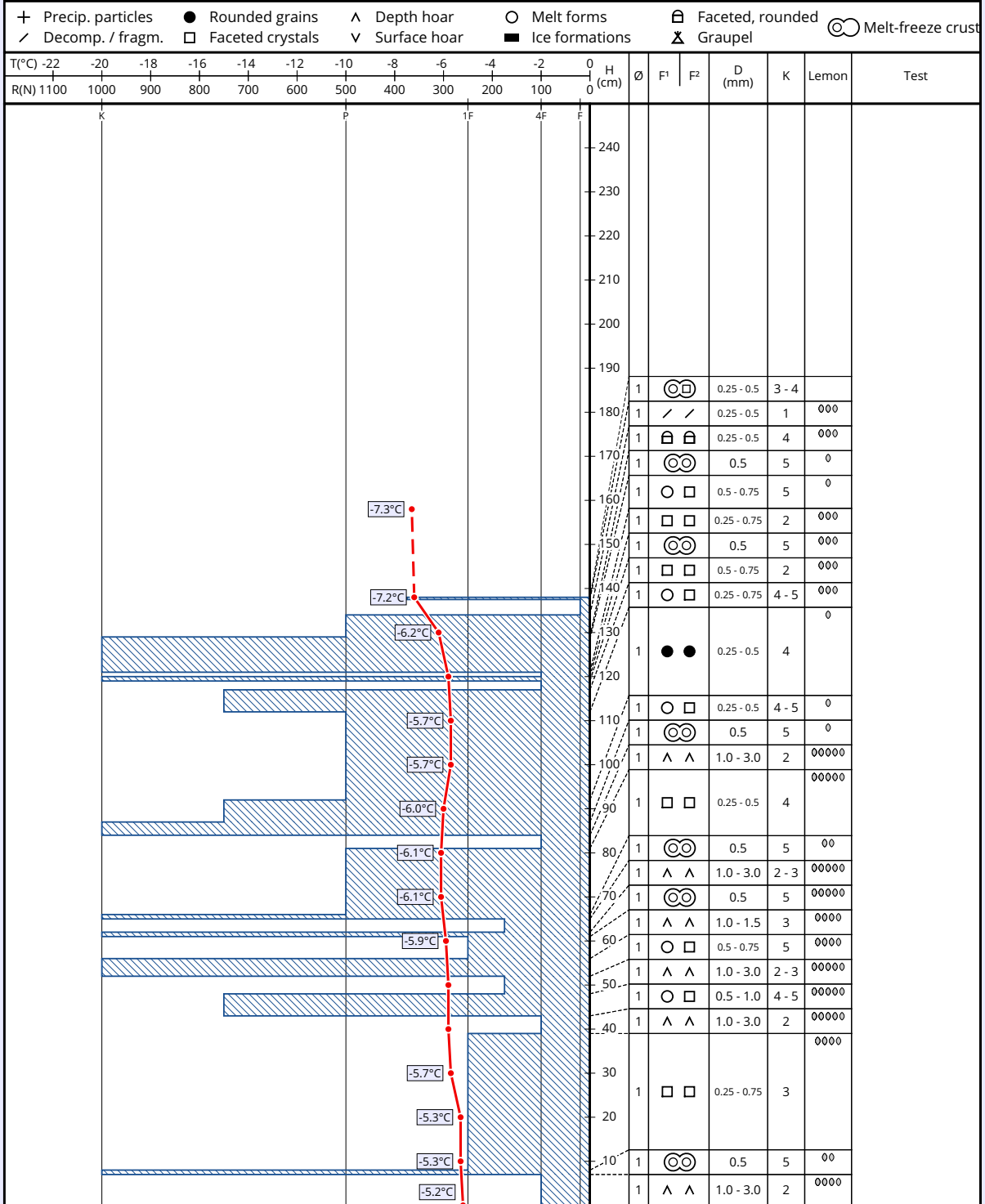
Appendix F   Comparison in Lia on the 3rd of May
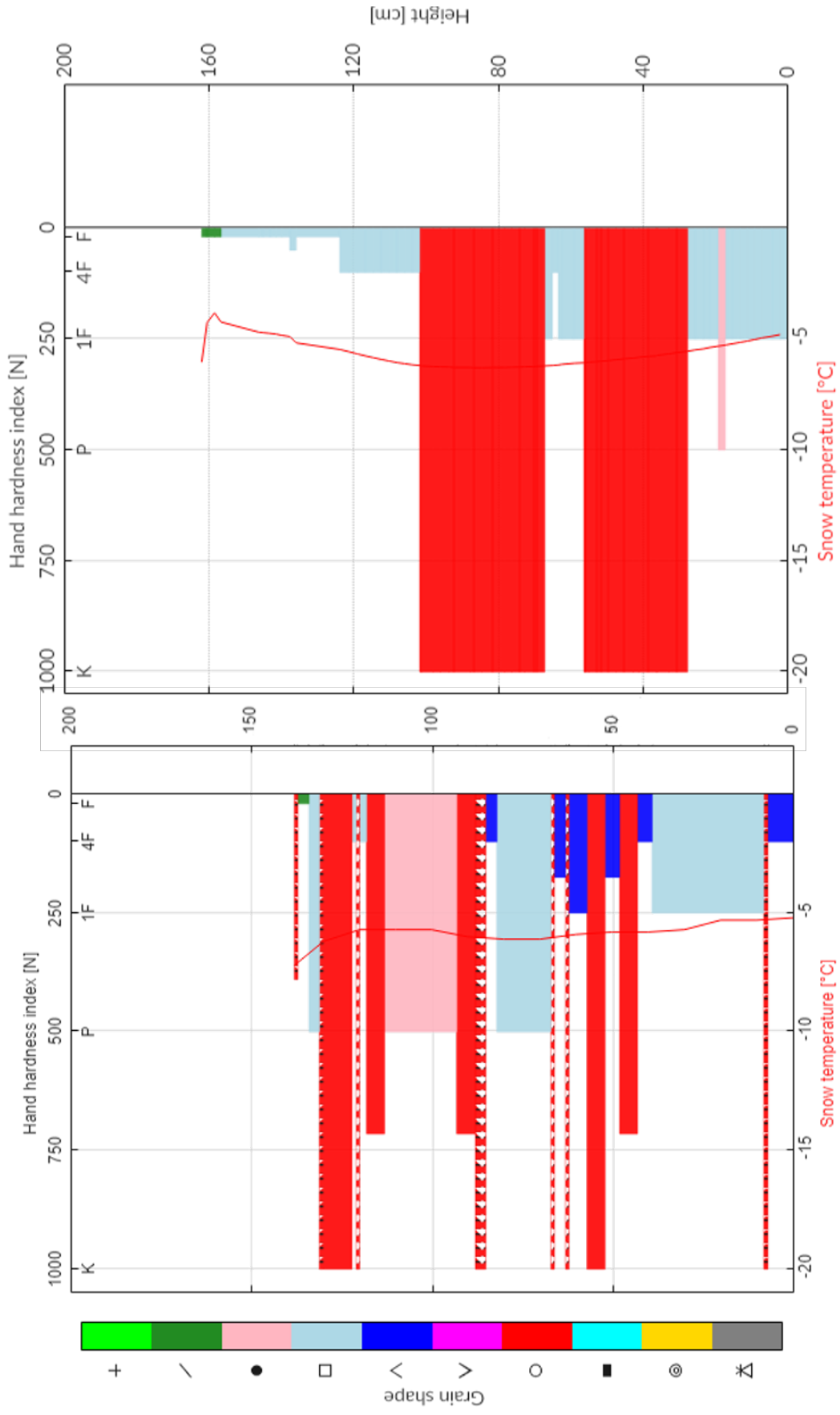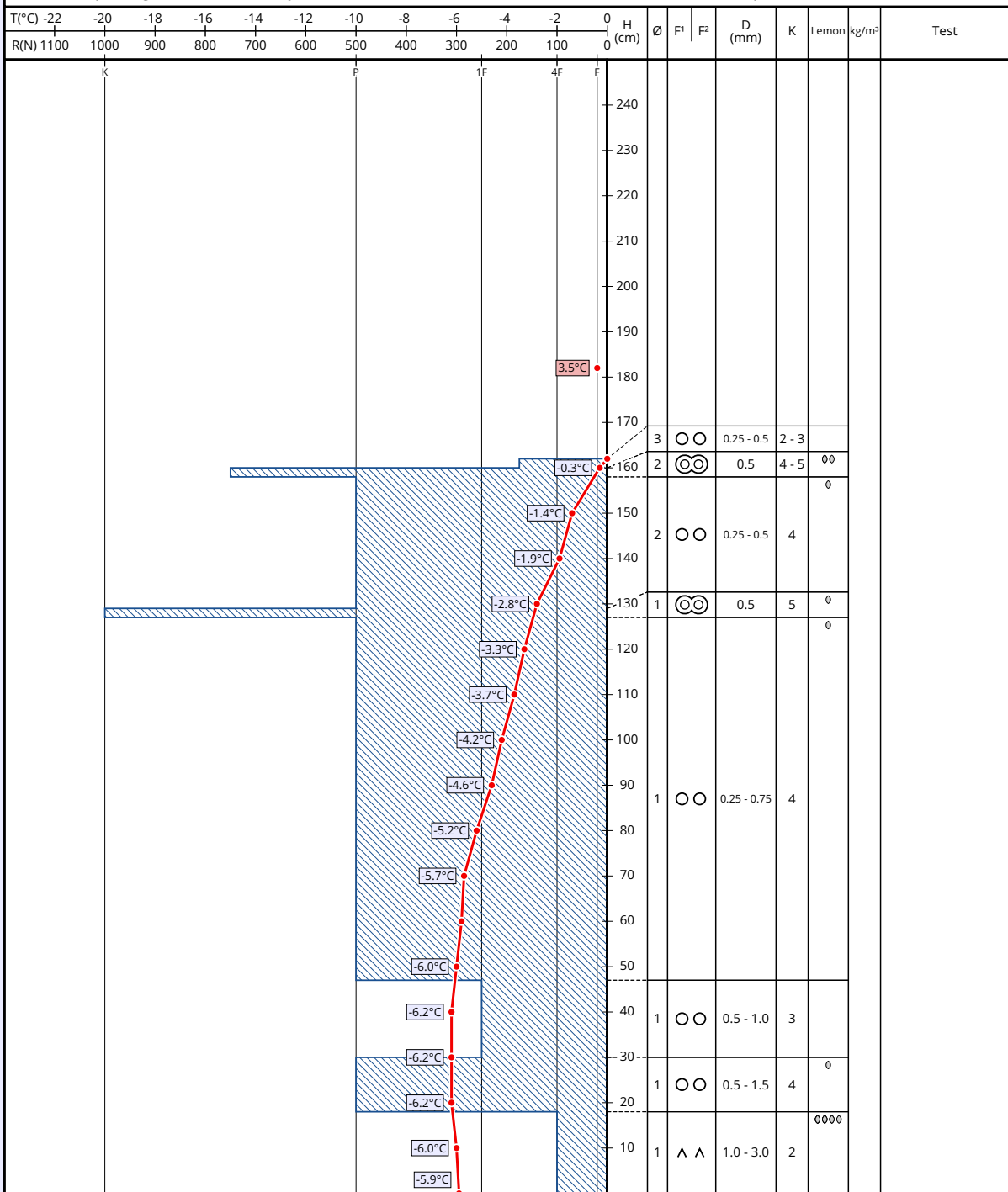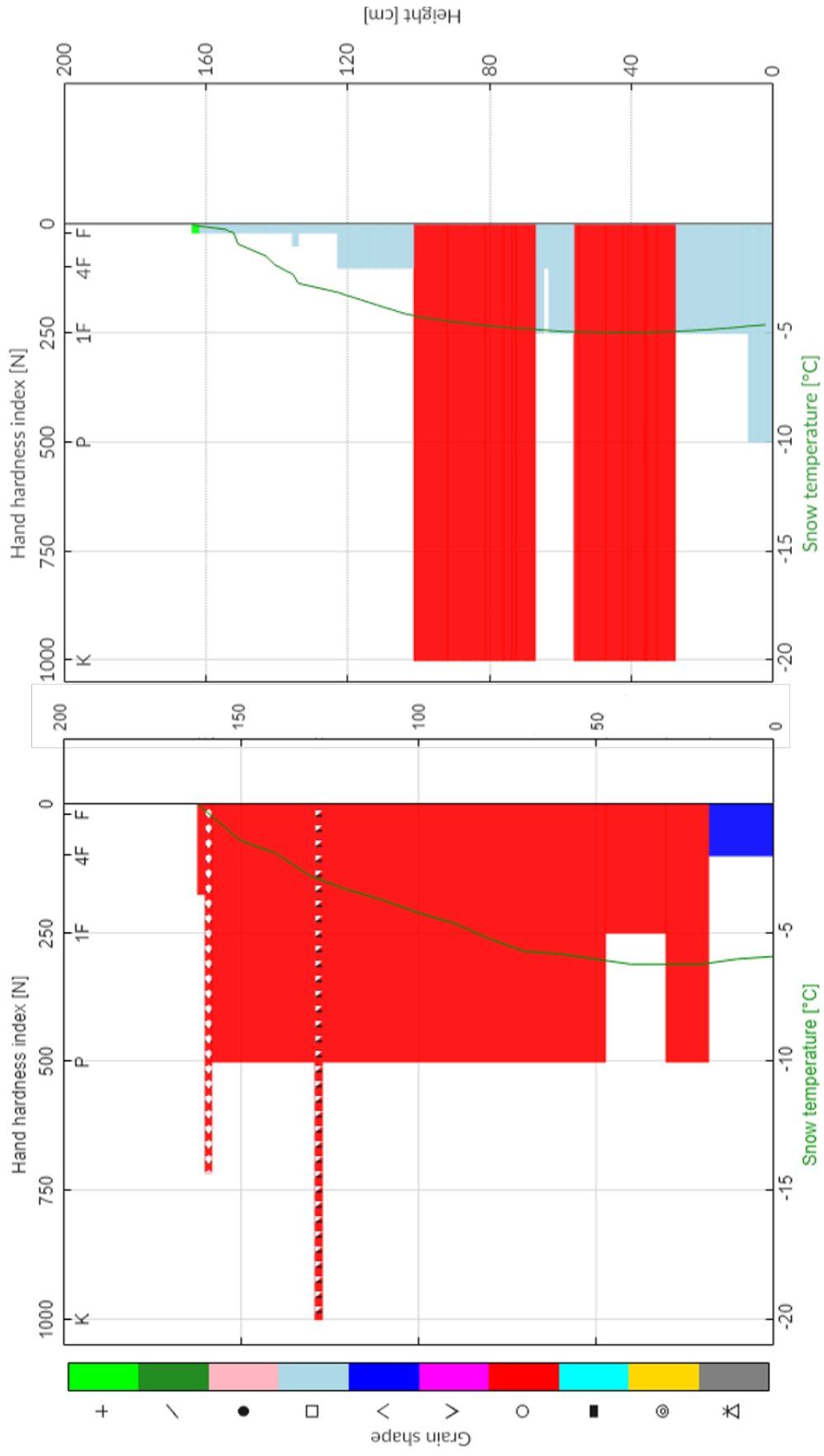

Figure 66: Comparison between the **field** on left side and the **model** on right side in **Lia** on the 3rd of May

Snowprofile: Nybyen Snow Station

Name: Martin Praz and Alex Prokop	**e-mail:** alexander.prokop@unis.no	**Observation date:** 27. Mar. 2018 13:00

Location: Nybyen Snow Station	**Elevation:** 358 m	**Air temperature:** -15.0°C
Subregion: [n/def]	**Incline [°]:** 34°	**Precipitation:** No precipitation
Region: Other	**Aspect:** W	**Intensity:**
Country: Other	**Wind speed:** Calm (0 km/h)	**Sky condition:** Few (1/8 - 2/8)
Lat/Long : 78.1991° / 15.609°	**Wind direction:**	**Profile-class:** not classified

+ Precip. particles	● Rounded grains	∧ Depth hoar	○ Melt forms	⬠ Faceted, rounded	◎ Melt-freeze crust
╱ Decomp. / fragm.	☐ Faceted crystals	∨ Surface hoar	■ Ice formations	⤬ Graupel	

Comments:
CT 20@140.0cm: resistant break planar (RP)
ECT 31: no break

H (cm)	Ø	F¹	F²	D (mm)	K	Lemon	Test
170	1	●	╱	0.25 - 0.5	1		
160	1	●	╱	0.5 - 0.75	2	00	
150	1	◎◎		0.5 - 1.0	5	00	
140	1	☐ ☐		0.25 - 0.5	2	000	CT20
130	1	○ ○		0.25 - 0.75	4	000	
120	1	○ ○		0.25 - 0.75	3	0	34°
90	1	○ ○		0.25 - 0.75	4	0	
60	1	◎⬠		0.5 - 1.0	4 - 5	0	
40	1	☐ ○		0.25 - 0.5	3	0	
10	1	∧ ○		1.0 - 3.0	2 - 3	000	

Temperature readings: -15.0°C, -20.0°C, -16.0°C, -14.0°C, -13.0°C, -12.3°C, -11.6°C, -11.3°C, -10.7°C, -10.5°C, -9.9°C, -9.4°C, -8.4°C, -7.8°C, -6.8°C, -6.8°C, -5.9°C, -5.9°C, -5.8°C
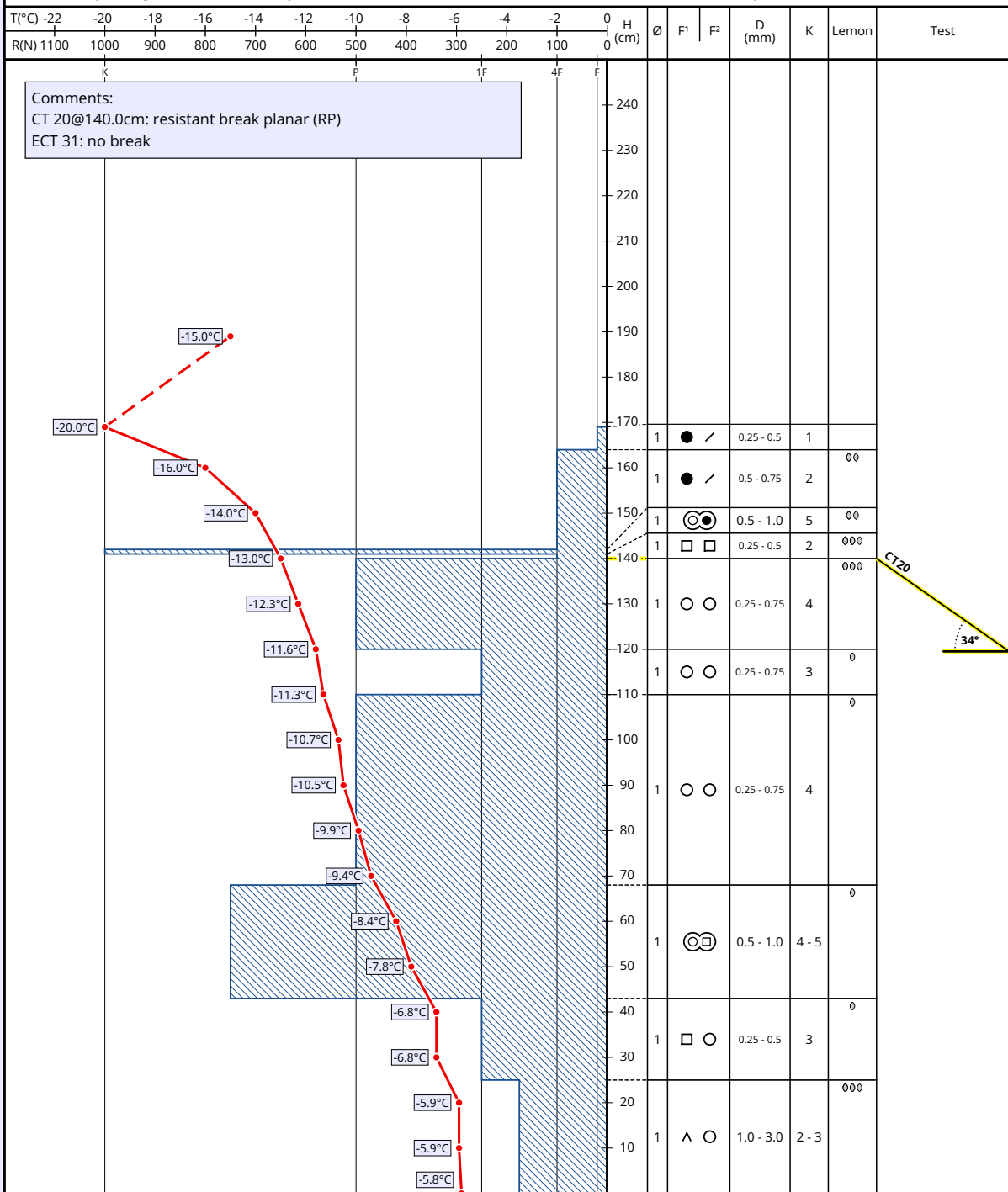
Appendix H Comparison in Nybyen on the 27th of March

Figure 67: Comparison between the **field** on left side, the **model** in the middle and the **model with wind data overestimation** on right side in **Nybyen** on the 27th of March

Appendix I Snow profile : Nybyen station on the 24th of April

Snowprofile: Nybyen Snow Station

Name: Martin Praz	**e-mail:** prazmartin@gmail.com	**Observation date:** 24. Apr. 2018 13:00
Location: Nybyen Snow Station	**Elevation:** 358 m	**Air temperature:** -15.0°C
Subregion: [n/def]	**Incline [°]:** 34°	**Precipitation:** No precipitation
Region: Other	**Aspect:** W	**Intensity:**
Country: Other	**Wind speed:** Gentle (< 20 km/h)	**Sky condition:** Clear (0/8)
Lat/Long : 78.1991° / 15.609°	**Wind direction:** S	**Profile-class:** not classified

Symbol	Description	Symbol	Description	Symbol	Description	Symbol	Description	Symbol	Description	Symbol	Description
+	Precip. particles	●	Rounded grains	∧	Depth hoar	O	Melt forms	⌂	Faceted, rounded	∞	Melt-freeze crust
∕	Decomp. / fragm.	□	Faceted crystals	∨	Surface hoar	■	Ice formations	⋊	Graupel		

66

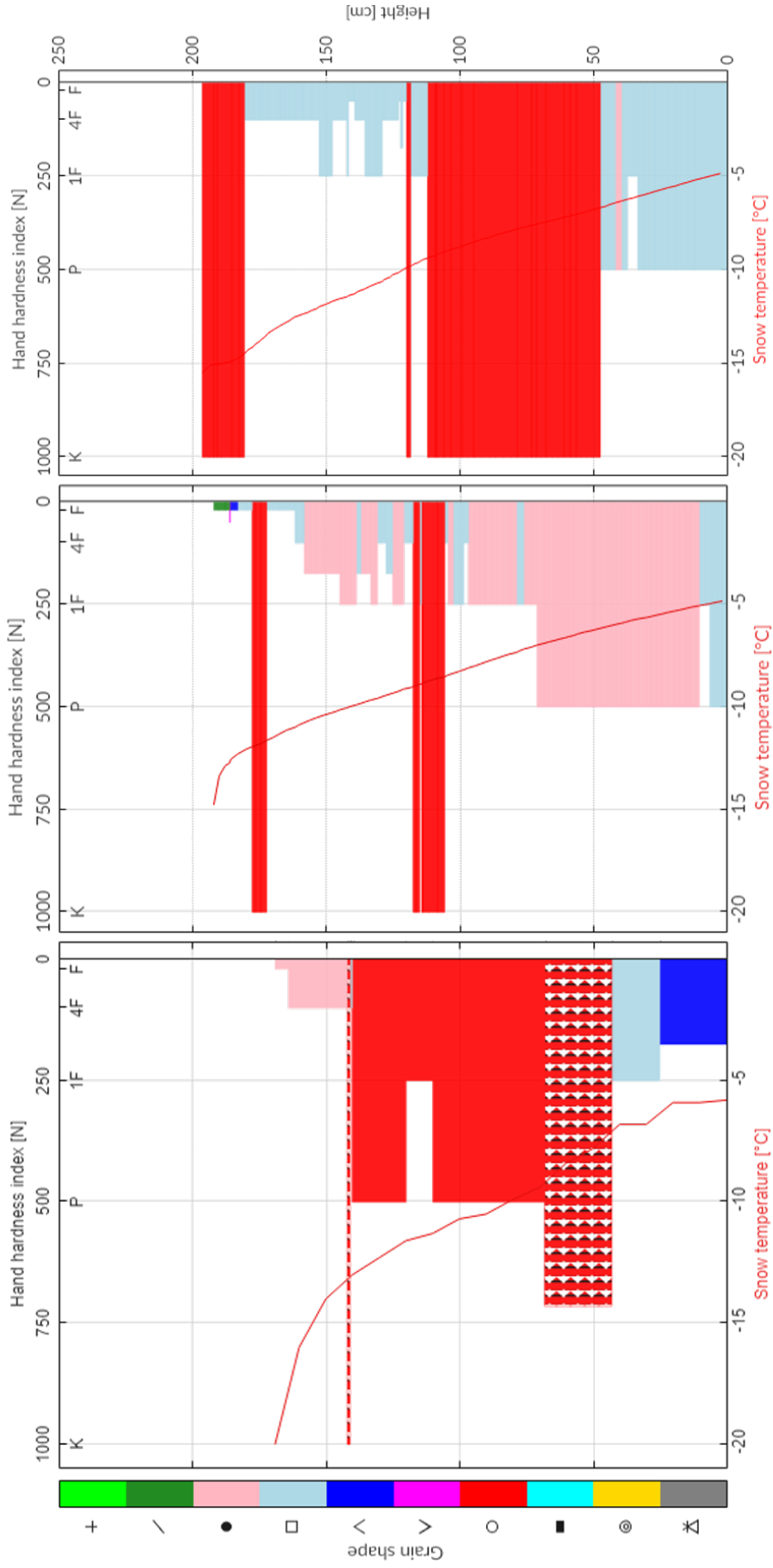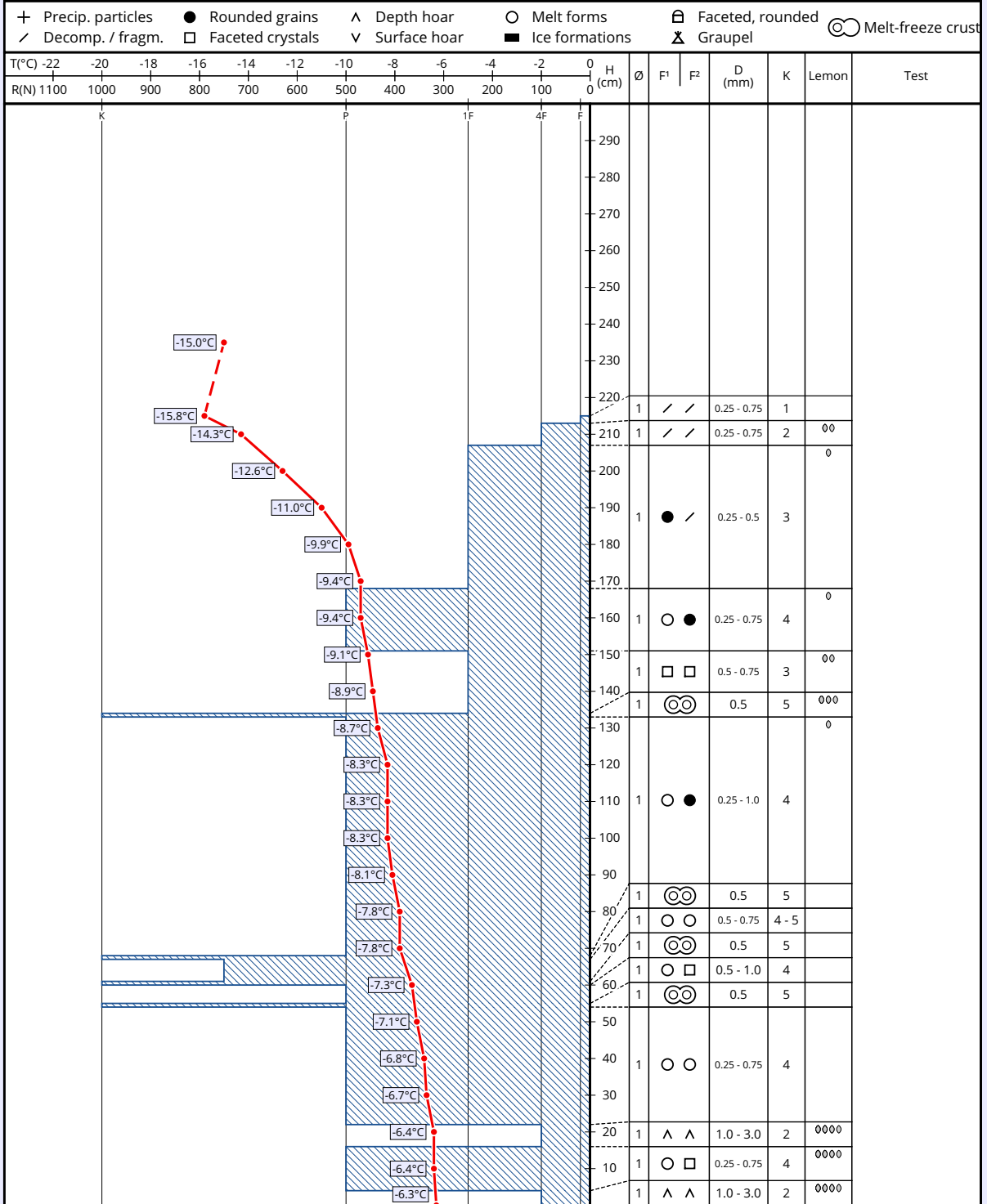# Appendix J   Comparison in Nybyen on the 24th of April
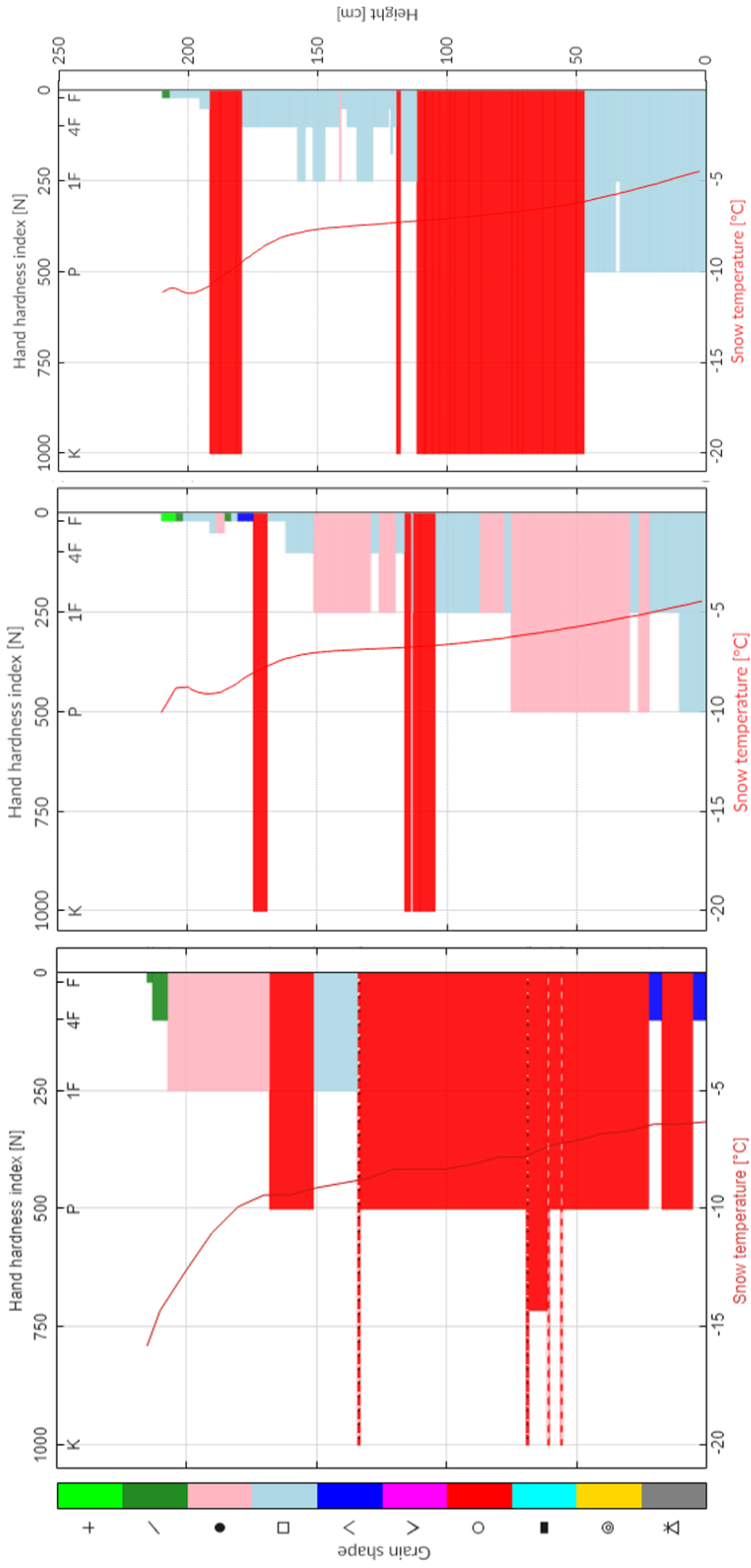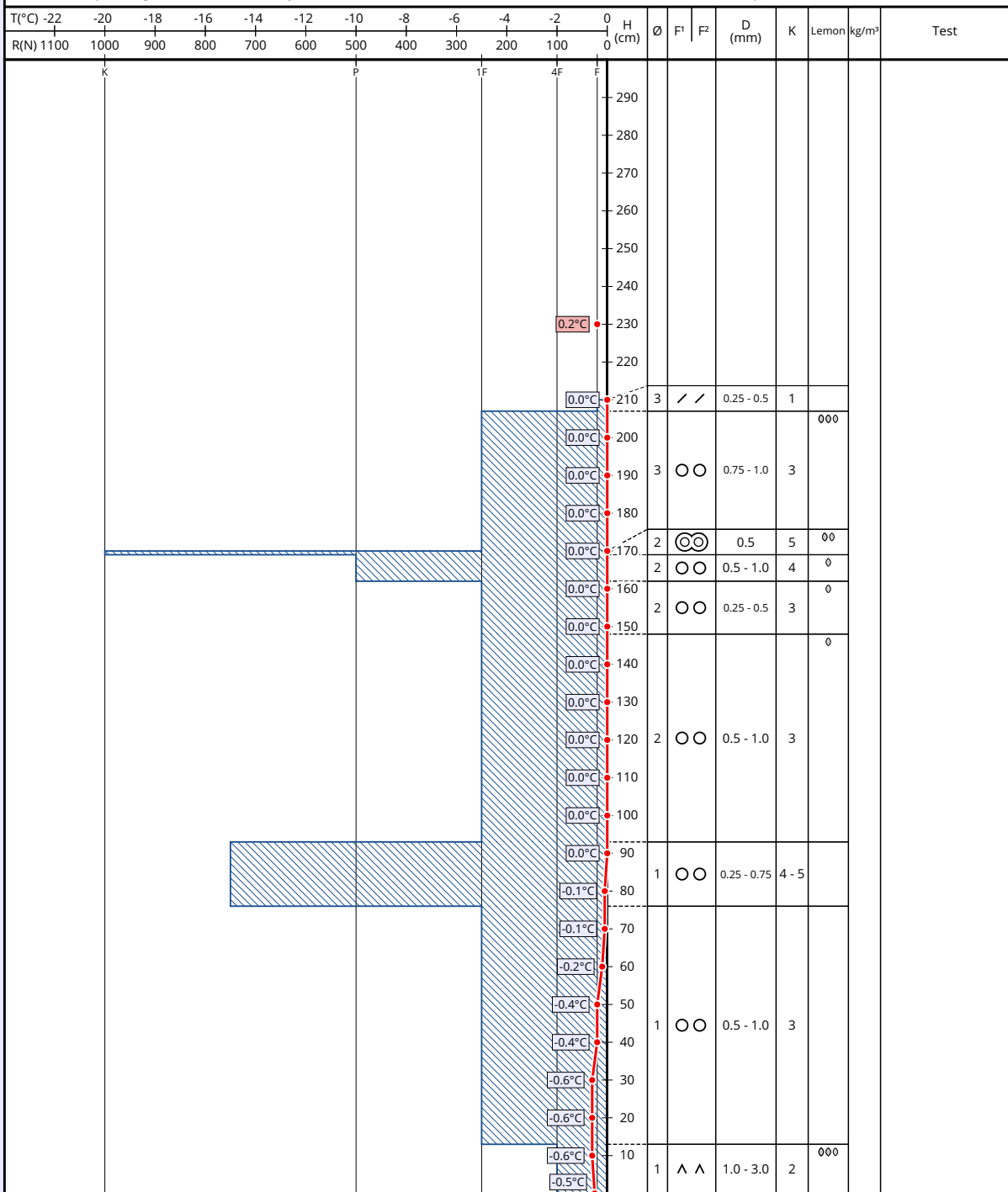

Figure 68: Comparison between the **field** on left side, the **model** in the middle and the **model with wind data overestimation** on right side in **Nybyen** on the 24th of April

Snowprofile: Nybyen Snow Station

Name: Martin Praz	**e-mail:** prazmartin@gmail.com	**Observation date:** 19. May. 2018 14:00
Location: Nybyen Snow Station	**Elevation:** 358 m	**Air temperature:** 0.2°C
Subregion: [n/def]	**Incline:** 34°	**Precipitation:** Sleet
Region: Other	**Aspect:** W	**Intensity:** Light
Country: Other	**Wind speed:** Gentle (< 20 km/h)	**Sky condition:** Overcast (8/8)
Lat/Long : 78.1991° / 15.609°	**Wind direction:** S	**Profile-class:** not classified

Legend:
- + Precip. particles
- / Decomp. / fragm.
- ● Rounded grains
- □ Faceted crystals
- ∧ Depth hoar
- ∨ Surface hoar
- ○ Melt forms
- ■ Ice formations
- ⬠ Faceted, rounded
- X Graupel
- ⊙⊙ Melt-freeze crust

H (cm)	T	Ø	F¹	F²	D (mm)	K	Lemon	kg/m³	Test
230	0.2°C								
210	0.0°C	3	/ /		0.25 - 0.5	1			
200	0.0°C						000		
190	0.0°C	3	○ ○		0.75 - 1.0	3			
180	0.0°C								
170	0.0°C	2	⊙⊙		0.5	5	00		
160	0.0°C	2	○ ○		0.5 - 1.0	4	0		
150	0.0°C	2	○ ○		0.25 - 0.5	3	0		
140	0.0°C						0		
130	0.0°C								
120	0.0°C	2	○ ○		0.5 - 1.0	3			
110	0.0°C								
100	0.0°C								
90	0.0°C	1	○ ○		0.25 - 0.75	4 - 5			
80	-0.1°C								
70	-0.1°C								
60	-0.2°C								
50	-0.4°C	1	○ ○		0.5 - 1.0	3			
40	-0.4°C								
30	-0.6°C								
20	-0.6°C								
10	-0.6°C	1	∧ ∧		1.0 - 3.0	2	000		
0	-0.5°C								

T(°C): -22, -20, -18, -16, -14, -12, -10, -8, -6, -4, -2, 0
R(N): 1100, 1000, 900, 800, 700, 600, 500, 400, 300, 200, 100, 0

K, P, 1F, 4F, F

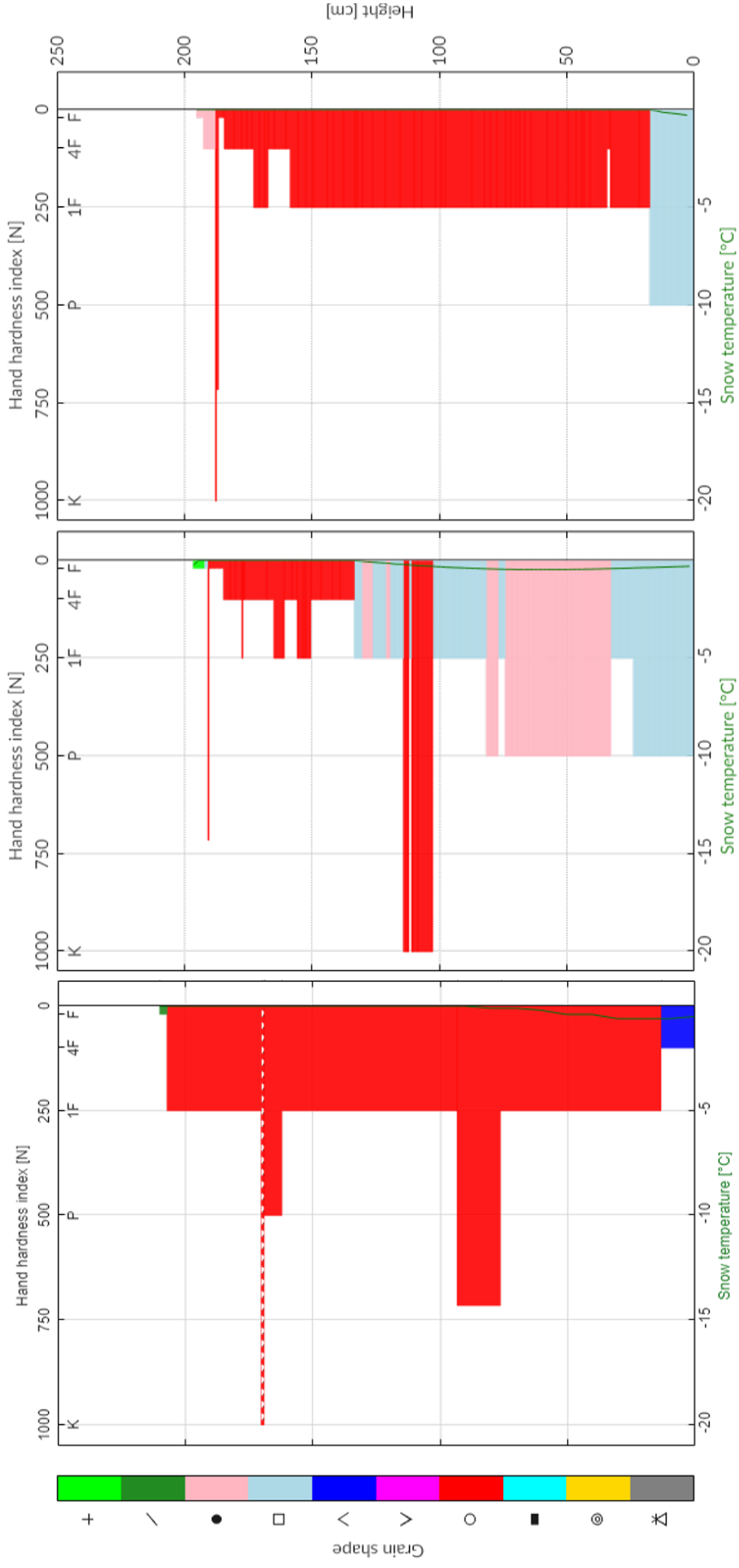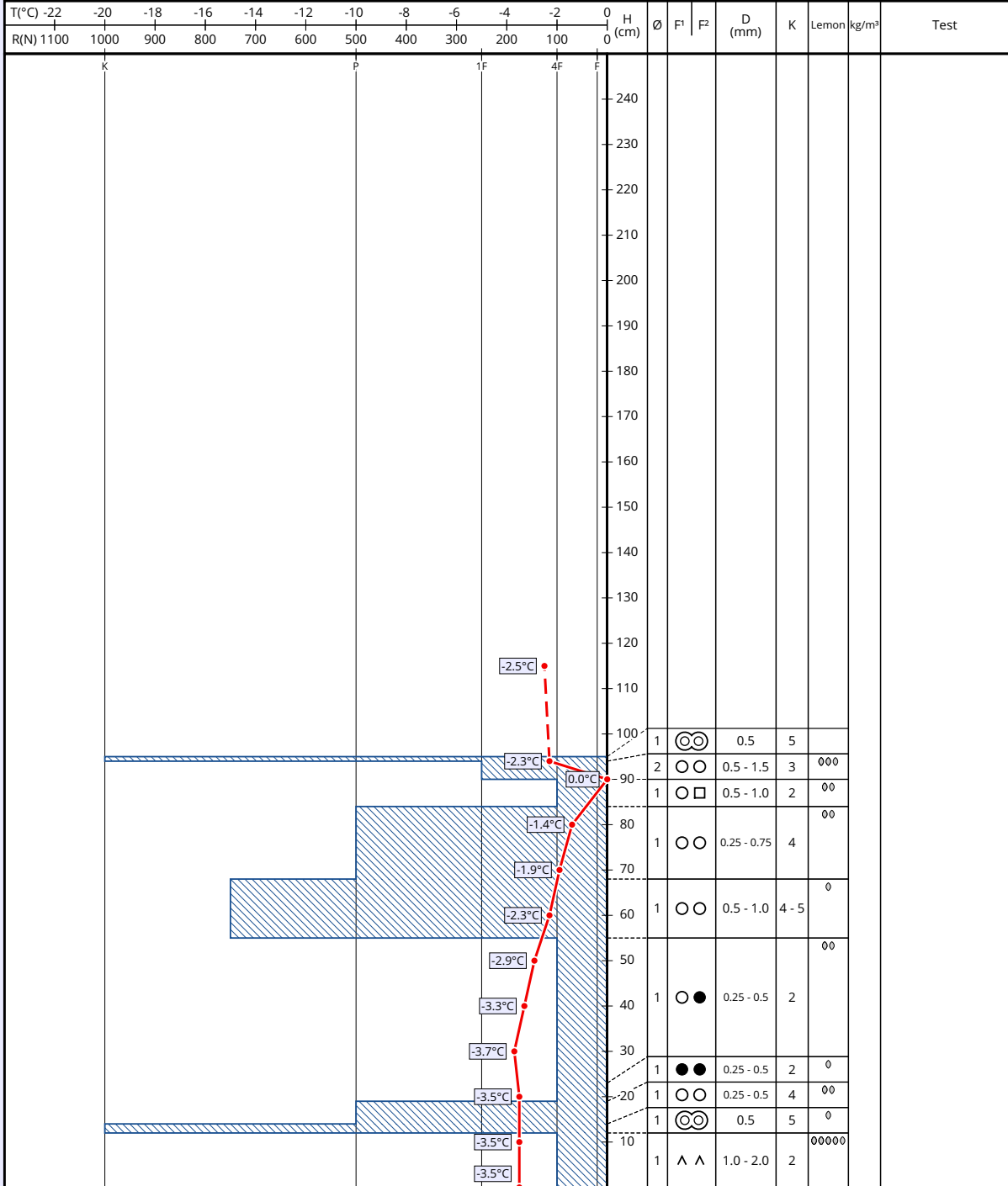# Appendix L   Comparison in Nybyen on the 19th of May

Figure 69: Comparison between the **field** on left side, the **model** in the middle and the **model with wind data overestimation** on right side in **Nybyen** on the 19th of May

Appendix M   Snow profile : Sverdruphamaren on the 14th of May

Snowprofile: Sverdruphamaren

Name: Martin Praz	**e-mail:** martin.praz@epfl.ch	**Observation date:** 14. May. 2018 14:00

Location: Sverdruphamaren	**Elevation:** 450 m	**Air temperature:** -2.5°C
Subregion: [n/def]	**Incline:** 39°	**Precipitation:** No precipitation
Region: Other	**Aspect:** NE	**Intensity:**
Country: Other	**Wind speed:** Gentle (< 20 km/h)	**Sky condition:** Few (1/8 - 2/8)
Lat/Long : 78.2102° / 15.5665°	**Wind direction:** W	**Profile-class:** not classified

Legend:
- $+$ Precip. particles
- $\diagup$ Decomp. / fragm.
- ● Rounded grains
- □ Faceted crystals
- ∧ Depth hoar
- ∨ Surface hoar
- ○ Melt forms
- ▬ Ice formations
- ⬠ Faceted, rounded
- ✕ Graupel
- ◎ Melt-freeze crust

Temperature profile readings (from top to bottom):
-2.5°C, -2.3°C, 0.0°C, -1.4°C, -1.9°C, -2.3°C, -2.9°C, -3.3°C, -3.7°C, -3.5°C, -3.5°C, -3.5°C

H (cm)	Ø	F¹ F²	D (mm)	K	Lemon	kg/m³	Test
~100	1	◎	0.5	5			
~95	2	○ ○	0.5 - 1.5	3		000	
~90	1	○ □	0.5 - 1.0	2		00	
~80	1	○ ○	0.25 - 0.75	4		00	
~60	1	○ ○	0.5 - 1.0	4 - 5		0	
~40	1	○ ●	0.25 - 0.5	2		00	
~28	1	● ●	0.25 - 0.5	2		0	
~20	1	○ ○	0.25 - 0.5	4		00	
~15	1	◎	0.5	5		0	
~10	1	∧ ∧	1.0 - 2.0	2		00000	

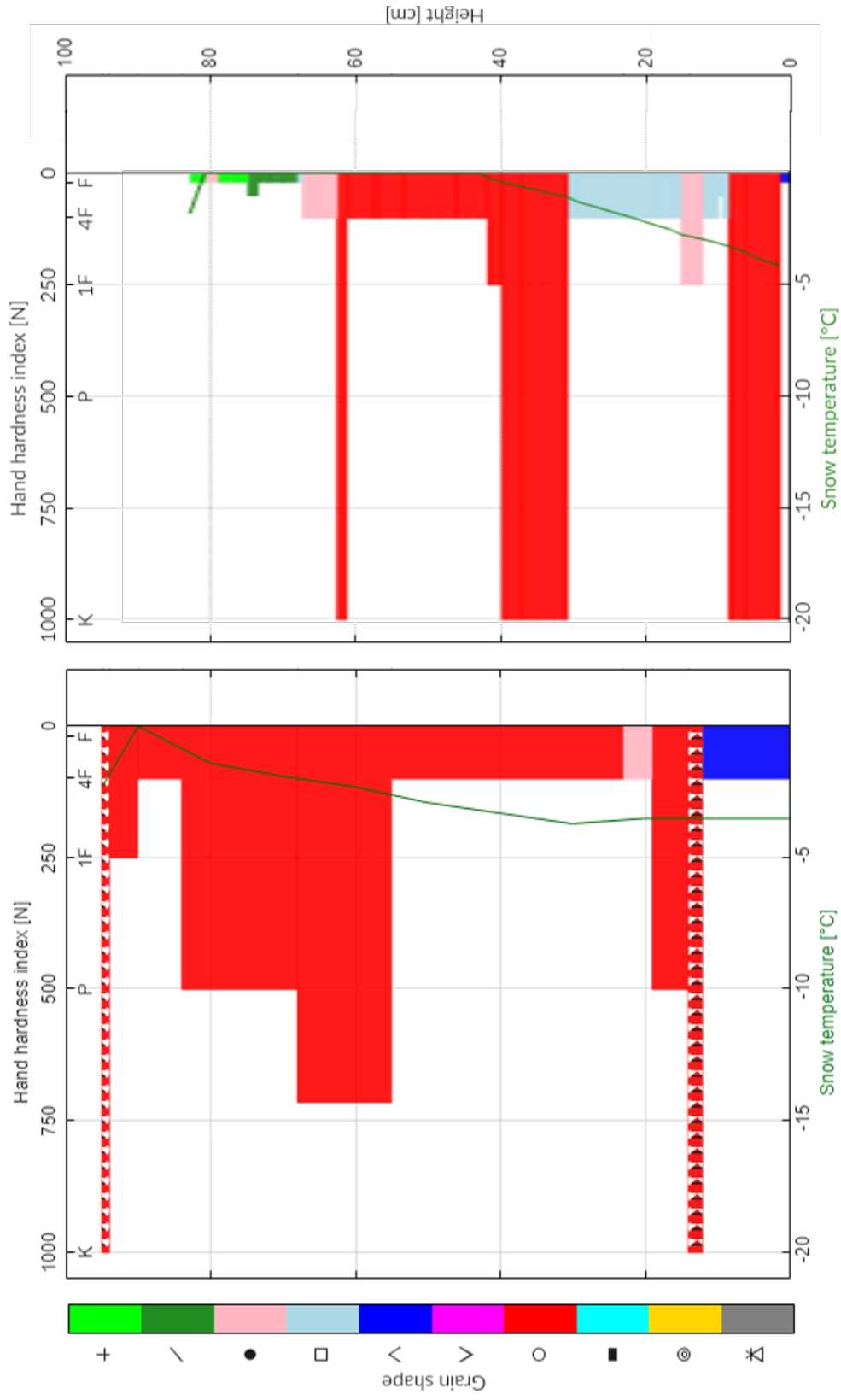# Appendix N   Comparison in Sverdruphamaren on the 14th of May

Figure 70: Comparison between the **field** on left side and the **model** on right side in **Sverdruphamaren** on the 14th of May
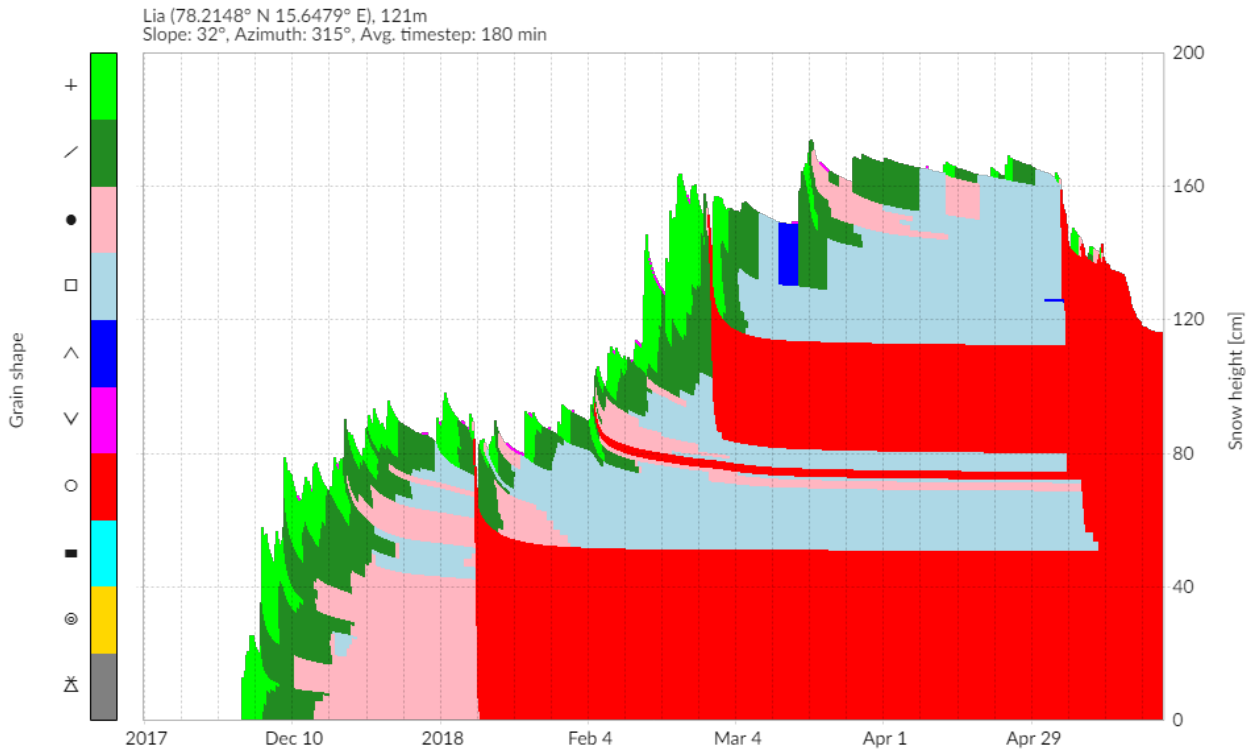
Appendix O Effect of the shortwave correction

Figure 71: Simulation of grain shape in **Lia** from the 11th of November until the 24th of May, **without shortwave radiation correction**, without mask and with wind speed equal to 50 % of raw data
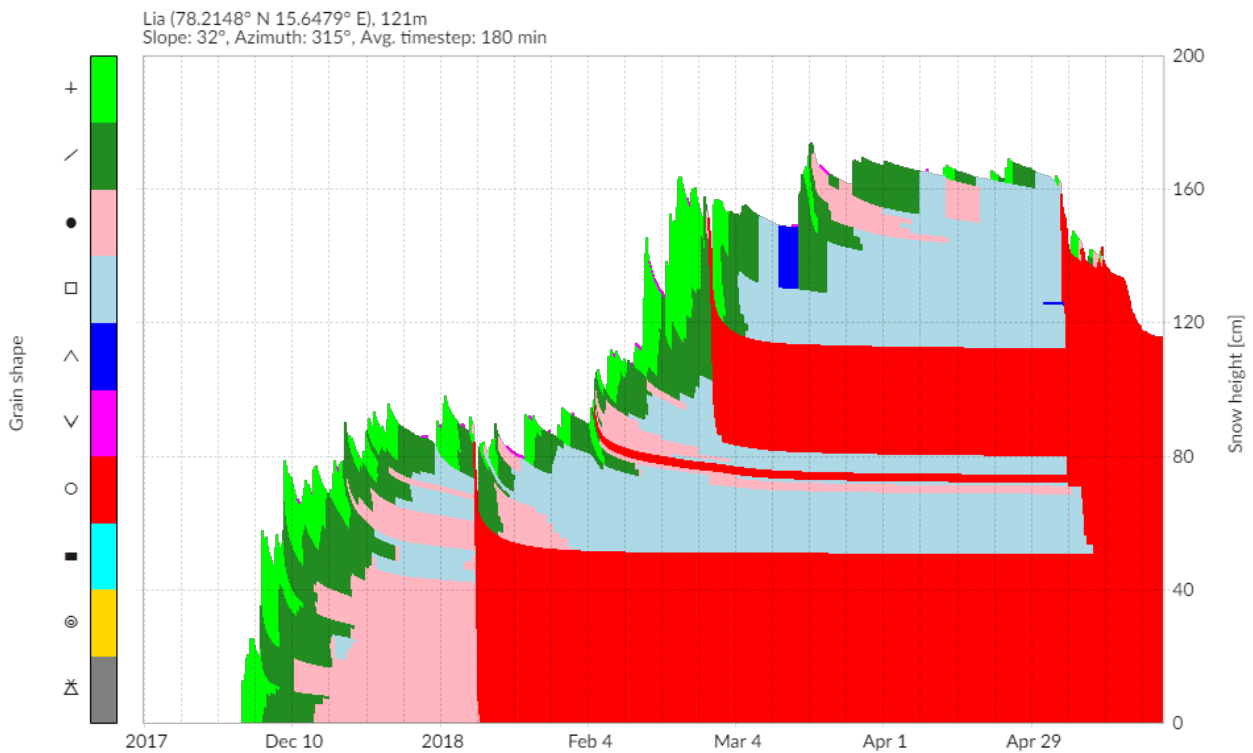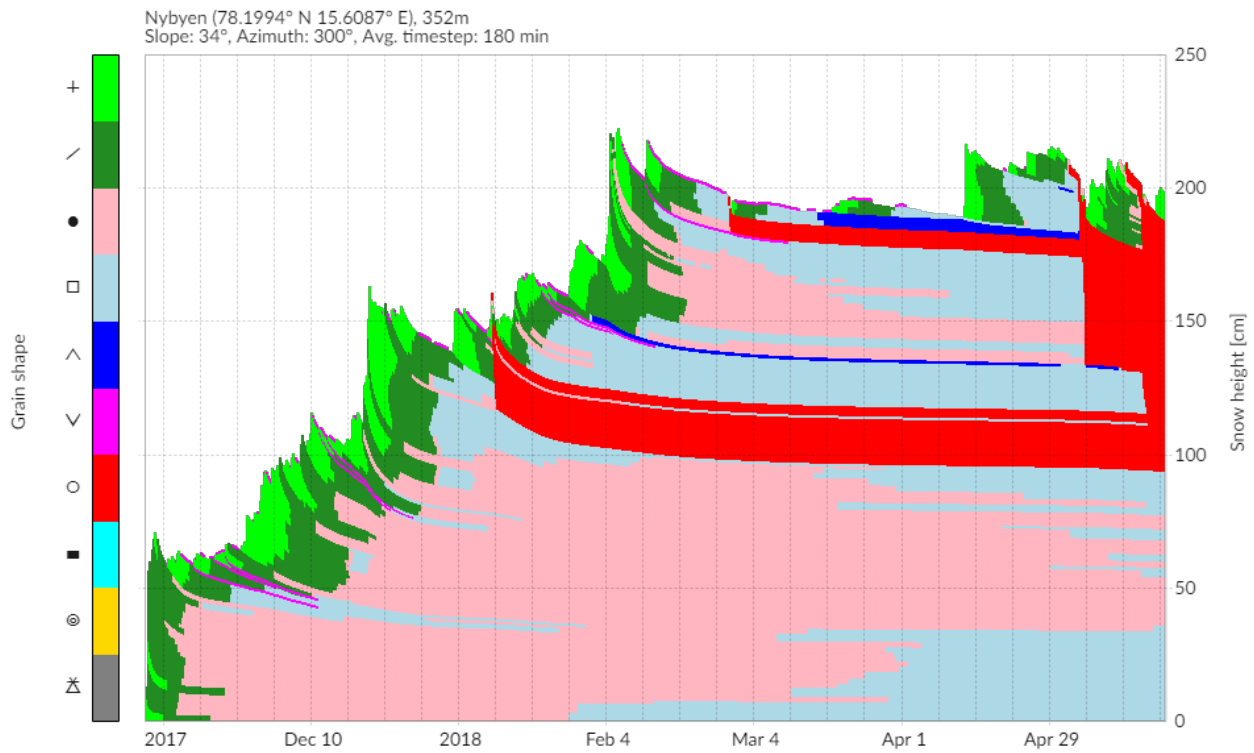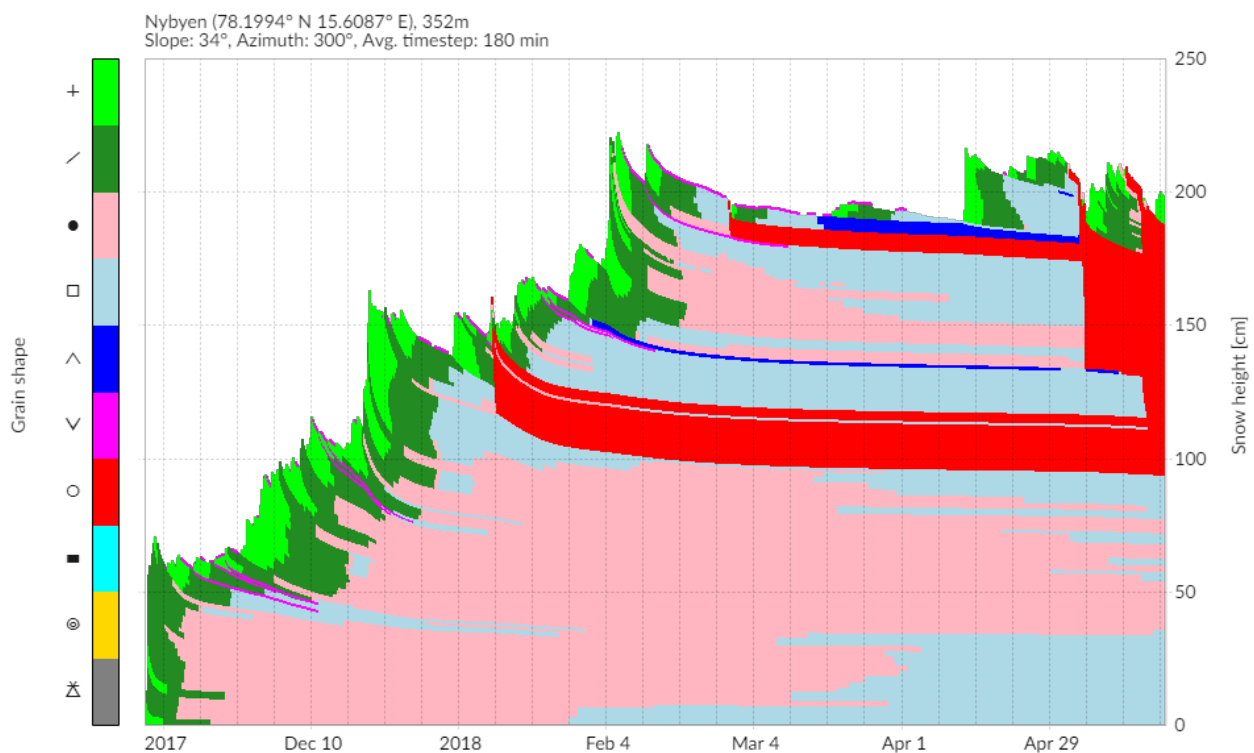

Figure 72: Simulation of grain shape in **Lia** from the 11th of November until the 24th of May, **with shortwave radiation correction**, without mask and with wind speed equal to 50 % of raw data

Figure 73: Simulation of grain shape in **Nybyen** from the 8th of November until the 21th of May, **without shortwave radiation correction**, without mask and with wind speed equal to 50 % of raw data

Figure 74: Simulation of grain shape in **Nybyen** from the 8th of November until the 21th of May, **with shortwave radiation correction**, without mask and with wind speed equal to 50 % of raw data
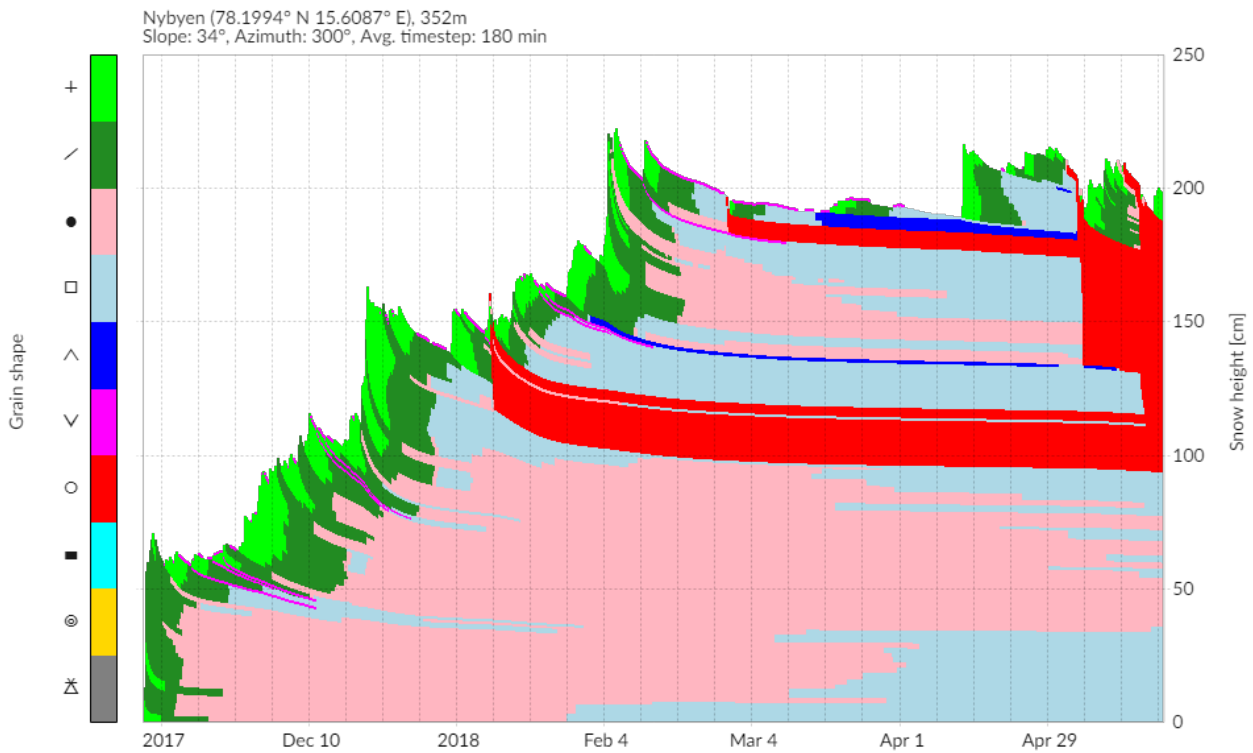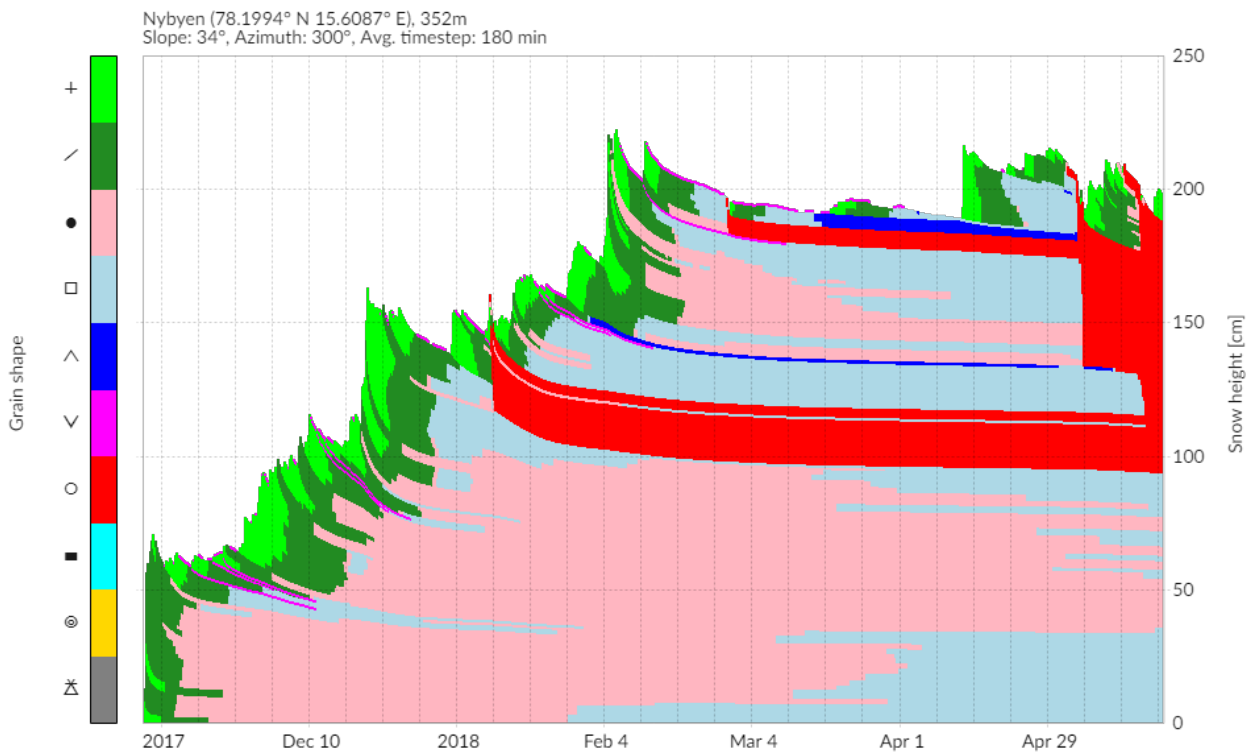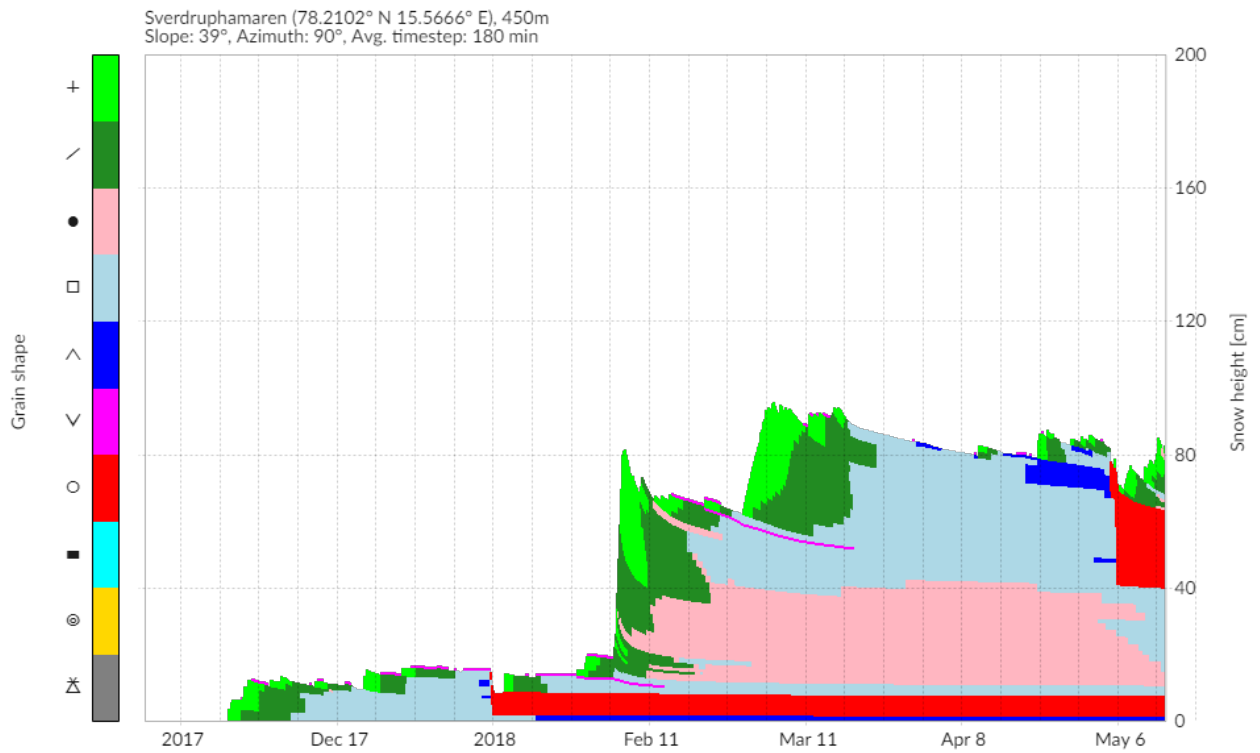
Appendix P   Effect of the mask

Figure 75: Simulation of grain shape in **Nybyen** from the 8th of November until the 21th of May, with shortwave radiation correction, **without mask** and with wind speed equal to 50 % of raw data

Figure 76: Simulation of grain shape in **Nybyen** from the 8th of November until the 21th of May, with shortwave radiation correction, **with mask** and with wind speed equal to 50 % of raw data
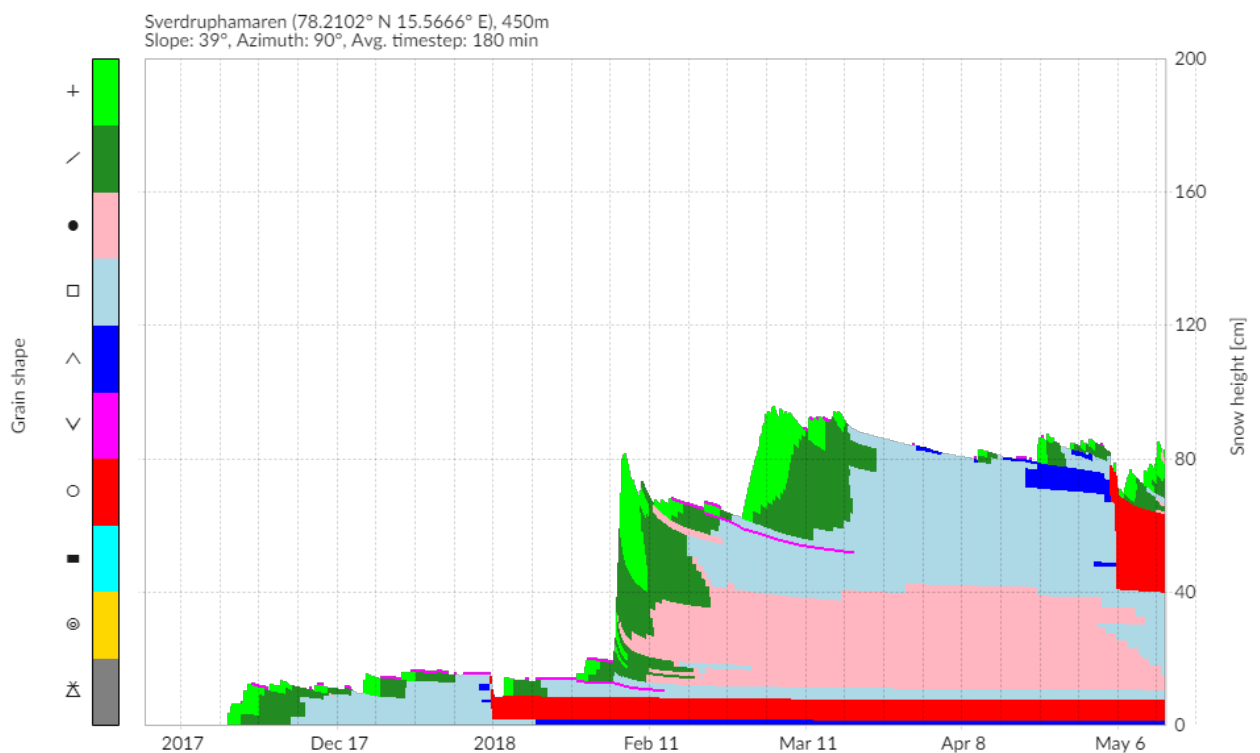
Figure 77: Simulation of grain shape in **Sverdruphamaren** from the 12th of November until the 16th of May, with shortwave radiation correction, **without mask** and with wind speed equal to 50 % of raw data

Figure 78: Simulation of grain shape in **Sverdruphamaren** from the 12th of November until the 16th of May, with shortwave radiation correction, **with mask** and with wind speed equal to 50 % of raw data
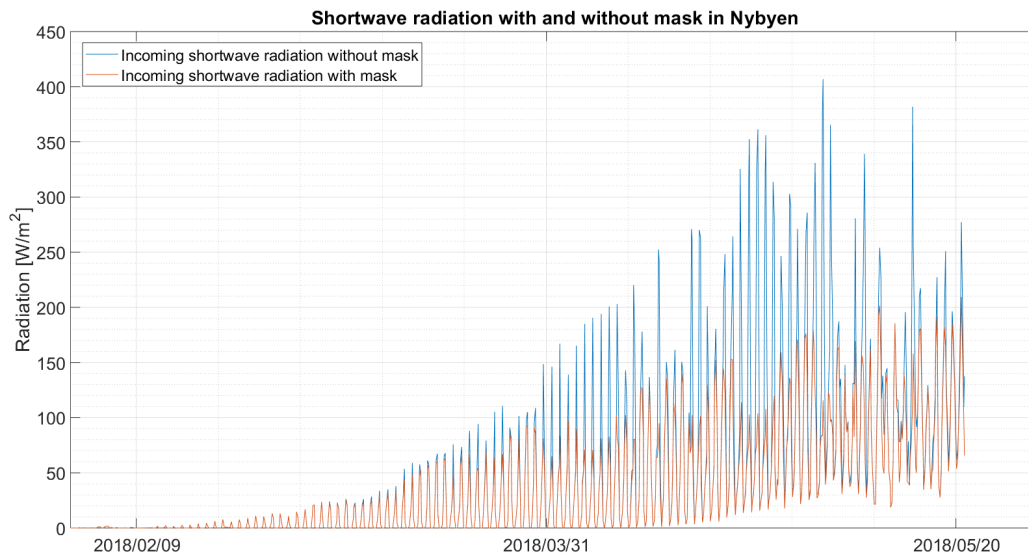
Figure 79: Shortwave radiation from output file in **Nybyen** from the 15th of February until the 21th of May, with mask and without
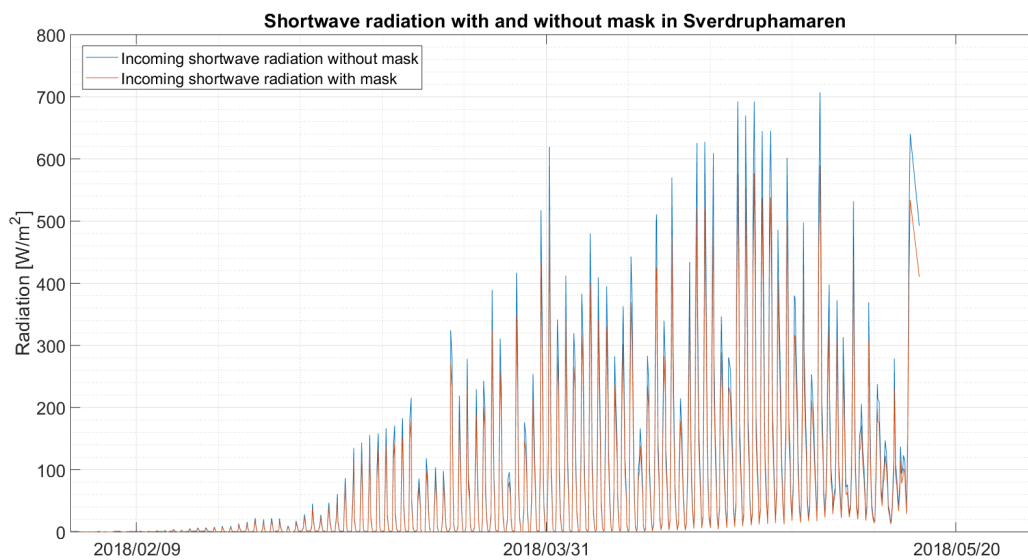

Figure 80: Shortwave radiation from output file in **Sverdruphamaren** from the 15th of February until the 16th of May, with mask and without

.

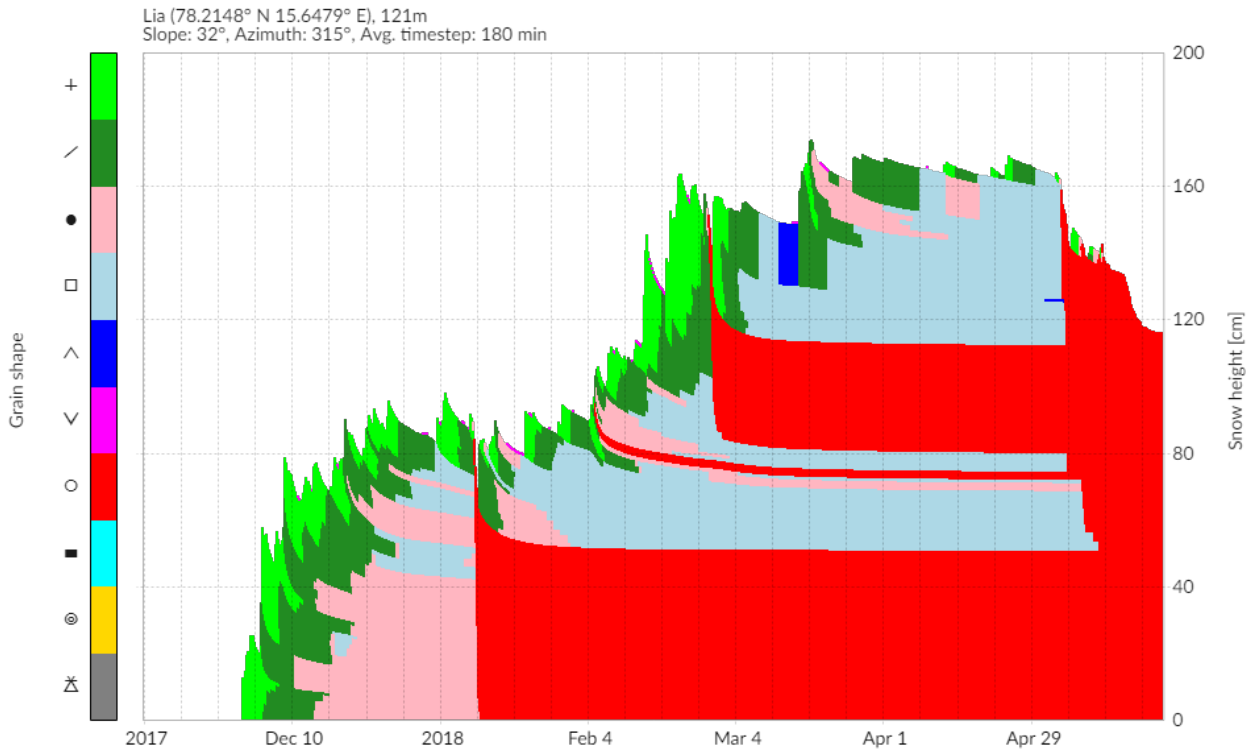# Appendix Q Effect of the boundary conditions

Figure 81: Simulation of grain shape in **Lia** from the 11th of November until the 24th of May, with shortwave radiation correction, with mask and with wind speed equal to 50 % of raw data and using **Dirichlet boundary condition**
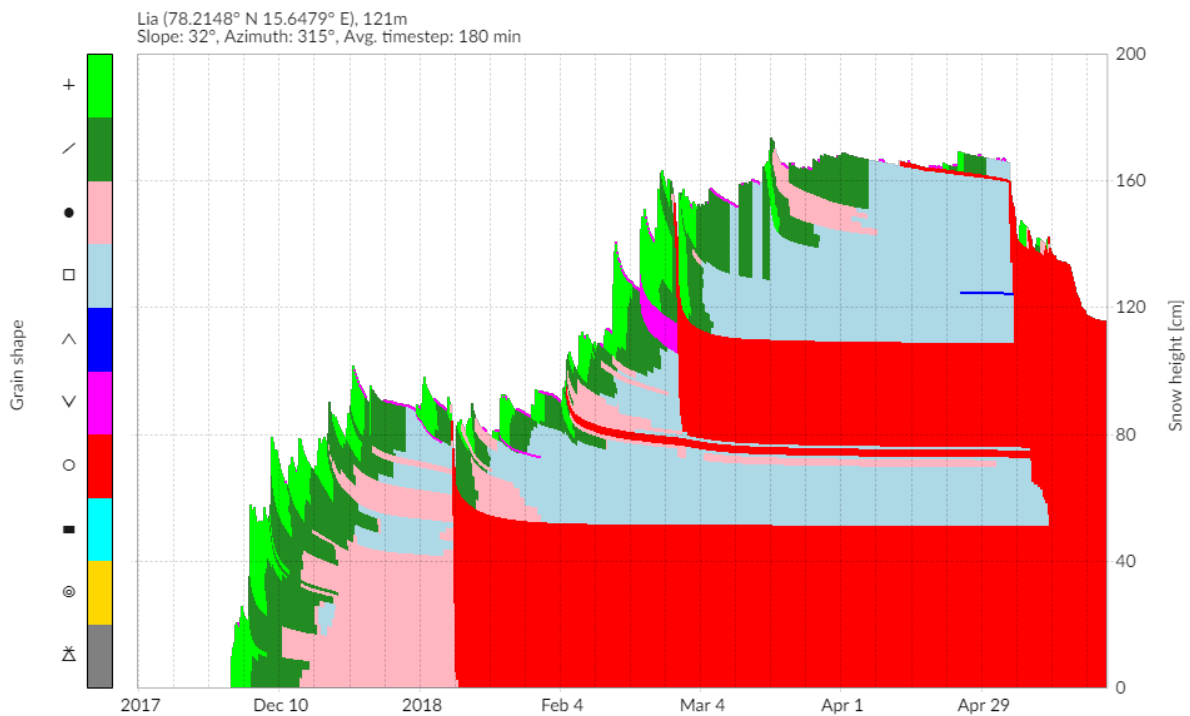

Figure 82: Simulation of grain shape in **Lia** from the 11th of November until the 24th of May, with shortwave radiation correction, with mask, with wind speed equal to 50 % of raw data and using **Neumann boundary condition**

Figure 83: Simulation of grain shape in **Sverdruphamaren** from the 12th of November until the 16th of May, with shortwave radiation correction, with mask, with wind speed equal to 50 % of raw data and using **Dirichlet boundary condition**

Figure 84: Simulation of grain shape in **Sverdruphamaren** from the 12th of November until the 16th of May, with shortwave radiation correction, with mask, with wind speed equal to 50 % of raw data and using **Neumann boundary condition**
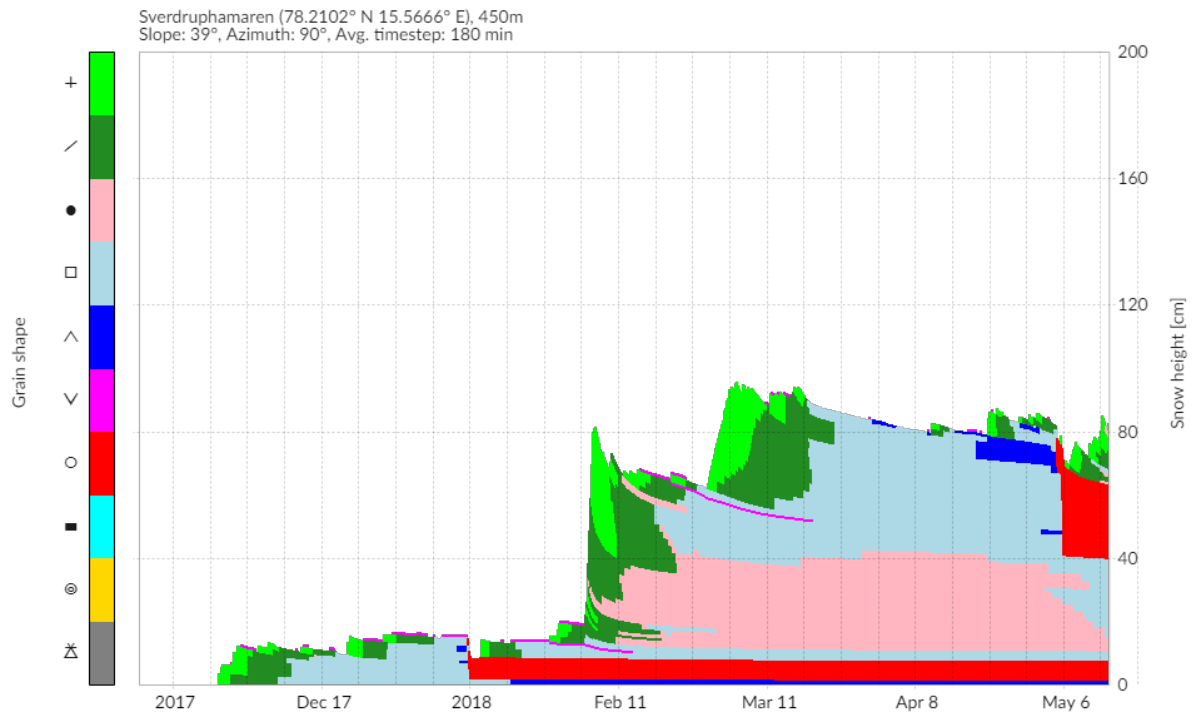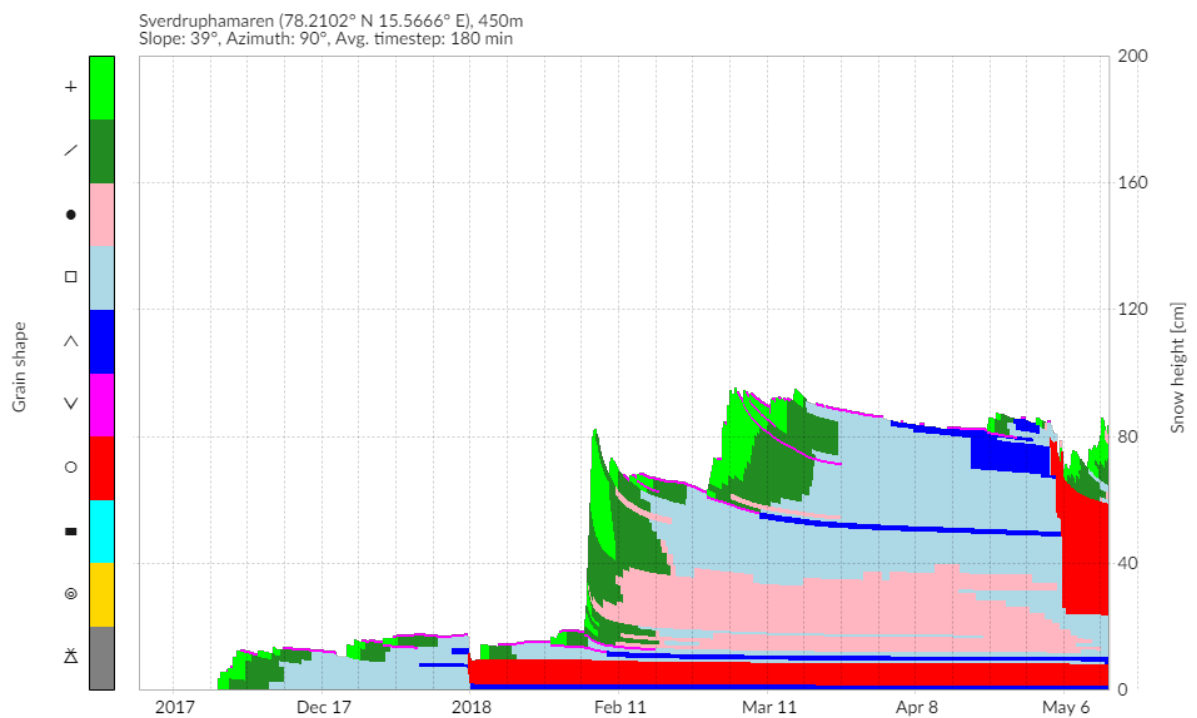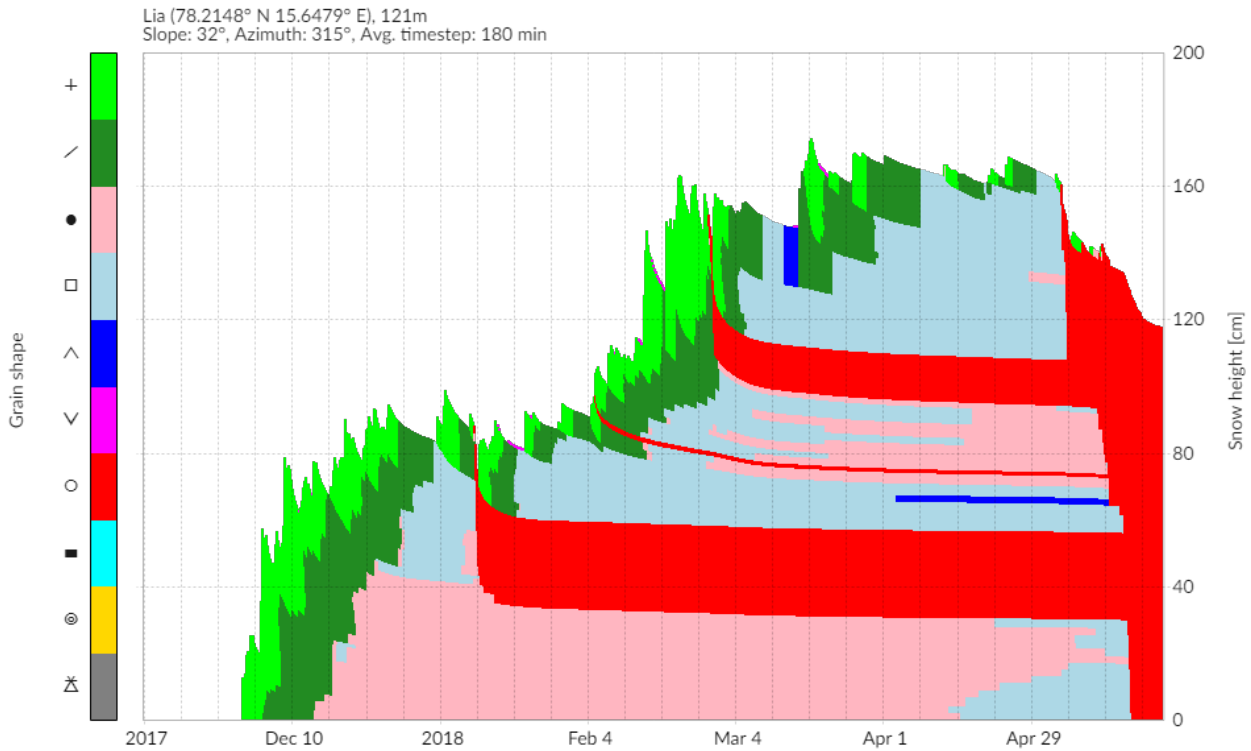
Appendix R Effect of wind in Lia

Figure 85: Simulation of grain shape in **Lia** from the 11th of November until the 24th of May, with shortwave radiation correction, **with mask** and with wind speed equal to **25 %** of raw data

Figure 86: Simulation of grain shape in **Lia** from the 11th of November until the 24th of May, with shortwave radiation correction, with mask and with wind speed equal to **62.5 %** of raw data

Figure 87: Simulation of grain shape in **Lia** from the 11th of November until the 24th of May, with shortwave radiation correction, with mask and with wind speed equal to **75 %** of raw data
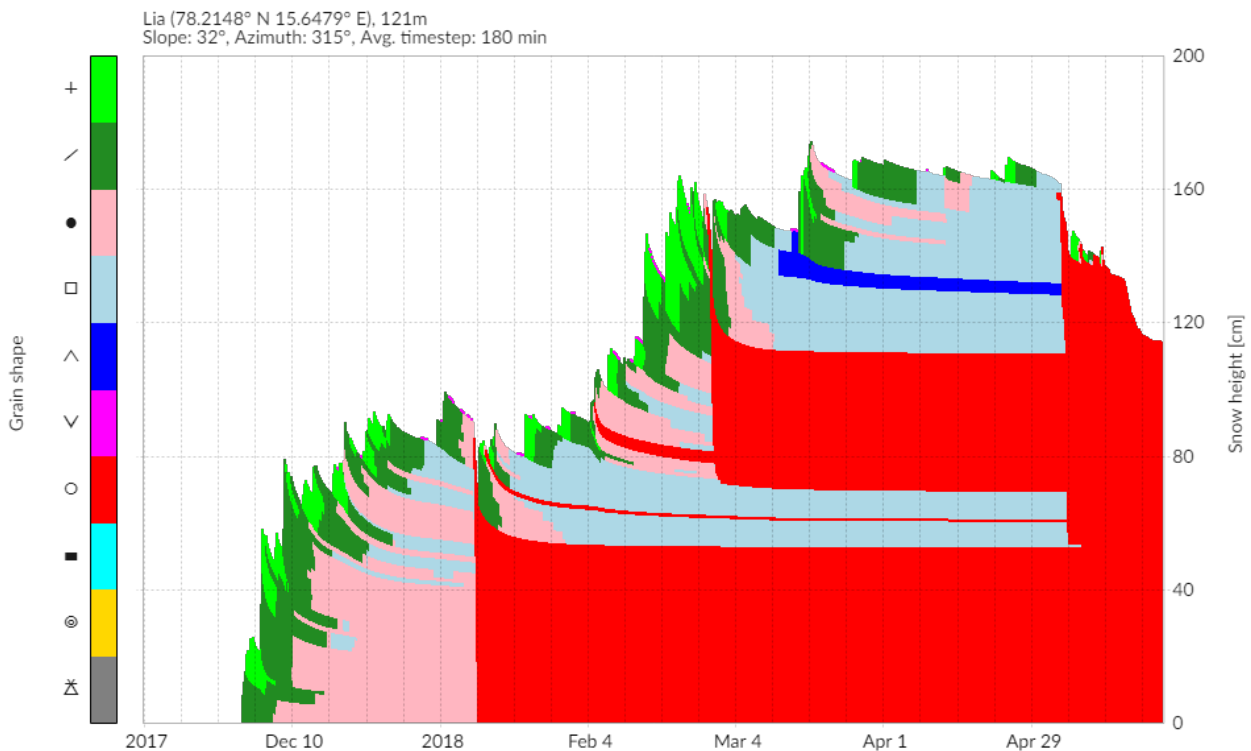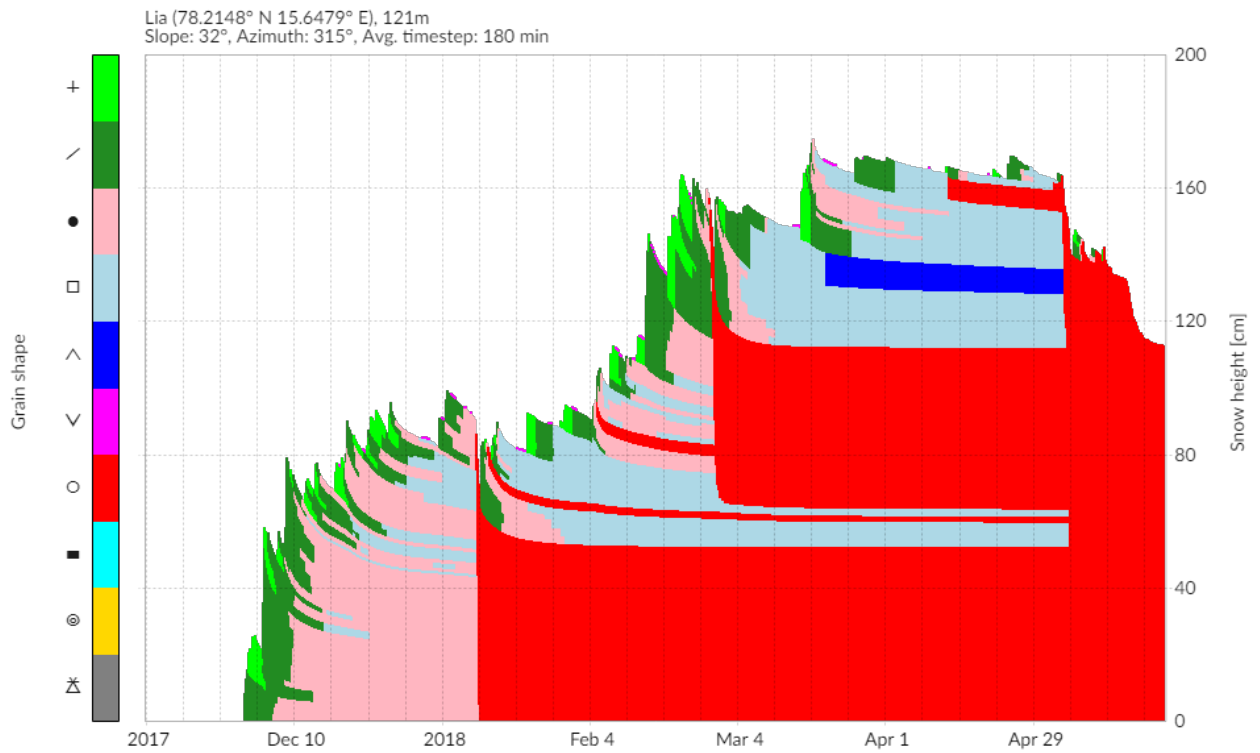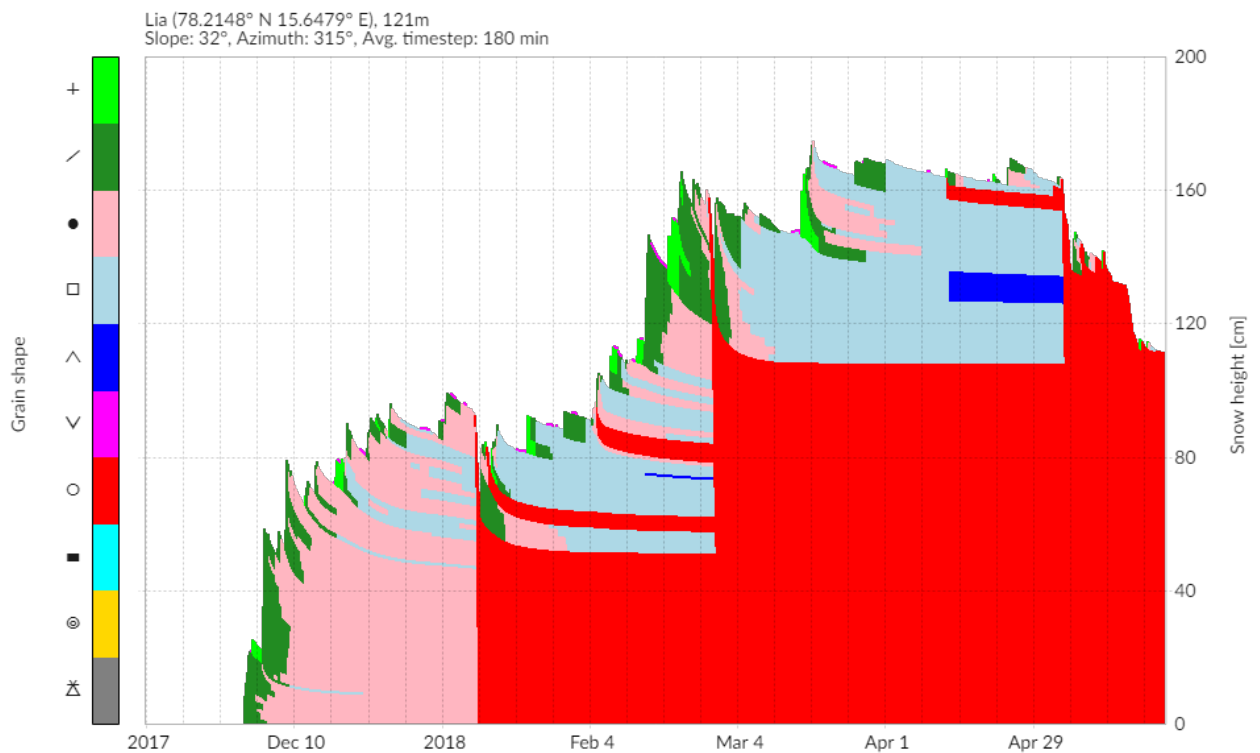

Figure 88: Simulation of grain shape in **Lia** from the 11th of November until the 24th of May, with shortwave radiation correction, with mask and with wind speed equal to **100 %** of raw data

Appendix S   Effect of wind in Sverdruphamaren

Figure 89: Simulation of grain shape in **Sverdruphamaren** from the 12th of November until the 16th of May, with shortwave radiation correction, with mask and with wind speed equal to **25 %** of raw data

Figure 90: Simulation of grain shape in **Sverdruphamaren** from the 12th of November until the 16th of May, with shortwave radiation correction, with mask and with wind speed equal to **50 %** of raw data

Figure 91: Simulation of grain shape in **Sverdruphamaren** from the 12th of November until the 16th of May, with shortwave radiation correction, with mask and with wind speed equal to **75 %** of raw data
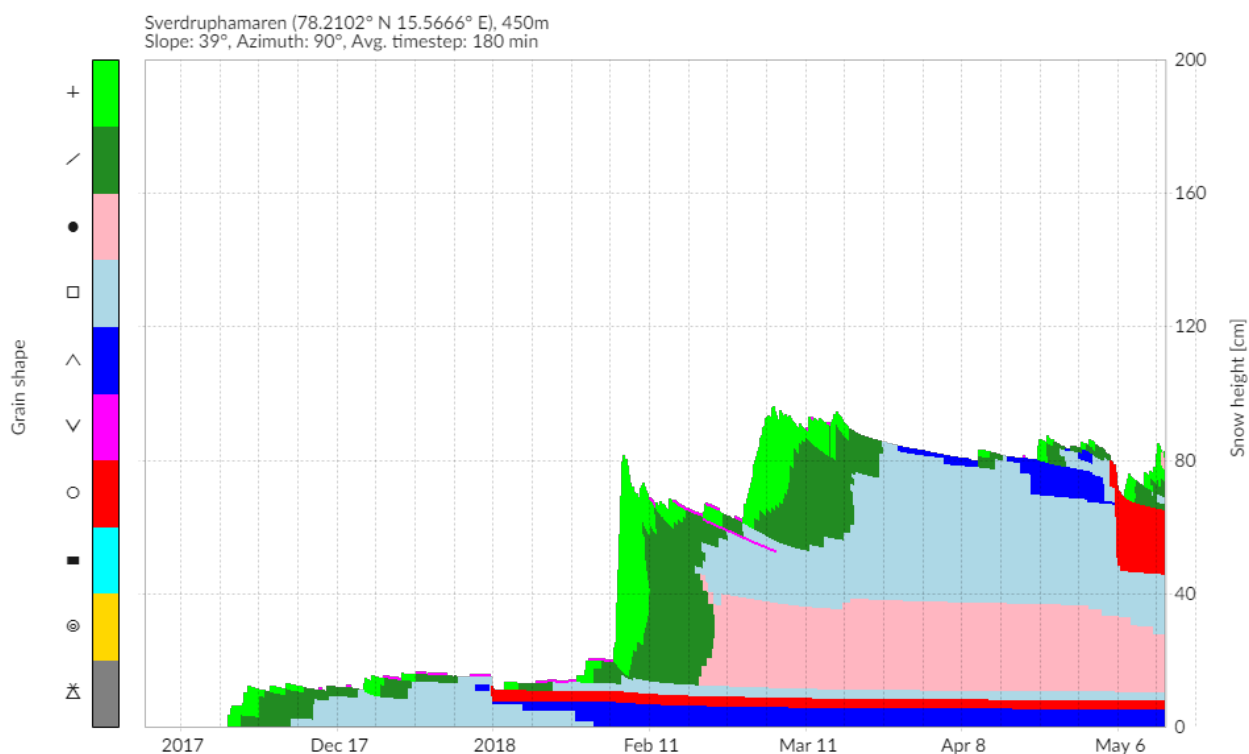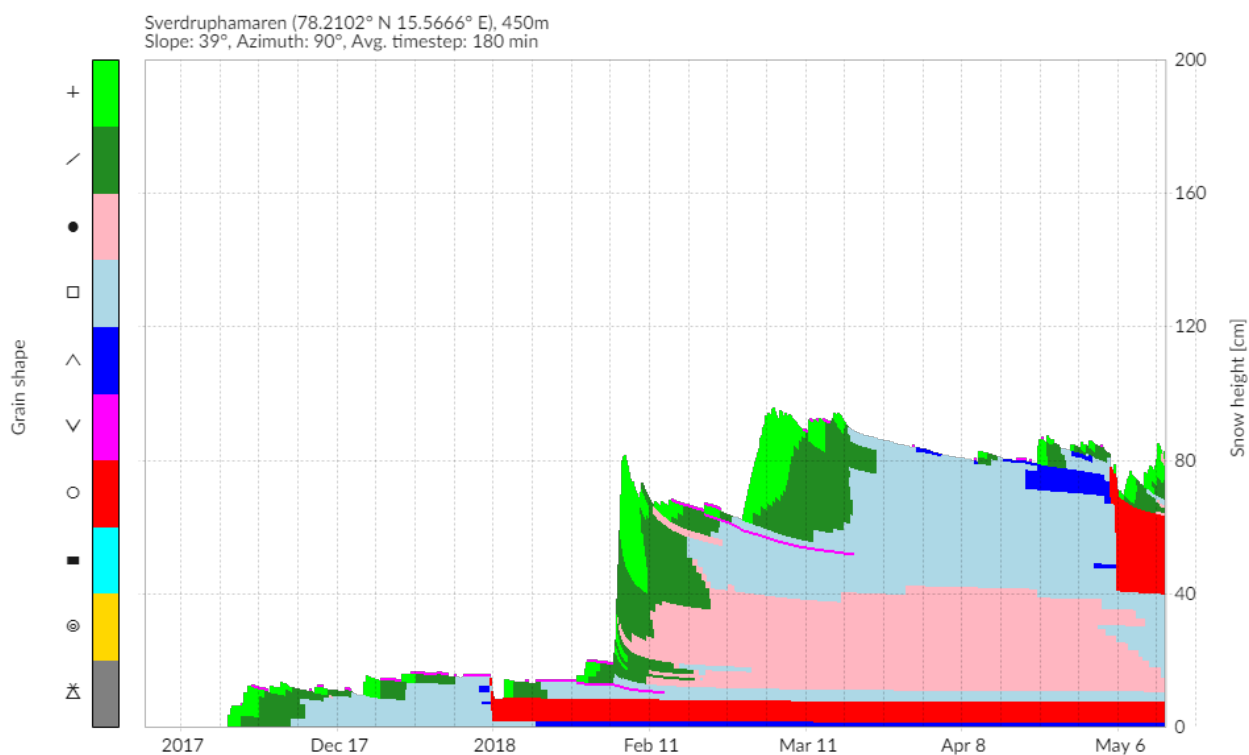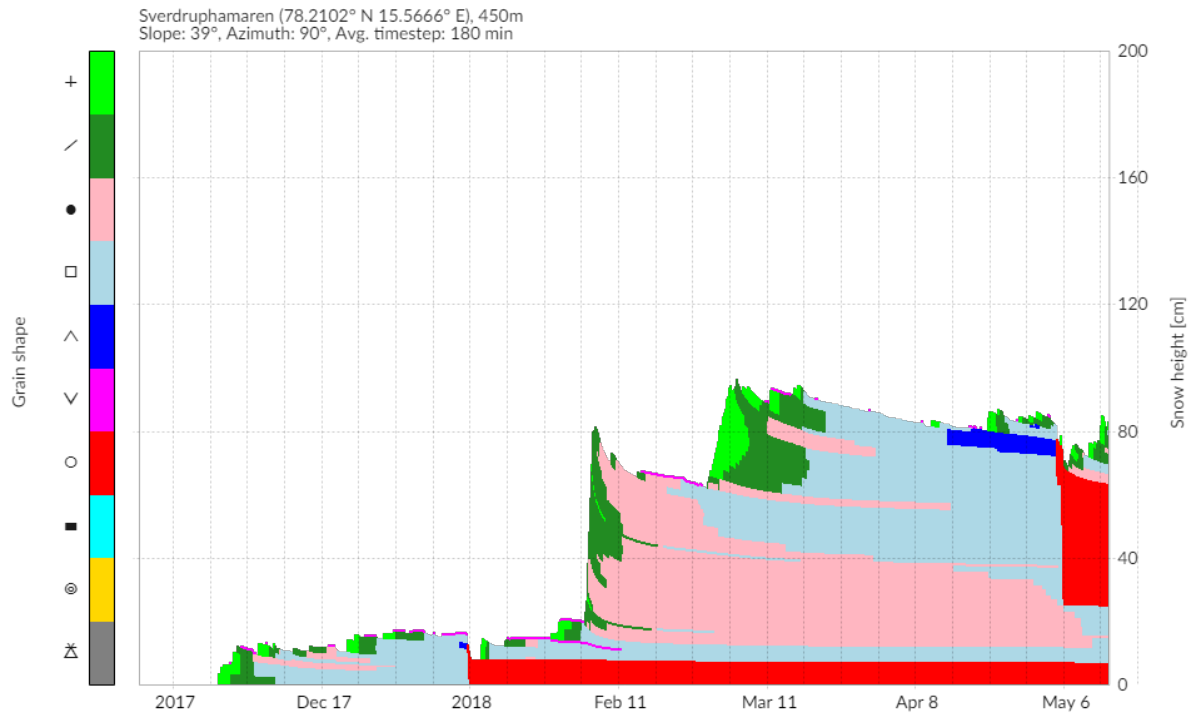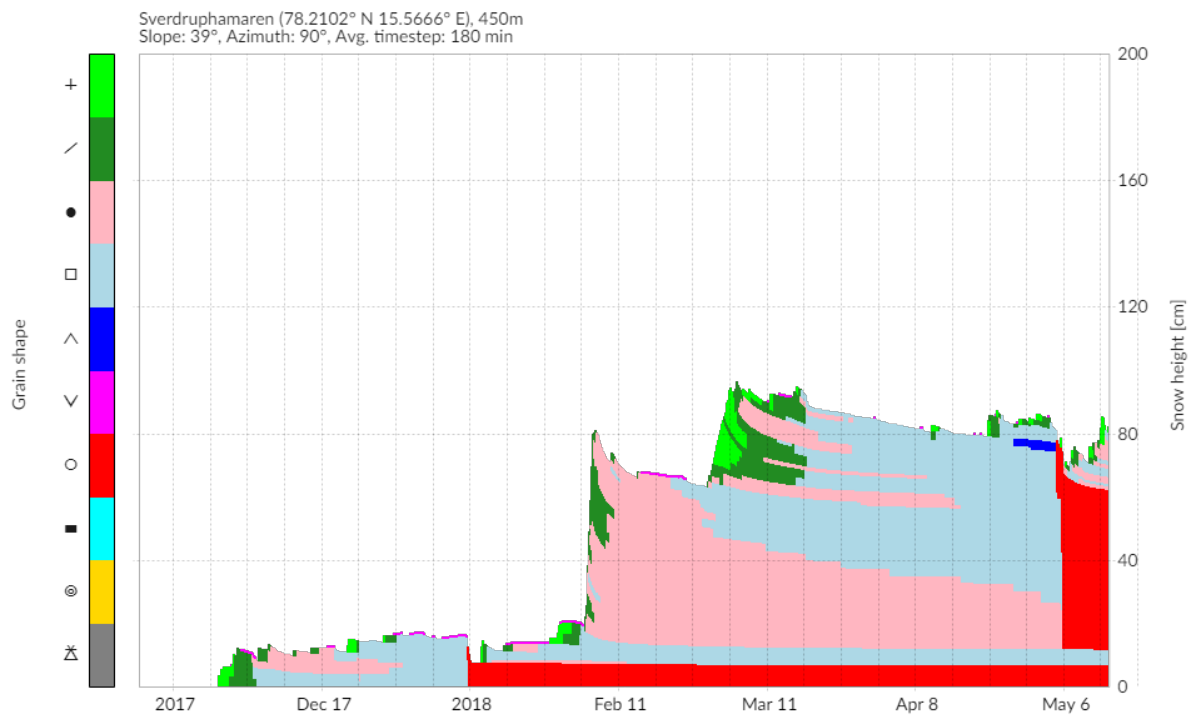

Figure 92: Simulation of grain shape in **Sverdruphamaren** from the 12th of November until the 16th of May, with shortwave radiation correction, with mask and with wind speed equal to **100 %** of raw data

References

[1] `https://www.ssb.no/en/befolkning/artikler-og-publikasjoner/_attachment/294354?_ts=` `15a12de02c0` consulted on the 21st of June 2018. Information about Svalbard, page 6 and 19.

[2] `https://www.ssb.no/en/befolkning/statistikker/befsvalbard` consulted on the 21st of June 2018. Infoamtion about the inhabitants of Longyearbyen.

[3] `https://geminiresearchnews.com/2017/02/force-deadly-polar-bears/` consulted on the 21st of June 2018. Article title : "A force more deadly than polar bears", 16.02.2017, Nancy Bazilchuk.

[4] M. Lehning, H. Huwald, J. Gaume, A. Kahl. 2017. Physics & Hydrology of Snow course. EPFL.

[5] C. Fierz, R.L Armstrong, Y. Durand, P. Etchevers, E. Greene, D.M McClung, K. Nishimura, P.K. Satyawali and S.A Sokratov. 2009. The International Classification for Seasonal Snow on the Ground. IHP-VII Technical Documents in Hydrology N°83, IACS Contribution N°1, UNESCO-IHP, Paris.

[6] C. Jaedicke. 2011. Drifting snow and snow accumulation in complex Arctic terrain: field experiments and numerical modelling. PhD thesis, Geophysical Institute, University of Bergen.

[7] J. W. Pomeroy, D. M. Gray Water Resources Research, Vol. 26, No. 7, Pages 1583-1594, July 1990. Saltation of Snow. National Hydrology Research Institute, Environment Canada, Saskatoon, Saskatchewan, Canada and Division of Hydrology, University of Saskatchewan, Saskatoon, Canada

[8] R. Sommerfeld and E. LaChapelle. 1970. The Classification of Snow Metamorphism. Journal of Glaciology, 9(55), 3-18. doi:10.3189/S0022143000026757

[9] G. E. Liston and M. Sturm. 1998. A snow-transport model for complex terrain. J. Glaciol., 44, 498–516

[10] G.E. Liston and M. Sturm. 2002. Winter precipitation patterns in arctic Alaska determined from a blowing-snow model and snow-depth observations. J. Hydromet., 3(6), 646–659.

[11] O. Bruland, G.E. Liston, J. Vonk, K. Sand and Å. Killingtveit. 2004. Modelling the snow distribution at two high arctic sites at Svalbard, Norway, and at an alpine site in central Norway. Nord. Hydrol., 35(3), 191–208.

[12] `https://www.umr-cnrm.fr/spip.php?article265&lang=fr` consulted on the 4th of July, CNRM website, information about CROCUS.

[13] V. Vionnet, E. Brun, S. Morin, A. Boone, S. Faroux, and al.. 2012 The detailed snowpack scheme Crocus and its implementation in SURFEX v7.2. Geoscientific Model Development, European Geosciences Union, 5, pp.773- 791. <10.5194/gmd-5-773-2012>. <insu-00844645>

[14] `https://www.slf.ch/en/services-and-products/snowpack.html`, consulted on the 18th of June 2018. Basic information about SNOWPACK.

[15] P. Bartelt and M. Lehning. 2002. A pysical SNOWPACK model for the Swiss avalanche warning. Part I: numerical model. WSL, Swiss Federal Institute for Snow and Avalanche Research, SLF, Flüelastrasse 11, CH-7260 Davos Dorf, Switzerland. Cold Regions Science and Technology 35 123– 145.

[16] M. Lehning, P. Bartelt, B. Brown, C. Fierz and P. Satyawali. 2002. A physical SNOWPACK model for the Swiss avalanche warning Part II. Snow microstructure. WSL, Swiss Federal Institute for Snow and Avalanche Research, SLF, Flüelastrasse 11, CH-7260 Davos Dorf, Switzerland. Cold Regions Science and Technology 35 147– 167.

[17] M. Lehning, P. Bartelt, B. Brown, C. Fierz. A physical SNOWPACK model for the Swiss avalanche warning Part III. 2002. Meteorological forcing, thin layer formation and evaluation. WSL, Swiss Federal Institute for Snow and Avalanche Research, SLF, Flüelastrasse 11, CH-7260 Davos Dorf, Switzerland. Cold Regions Science and Technology 35 169– 184.

[18] `https://models.slf.ch/docserver/snowpack/html/index.html` Documentation online of SNOWPACK.

[19] M. Kottek, J. Grieser, C. Beck, B. Rudolf, and F. Rubel. 2006. World map of the Koeppen-Geiger climate classification updated. Meteorologische Zeitschrift 15/3:259–263.

[20] M. Eckerstorfer and H.H. Christiansen. 2011. The "High Arctic Maritime Snow Climate" in Central Svalbard. Arctic, Antarctic, and Alpine Research 43(1):11-21.

[21] Norwegian Meteorological Institute.

[22] Brage B. Hansen, Ketil Isaksen, Rasmus E. Benestad, Jack Kohler, Åshild Ø Pedersen, Leif E. Loe, Steffen J. Coulson, Lan Otto Larsen, and Øystein Varpe. 2014. Warmer and wetter winters: characteristics and implications of an extreme weather event in the High Arctic. Environ. Res. Lett. 9 114021

[23] O. Humlum. 2002. Modelling late 20th-century precipitation in Nordenskiold Land, Svalbard, by geomorphic means. Norsk Geografisk Tidsskrift–Norwegian Journal of Geography 56:96–103.

[24] C. Jaedicke and P. Gauer. 2005. The influence of drifting snow on the location of glaciers on western Spitsbergen, Svalbard. Annals of Glaciology 42:237–242.

[25] D.M. McClung and P. Schaerer. 2006. The Avalanche Handbook. 3rd edition. Seattle The Mountaineers. 342 pp.

[26] F. Dominé, A. Cabanes, L. Legagneux. 2002. Structure, microphysics, and surface area of the Arctic snowpack near Alert during the ALERT 2000 campaign. CNRS, Laboratoire de Glaciologie et Géophysique de l'Environnement, BP 96, 38402 Saint Martin d'Hères cedex, France. Atmospheric Environment 36 2753–2765.

[27] `https://www.slf.ch/en/avalanche-bulletin-and-snow-situation/measured-values/description-of-automated-stations.html`

[28] `http://toposvalbard.npolar.no/`, consulted on the 9rd of June, information about the distances and the name of locations.

[29] Kevin J. Rennert, Gerard Roe, Jaakko Putkonen and Cecilia M. Bitz. 2009. Soil Thermal and Ecological Impact of Rain on Snow Events in the Circumpolar Arctic. University of Washington, Seattle, Washington. 2302 Journal of Climate, Volume 2.

[30] `http://www.npolar.no/en/the-arctic/svalbard/`, consulted on the 3rd of June, information about the duration about the polar night and the polar day.

[31] Eirik J. Førland, Rasmus Benestad, Inger Hanssen-Bauer, Jan Erik Haugen, and Torill Engen Skaugen. 2011. Temperature and Precipitation Development at Svalbard 1900–2100. Advances in Meteorology, vol. 2011, Article ID 893790, 14 pages.
`https://doi.org/10.1155/2011/893790`

[32] T.F. Stocker, D. Qin, G.-K. Plattner, L.V. Alexander, S.K. Allen, N.L. Bindoff, F.-M. Bréon, J.A. Church, U. Cubasch, S. Emori, P. Forster, P. Friedlingstein, N. Gillett, J.M. Gregory, D.L. Hartmann, E. Jansen, B. Kirtman, R. Knutti, K. Krishna Kumar, P. Lemke, J. Marotzke, V. Masson-Delmotte, G.A. Meehl, I.I. Mokhov, S. Piao, V. Ramaswamy, D. Randall, M. Rhein, M. Rojas, C. Sabine, D. Shindell, L.D. Talley, D.G. Vaughan and S.-P. Xie. 2013. Technical Summary. In: Climate Change 2013: The Physical Science Basis. Contribution of Working Group I to the Fifth Assessment Report of the Intergovernmental Panel on Climate Change [Stocker, T.F., D. Qin, G.-K. Plattner, M. Tignor, S.K. Allen, J. Boschung, A. Nauels, Y. Xia, V. Bex and P.M. Midgley (eds.)]. Cambridge University Press, Cambridge, United Kingdom and New York, NY, USA.

[33] `eklima.met.no` Precipitation data

[34] John Stimberis and Charles M. Rubin. 2011. Glide avalanche response to an extreme rain-on-snow event, Snoqualmie Pass, Washington, USA. 468, Journal of Glaciology, Vol. 57, No. 203.

[35] A. Dai. 2008. Temperature and pressure dependence of the rain-snow phase transition over land and ocean, Geophys. Res. Lett., 35, L12802, doi:10.1029/2008GL033295.

[36] H. Conway and C.F. Raymond. 1993. Snow stability during rain. Geophysics Program AK-50, University of Washington, Seattle, Washington 98195, U.S.A. Journal of Glaciology, Vol. 39, No. 133.

[37] M. Lonardi. 2018. Characterization of Wind Channeling Around Longyearbyen, Svalbard. Uppsala University, Disciplinary Domain of Science and Technology, Earth Sciences, Department of Earth Sciences, LUVAL.